

# Publikace I

## RESEARCH ARTICLE

# Atmospheric pressure chemical ionization mass spectrometry at low flow rates: Importance of ion source housing

Timotej Strmeň<sup>1,2</sup> | Vladimír Vrkoslav<sup>1</sup> | Zuzana Bosáková<sup>2</sup> | Josef Cvačka<sup>1,2</sup> 

<sup>1</sup>Institute of Organic Chemistry and Biochemistry of the Czech Academy of Sciences, Flemingovo nám. 2, CZ-166 10 Prague 6, Czech Republic

<sup>2</sup>Department of Analytical Chemistry, Faculty of Science, Charles University in Prague, Hlavova 2030/8, CZ-128 43 Prague 2, Czech Republic

**Correspondence**

J. Cvačka, Institute of Organic Chemistry and Biochemistry of the Czech Academy of Sciences, Flemingovo nám. 2, CZ-166 10 Prague 6, Czech Republic.  
Email: josef.cvacka@uochb.cas.cz

**Funding information**

Charles University in Prague, Grant/Award Number: Project SVV260440; Czech Science Foundation, Grant/Award Number: 16-01639S

**Rationale:** Hyphenation of atmospheric pressure chemical ionization (APCI) mass spectrometry with capillary and micro high-performance liquid chromatography (HPLC) is attractive for many applications, but reliable ion sources dedicated to these conditions are still missing. There are a number of aspects to consider when designing such an ion source, including the susceptibility of the ionization processes to ambient conditions. Here we discuss the importance of ion source housing for APCI at low flow rates.

**Methods:** Selected compounds dissolved in various solvents were used to study ionization reactions at 10  $\mu\text{L}/\text{min}$  flow rate. APCI spectra were generated using the Ion Max-S source (Thermo Fisher Scientific) operated with or without the ion source housing.

**Results:** The APCI spectra of most compounds measured in the open and enclosed ion sources were markedly different. The differences were explained by water and oxygen molecules that entered the plasma region of the open ion source. Water tended to suppress charge transfer processes while oxygen diminished electron capture reactions and prevented the formation of acetonitrile-related radical cations useful for localizing double bonds in lipids. The effects associated with the ion source housing were significantly less important for compounds that are easy to protonate or deprotonate.

**Conclusions:** The use of ion source housing prevented alternative ionization channels leading to unwanted or unexpected ions. Compared with the conventional flow rate mode (1 mL/min), the effects of ambient air components were significantly higher at 10  $\mu\text{L}/\text{min}$ , emphasizing the need for ion source housing in APCI sources dedicated to low flow rates.

## 1 | INTRODUCTION

Liquid chromatography/mass spectrometry (LC/MS) is a key analytical method in life science research. It is widely used in various “omics” aiming at the collective characterization and quantification of pools of biological molecules. LC/MS analyses are increasingly performed in a down-sized format with nano- and micro-bore chromatography columns, which yield less dilution and thus provide enhanced sensitivity.<sup>1</sup> Low flow rate LC/MS systems are attractive

not only for proteomics, but also for small molecule analysis and metabolomics.<sup>2</sup> Nowadays, the LC/MS methods rely almost exclusively on electrospray ionization (ESI), which is suitable for the analysis of a wide range of compounds. It works particularly well for species that exist as ions in solution or those with acidic or basic functionality but is less efficient or inefficient at ionizing less polar compounds.<sup>3</sup> Unlike ESI, atmospheric pressure chemical ionization (APCI) is based on gas-phase processes. APCI-MS allows the analysis of medium polar to non-polar substances with good sensitivity,

which makes it a complementary ionization technique to ESI. APCI is very compatible with a broad range of solvents, regardless of their polarity. While ESI is susceptible to ion suppression caused by competition for a charge during the ionization,<sup>4</sup> the APCI process is significantly less affected by the matrix.<sup>5</sup> APCI-MS thus has the potential to become a complementary ionization technique for complex samples containing many analytes, e.g., in metabolomics or lipidomics.

The ions formed in APCI sources result from primary and secondary processes, which strongly depend on the chemical nature of all the species involved, the ion source design and experimental conditions. Cluster ions are readily formed in the ion sources and they are involved in the ionization mechanisms.<sup>6</sup> The nebulizer gas governs primary ionization. A corona discharge in nitrogen provides radical cations such as  $N_2^{+\bullet}$  and  $N_4^{+\bullet}$ , which in dry air further react with molecular oxygen to yield  $O_2^{+\bullet}$  and  $O_4^{+\bullet}$ , together with small amounts of  $NO^+$ .<sup>7,8</sup> Primary ionization of dry air in the negative ion mode affords  $O_2^{-\bullet}$  and  $O_4^{-\bullet}$ , which in humid air readily form clusters with water.<sup>8</sup> After the introduction of the solvent into an APCI source, further reactions take place including proton transfer, charge transfer, or reactions with electrons. The resulting cocktail of charged species reacts with the analyte molecules via several mechanisms.<sup>9</sup> Transfer of a proton from the reactant ion to an analyte happens when the proton affinity (PA) of the analyte is higher than that of the molecule from which the reactant ion has been formed. Charge transfer occurs when the analyte has lower ionization energy (IE) than the molecule from which the reactant ion has been formed. Charge transfer in the negative ion mode (reaction with  $O_2^{-\bullet}$ ) takes place when the electron affinity (EA) of the analyte is higher than that of molecular oxygen (0.451 eV).<sup>10,11</sup> Some organic compounds with positive EA values may interact with thermal or near-thermal electrons by resonance or dissociative electron capture.<sup>12</sup> The ionization pathways taking place in the positive and negative APCI are summarized, for instance, elsewhere.<sup>9,10</sup> In addition to these processes, various solvent adducts<sup>13</sup> or products of gas-phase chemical reactions<sup>14</sup> can be formed. Despite the complex chemistry, APCI mass spectra are informative and their interpretation is usually simple. Most analytes provide protonated or deprotonated molecules. Compounds with low PA and IE values provide radical cations, which can be utilized for sensitive detection or structure elucidation.<sup>15,16</sup>

APCI-MS is a technique compatible with the high flow rates used in conventional HPLC. Commercial ion sources operate best at approximately 1 mL/min and accept flow rates between hundreds of  $\mu$ L and 2–3 mL/min. Therefore, they cannot be combined with micro- and capillary LC. Several concepts for low flow rate APCI sources have been proposed,<sup>17–22</sup> but additional development is needed to design more robust, sensitive, and reliable devices. There are many technical issues related to APCI source design. Here we would like to focus on the chamber, which isolates the ionization region from the external environment, i.e., ion source housing. While older designs of low flow rate APCI sources were enclosed in a housing,<sup>18,19</sup> papers that are more recent suggest ion sources operating in the open atmosphere.<sup>20–22</sup>

A typical commercial APCI source is maintained at atmospheric pressure and its inner volume is several hundred mL. The housings are commonly made of metallic materials, such as aluminum alloys, and they have a window for easily observing the interior of the ion source. The housing protects users from dangerous and irritating solvent vapors and prevents accidental touching of hot surfaces and metal parts under high voltage. The housing also largely prevents unwanted reactants from entering the ionization zone but, because it does not provide absolute sealing, air components such as water may enter the ion source.<sup>6</sup> The source housing is commonly used also in conventional ESI and atmospheric pressure photoionization (APPI) sources, but it is usually absent in API sources operating at low flow rates. For instance, the ionization regions of nano- or microelectrospray sources are only lightly protected to prevent an electric shock hazard. Most ambient ionization procedures are carried out in the open atmosphere, without any housing, for instance, desorption electrospray (DESI),<sup>23</sup> desorption atmospheric pressure photoionization (DAPPI),<sup>24</sup> or desorption atmospheric pressure chemical ionization (DAPCI).<sup>25</sup>

In this work, we discuss the importance of the ion source housing for APCI operated at  $\mu$ L/min flow rates. Mass spectra recorded using two APCI sources were compared. The sources were virtually identical, with the exception of the ion source housing, which was present or absent. Selected analytes dissolved in solvents of various polarities were used to study gas-phase processes taking place in the enclosed and open APCI sources.

## 2 | EXPERIMENTAL

### 2.1 | Chemicals

Pyrene (98%), squalene ( $\geq 98\%$ ), tetradec-1-yne ( $\geq 97\%$ ), palmitoyl oleate (99%), (2,2,6,6-tetramethylpiperidin-1-yl)oxyl (TEMPO; 98%), picric acid ( $\geq 98\%$ ), 2-hydroxy-5-nitrobenzoic acid (99%), 4-hydroxyaniline, (>98%), *N*-(4-hydroxyphenyl)acetamide (paracetamol;  $\geq 98.0\%$ ), 4-amino-*N*-(1,3-thiazol-2-yl)benzenesulfonamide (sulfathiazole;  $\geq 98\%$ ), carbon disulfide (anhydrous,  $\geq 99\%$ ), ethyl acetate ( $\geq 99.7\%$ ), and *n*-hexane ( $\geq 99.0\%$ ) were purchased from Sigma-Aldrich (St Louis, MO, USA). Trielaidin (>99%) was obtained from Nu-Chek Prep (Elysian, MN, USA). Tetradecan-2-one was prepared from tetradec-1-ene as described in the supporting information. Tetradecanal synthesized by pyridinium chlorochromate oxidation of tetradecan-1-ol was kindly provided by Dr Pavlína Kyjaková (IOCB Prague, Czech Republic). Methanol (gradient grade for LC) and toluene ( $\geq 99.9\%$ ) were from Merck (Darmstadt, Germany). Acetonitrile ( $\geq 99.9\%$ ) was purchased from VWR Chemicals (Radnor, PA, USA). Chloroform (p.a., stabilized with 1% of ethanol) from Penta (Prague, Czech Republic) was purified to remove the stabilizer and water residues. It was shaken three times with 1/10 vol. of sulfuric acid, washed with water, dried over calcium chloride, and distilled. Both deuterium oxide (99.9% D) and chloroform-d (99.8% D) were purchased from Euriso-top (Saint-Aubin, France). Water was prepared using a Milli-Q integral system (Merck Millipore, Burlington, MA, USA). The

analyte solutions were prepared at the concentration of 100  $\mu\text{mol/L}$  with the following exceptions: TEMPO, squalene, and trielaidin (50  $\mu\text{mol/L}$ ), picric and 2-hydroxy-5-nitrobenzoic acid (300  $\mu\text{mol/L}$ ) and tetradec-1-yne and 4-hydroxyaniline (1 mg/mL). Gaseous nitrogen ( $\geq 99.999\%$   $\text{N}_2$ ,  $\leq 3$  ppmv  $\text{O}_2$ ,  $\leq 2$  ppmv  $\text{H}_2\text{O}$ ,  $\leq 0.2$  ppmv  $\text{C}_m\text{H}_n$ ) and synthetic air (5.0, hydrocarbon free, 79.5%  $\text{N}_2$ , 20.5%  $\text{O}_2$ ,  $\leq 5$  ppmv  $\text{H}_2\text{O}$ ,  $\leq 0.5$  ppmv  $\text{CO}_2$ ), both from Messer (Bad Soden, Germany), were used for sample nebulization.

### 2.1.1 | Safety consideration

The low autoignition temperature of carbon disulfide (90°C) may cause spontaneous ignition of its vapors leaving the APCI sprayer, especially at higher liquid flows and high probe temperatures in the open ion source.

## 2.2 | LCQ Fleet mass spectrometer

The low-resolution spectra were recorded with an LCQ Fleet ion-trap mass spectrometer (Thermo Fisher Scientific, Waltham, MA, USA). The instrument was operated either with the Ion Max-S API source fitted with the APCI probe (both from Thermo Fisher Scientific), hereafter referred to as the enclosed ion source, or with the same APCI source lacking the source housing (hereafter referred to as the open ion source). The Ion Max-S API consisted of a metal housing, which defined the internal volume of the source (approximately 475 mL). The angle of the probe was approximately 60° relative to the inlet capillary, and the distance between the probe and the inlet capillary was 13 mm. The corona discharge needle was mounted inside the ion source housing slightly off-axis, 6 mm from the inlet capillary and 10 mm from the probe. The pressure in the ion source housing was not measured, but probably remained at the atmospheric level because the source drain was open to the atmosphere.

The open ion source was built on a platform consisting of a profiled aluminum flange for attaching the entire device to the mass spectrometer and two steel rods for mounting a holder for a corona discharge needle on them. The probe was fixed in a clamp attached to a retort stand. The positions of the probe and the corona discharge needle (angles, distances) were carefully adjusted to be the same as in the enclosed ion source. The sheath and auxiliary gases (nitrogen in most cases) for the probe were taken from hose connectors located on the front panel of the LCQ Fleet instrument. The high voltage connector on the front panel of the instrument was used to power the corona discharge. The probe heater was powered from the Ion Max-S API source (unmounted, placed beside the spectrometer), which was connected to the front panel of the instrument using a cable with 15-pin D-SUB male/female connector. Photographs of the open ion source are provided in Figure S1 (supporting information). The open ion source was fully controlled from Xcalibur software (Thermo Fisher Scientific) in the same way as the enclosed ion source.

A cross-sectional view of the commercial APCI probe used in both ion sources can be found in a technical data sheet from Thermo Fisher Scientific.<sup>26</sup> The ion source parameters (temperatures, voltages) were manually optimized for each compound separately. For a given compound, the same parameters were used in both the open and the enclosed ion sources. The range of settings was as follows: capillary temperature 150–300°C, vaporizer temperature 250–300°C, corona discharge current 1.5–3.0  $\mu\text{A}$  for positive ions and 7.0  $\mu\text{A}$  for negative ions, nitrogen sheath gas flow rate 20–30 a.u. (11–14 L/s), nitrogen auxiliary gas flow rate 5–10 a.u. (4–6 L/s), capillary voltage 4–9 V for positive ions and –12 V for negative ions, and tube lens voltage 55–80 V for positive ions and –56 V for negative ions. The flow rates of gases were set in arbitrary units (a.u.); the corresponding volumetric flow rates were determined experimentally, see Figure S2 (supporting information). The samples were infused into the ion sources using a syringe pump operated at 10  $\mu\text{L}/\text{min}$ , which was a significantly lower flow rate than the optimum values recommended by the manufacturer (0.1–2 mL/min).<sup>26</sup> Data were evaluated using Xcalibur software (Thermo Fisher Scientific).

## 2.3 | LTQ Orbitrap XL mass spectrometer

High-resolution data were recorded using an LTQ Orbitrap XL mass spectrometer (Thermo Fisher Scientific) equipped with an Ion Max API source (i.e., an enclosed ion source) and operated at the same conditions as described for the LCQ Fleet.

## 2.4 | Mass spectrometry in the presence of D<sub>2</sub>O

The effect of moisture in APCI sources was probed with D<sub>2</sub>O. In the case of the open ion source, a 10-mL beaker with 8 mL of D<sub>2</sub>O was placed close to the inlet capillary of the mass spectrometer. Dry nitrogen gas flowing at 275 mL/min was bubbled through D<sub>2</sub>O to enhance the evaporation. In the case of the enclosed ion source, a small gas bubbler with 2.5 mL of D<sub>2</sub>O or H<sub>2</sub>O was connected to a Teflon tube with sheath gas. Prior to the introduction of the sample, D<sub>2</sub>O or H<sub>2</sub>O vapors were introduced into the APCI sources for 5 min.

## 2.5 | Temperature measurement inside the ion sources

The temperature of vapors inside the ion sources was measured using a Voltcraft IR 1200-50D thermometer equipped with a Type K chromel-alumel thermocouple (Conrad Electronic SE, Hirschau, Germany). Before the measurement, the corona discharge needle was removed and the sensor was placed inside the ion source, about 7 mm from the inlet capillary. The vaporizer and heated capillary temperatures were set at 250°C and 150°C, respectively. The temperature was recorded after 60 min of continuous ion source operation.

### 3 | RESULTS AND DISCUSSION

#### 3.1 | Positive ion mode: Protonation vs charge transfer

The effect of the ion source housing was evaluated using the products of the chemical reactions taking place in the ion sources. The first experiments were performed with pyrene. Polycyclic aromatic hydrocarbons are known to provide both protonated molecules and molecular ions in APCI, depending on the experimental conditions.<sup>27</sup> Therefore, the relative proportion of  $[M + H]^+$  ( $m/z$  203.1) and  $M^{+\bullet}$  ( $m/z$  202.1) can be used to monitor proton and charge transfer processes in the ion source. Pyrene dissolved in toluene was introduced at 10  $\mu\text{L}/\text{min}$  and 1 mL/min into the enclosed and open ion sources. Several settings of the sheath and auxiliary gases (nitrogen) were used to cover a wide range of conditions typically used at low and high flow rates. Histograms in Figure 1 show that the ionization of pyrene by charge transfer ( $m/z$  202.1,  $[M]^{+\bullet}$ ) prevailed over the formation of the protonated molecule ( $m/z$  203.1,  $[M + H]^+$ ) in the enclosed ion source at all conditions; the  $[M + H]^+ / [M]^{+\bullet}$  intensity ratios were less than one. The results for the open ion source were different. While charge transfer remained the dominant process at 1 mL/min, protonation prevailed at 10  $\mu\text{L}/\text{min}$  and the intensity ratio increased above one. The gas-phase ionization processes almost certainly changed due to the presence of other reactants such as water in the ion source. It is known that momentum transfer from the surrounding air to the nebulizer jet occurs, taking air constituents into the corona discharge region.<sup>28</sup> Since the volume of solvent vapors was small compared with the volume of nitrogen (see Table S1, supporting information), the amount of air drawn into the jet was similar at both flow rates (at the same nebulizer and auxiliary gas settings). However, the relative concentration of the solvent (toluene) in the jet was 100 $\times$  higher at 1 mL/min compared with 10  $\mu\text{L}/\text{min}$ . Therefore, we assume that the different ionization of pyrene at high and low flow rates stemmed from different

toluene/water ratios in the jet. To confirm the hypothesis that water is responsible for the enhanced protonation at the low flow rate, light and heavy water vapors were introduced into the enclosed ion source. Almost complete protonation or deuteration of pyrene was observed (Figures 2A–2C). In addition, blank APCI spectra recorded in the open ion source without any solvent showed the protonated water dimer at  $m/z$  37.0 together with protonated acetonitrile and acetone (from the laboratory environment) at  $m/z$  42.0 and 59.0, respectively. These ions were almost absent in the enclosed ion source (Figure S3, supporting information). Protonated water could not be detected since the instrument recorded ions from  $m/z$  20. It was concluded that water and possibly traces of common solvents in the external air were responsible for protonation of pyrene in the open ion source at 10  $\mu\text{L}/\text{min}$ . It can be summarized that the effect of ambient air on APCI processes is more pronounced at low flow rates than under conventional conditions.

The impact of ion source housing on the ionization processes was studied at the flow rate of 10  $\mu\text{L}/\text{min}$  in a systematic way. Mass spectra of squalene, pyrene, TEMPO, paracetamol, and sulfathiazole dissolved in various solvents were recorded. The relative proportions of proton transfer ( $[M + H]^+$ ) and charge transfer ( $M^{+\bullet}$ ) ions formed in the enclosed and open sources are given in Table 1; selected mass spectra including the spectra of solvents can be found in Figures S4 and S5 (supporting information). As expected, the analytes were completely or almost completely protonated in methanol, regardless of the presence or absence of the housing (except for squalene, which is insoluble in methanol). The PA of methanol is sufficiently low to ensure efficient proton transfer and any further protonation with water was thus not manifested. When dissolved in toluene, carbon disulfide or chloroform, the analytes were ionized differently in the enclosed and open ion sources (except for paracetamol and sulfathiazole, which were insoluble in these solvents). While protonated molecules dominated in the open ion source, the enclosed source spectra exhibited mostly molecular ions, which were readily formed by charge transfer reactions because the IE values of the

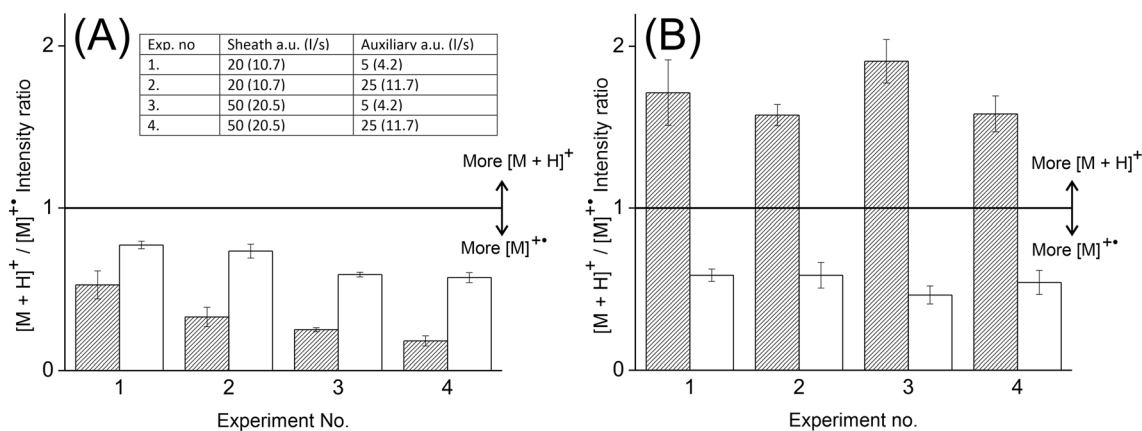


**FIGURE 1** Bar graphs showing intensity ratios of pyrene protonated molecule ( $[M + H]^+$ ;  $m/z$  203.1) and molecular ion ( $M^{+\bullet}$ ;  $m/z$  202.1). Pyrene was dissolved in toluene (25  $\mu\text{mol}/\text{L}$ ) and delivered at 10  $\mu\text{L}/\text{min}$  (hatched bars) and 1 mL/min (empty bars) into the A, enclosed and B, open APCI sources. The  $[M + H]^+$  intensities were corrected for the  $^{13}\text{C}$  isotope of  $M^{+\bullet}$ . Data represent averages of three measurements and the error bars describe standard deviations

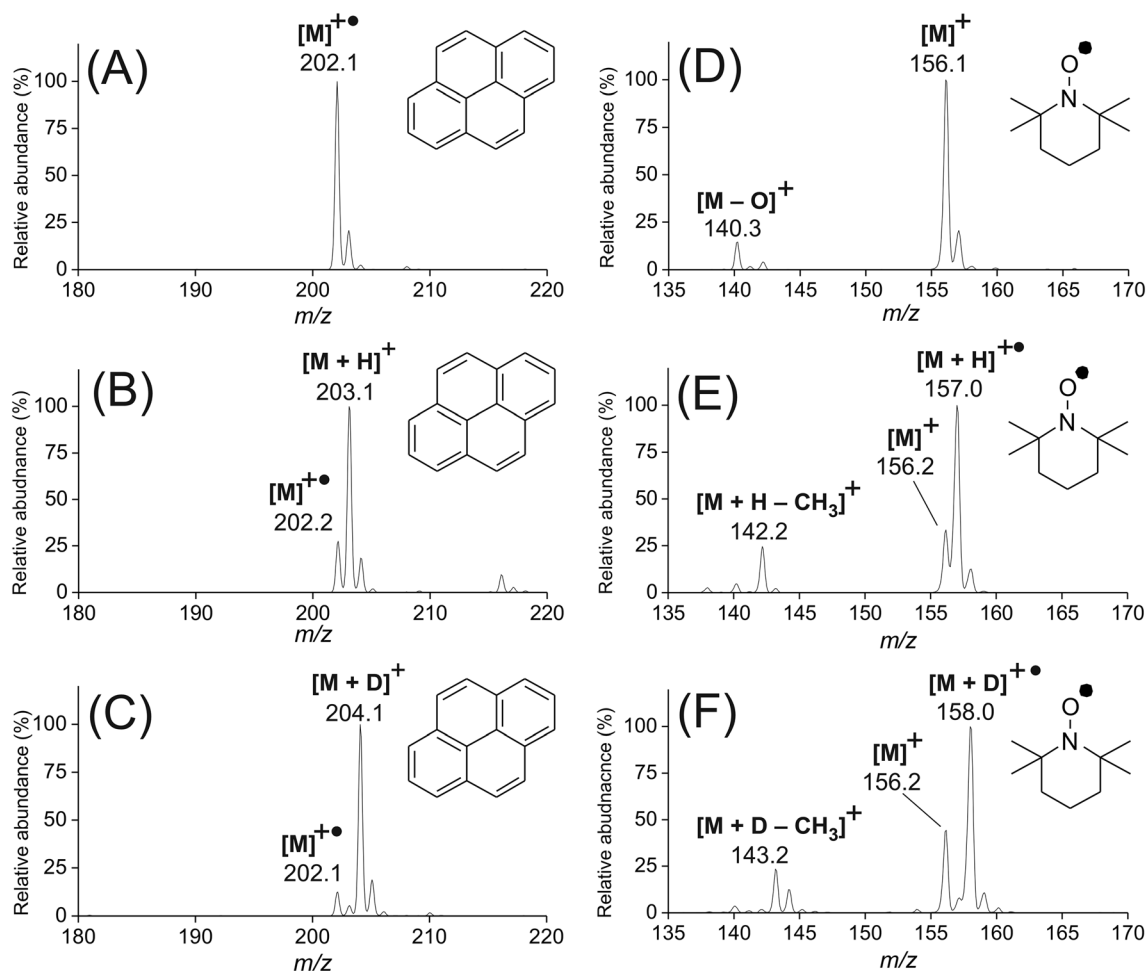


**FIGURE 2** APCI+ mass spectra of pyrene dissolved in chloroform (100  $\mu\text{mol/L}$ ) recorded in the enclosed ion source operated with A, dry nitrogen; B, nitrogen with  $\text{H}_2\text{O}$  vapors; and C, nitrogen with  $\text{D}_2\text{O}$  vapors as nebulizer gas. APCI+ mass spectra of TEMPO dissolved in carbon disulfide (50  $\mu\text{mol/L}$ ) recorded in the enclosed ion source operated with D, dry nitrogen; E, nitrogen with  $\text{H}_2\text{O}$  vapors; and F, nitrogen with  $\text{D}_2\text{O}$  vapors as nebulizer gas. The flow rate was 10  $\mu\text{L/min}$

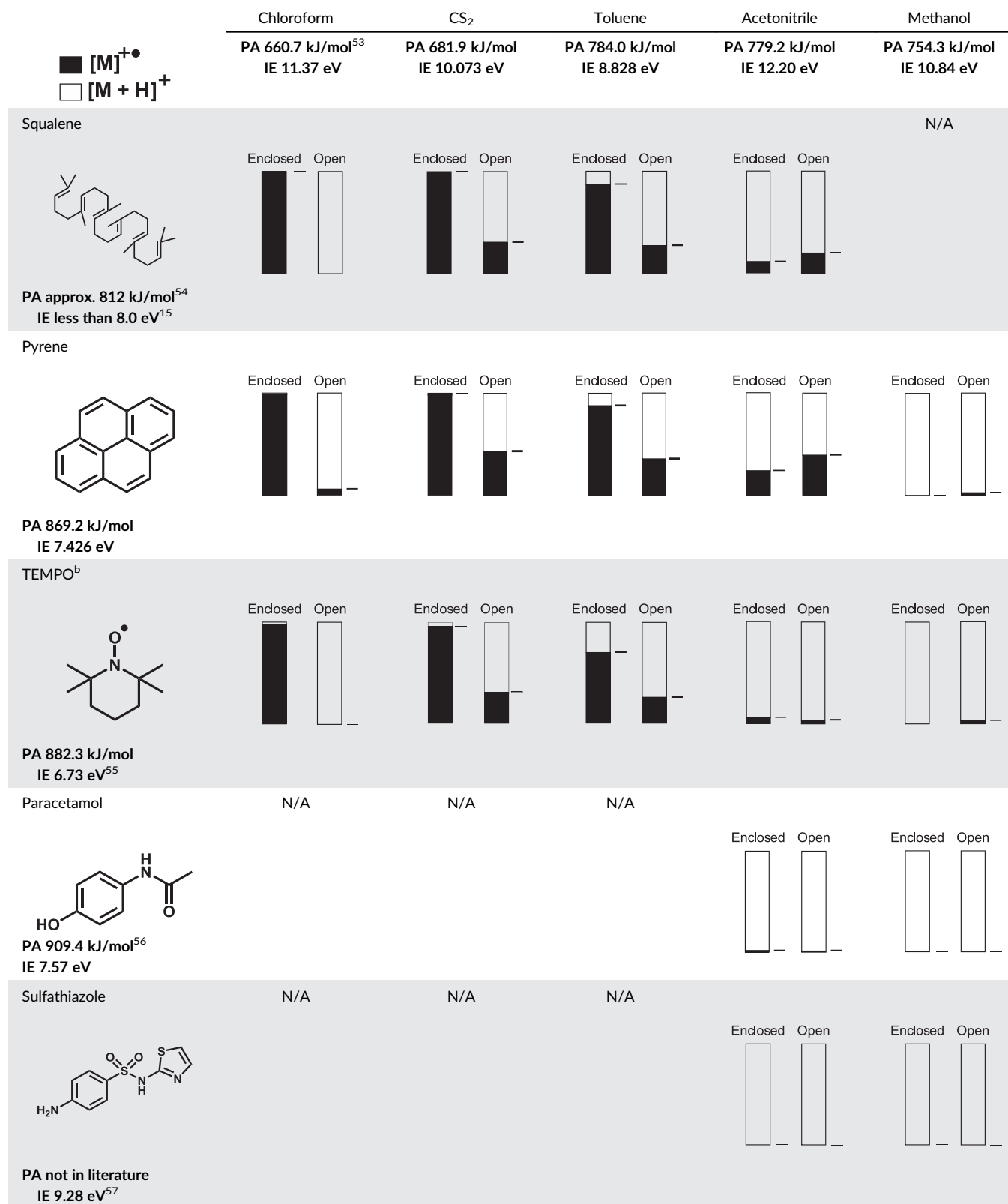
analytes are lower than those of the solvents. Protonation in the open ion source was explained by the presence of water from the surrounding air. As with pyrene, the introduction of  $\text{H}_2\text{O}$  or  $\text{D}_2\text{O}$  caused protonation or deuteration of TEMPO in the enclosed ion source (Figures 2D–2F). The  $\text{M}^+$  peak of TEMPO formed by charge transfer did not disappear completely, probably because of the low IE of this compound.

All the analytes were protonated in acetonitrile, but both hydrocarbons (squalene and pyrene) showed also significant amounts of molecular ions. Surprisingly, the open ion source provided more  $\text{M}^{+\bullet}$  for the hydrocarbons than the enclosed one. When we replaced the nebulizer nitrogen with dry synthetic air, pyrene provided almost exclusively radical cations (Figure 3). The APCI mass spectrum of acetonitrile showed radical species  $\text{CH}_3\text{CN}^{+\bullet}$ ,  $[(\text{CH}_3\text{CN})_2]^{+\bullet}$ , and  $[(\text{CH}_3\text{CN})_3]^{+\bullet}$ , which were not formed in nitrogen (Figure S6, supporting information). These ions were previously reported by Kolakowski et al.,<sup>29</sup> who suggested that these ions were formed by charge transfer reaction with oxygen, which has a lower IE than nitrogen (IE ( $\text{O}_2$ ) = 12.07 eV, IE ( $\text{N}_2$ ) = 15.58 eV<sup>30</sup>). Thus, increased

formation of hydrocarbon radical cations could be attributed to charge transfer reactions with acetonitrile-related radical ions produced by the action of oxygen in the open ion source.

### 3.2 | Negative ion mode: Deprotonation vs electron capture

Negative ions are formed in APCI by deprotonation, dissociative or non-dissociative electron capture, or anion addition.<sup>13</sup> Since all these reactions can be observed with nitroaromatic compounds,<sup>31</sup> picric acid and 2-hydroxy-5-nitrobenzoic acid were selected for the experiments. The mass spectra of 2-hydroxy-5-nitrobenzoic acid dissolved in methanol showed a deprotonated molecule at  $m/z$  182.0, accompanied by a  $\text{CO}_2$  loss fragment ion at  $m/z$  138.1 (Figure 4). The enclosed ion source spectra additionally displayed  $m/z$  166.0 consistent with  $[\text{M} - \text{OH}]^-$  (Figure 4A). Similarly, picric acid in methanol provided an  $[\text{M} - \text{OH}]^-$  ion at  $m/z$  212.1 at a much higher intensity in the enclosed ion source (cf. Figures 4C and 4D). Tandem

**TABLE 1** Relative intensities of radical cations and protonated molecules of the tested compounds formed in APCI at 10  $\mu\text{L}/\text{min}$  flow rate. The analytes were dissolved in 100% solvents<sup>a</sup>

<sup>a</sup>Data are averages for four consecutive measurements; standard deviation values are expressed by the thickness of a short line next to each histogram. The intensities of the  $[\text{M} + \text{H}]^+$  ion were corrected for the <sup>13</sup>C isotope of  $\text{M}^{+\bullet}$ . N/A means that the chemical was not sufficiently soluble or ionized in the particular solvent. If not stated otherwise, PA and IE values were taken from the NIST Chemistry WebBook.<sup>30</sup>

<sup>b</sup>Since TEMPO is a radical itself, the black color represents the even-electron cation  $\text{M}^+$  ( $m/z$  156.1), while the white color corresponds to the odd-electron ion  $[\text{M} + \text{H}]^{+\bullet}$  ( $m/z$  157.0).

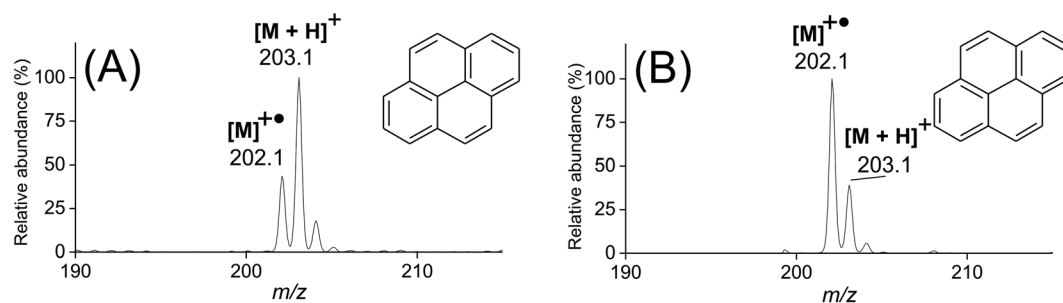


**FIGURE 3** APCI+ mass spectra of pyrene dissolved in acetonitrile (100  $\mu\text{mol/L}$ ) recorded in the enclosed ion source operated with A, dry nitrogen and B, dry synthetic air as nebulizer gas. The flow rate was 10  $\mu\text{L/min}$

mass spectrometry (MS/MS) experiments showed that the  $[\text{M} - \text{OH}]^-$  ions did not originate from collision activation of deprotonated molecules (Figures S7a and 7b, supporting information), but they could be obtained from  $\text{M}^{\bullet-}$  (Figure S7c, supporting information). Therefore, these ions were created by electron capture accompanied by the elimination of hydroxyl radicals. Very similar mass spectra were recorded for acetonitrile solutions (Figure S8, supporting information). Formation of  $[\text{M} - \text{OH}]^-$  in nitroaromatic compounds has been observed earlier in APCI<sup>31</sup> and thermospray ionization.<sup>32</sup> 2-Hydroxy-5-nitrobenzoic acid and picric acid easily captured electrons due to their high electron affinities (3.06 eV<sup>33</sup> and 3.89 eV,<sup>34</sup> respectively). The lower abundance or even absence of electron capture products in the open ion source can be explained by the presence of oxygen. Due to its positive electron affinity,<sup>11</sup> molecular oxygen depleted the number of free, low-energy electrons by reacting with them upon the formation of superoxide anion  $\text{O}_2^{\bullet-}$ .<sup>35,36</sup> The superoxide radical anion is strongly basic in the gas phase, thus enhancing the deprotonation

of analytes.<sup>37</sup> Blank APCI spectra of laboratory air showed the superoxide anion  $\text{O}_2^{\bullet-}$  at  $m/z$  32.0 (Figure S9, supporting information). Furthermore, the presence of  $\text{O}_2^{\bullet-}$  in the ion source was demonstrated by the reaction with 4-hydroxyaniline. The superoxide anion induces oxidative ionization of some phenolic compounds yielding  $[\text{M} - 2\text{H}]^{\bullet-}$  ions.<sup>38</sup> This ion ( $m/z$  107.2) was indeed observed at high intensity in the open source (Figure 5A), while only a negligible signal of the ion was detected in the enclosed source (Figure 5B). When synthetic air was used as a nebulizer gas, the  $[\text{M} - 2\text{H}]^{\bullet-}$  ion was also observed in the enclosed ion source (Figure 5C). Clearly, oxygen in the APCI source strongly affected the formation of negatively charged ions by suppressing electron capture reactions. The electron capture processes can also be diminished if halogenated solvents with high electron affinities are used.<sup>39</sup> Indeed, no electron capture products were detected for picric acid in chloroform (EA ( $\text{CHCl}_3$ ) = 0.622 eV<sup>30</sup>), even in the enclosed source (Figure S10, supporting information).

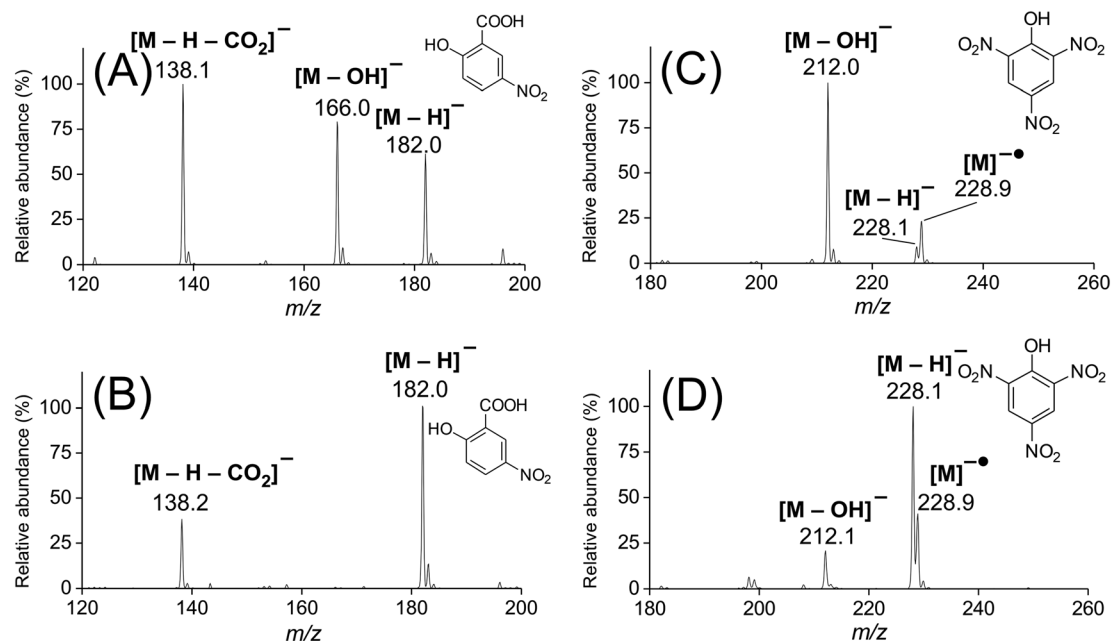


**FIGURE 4** APCI- mass spectra of A, B, 2-hydroxy-5-nitrobenzoic acid and C, D, picric acid dissolved in methanol (300  $\mu\text{mol/L}$ ) and recorded in A, C, the enclosed ion source and B, D, the open ion source operated with dry nitrogen nebulizer gas. The flow rate was 10  $\mu\text{L/min}$



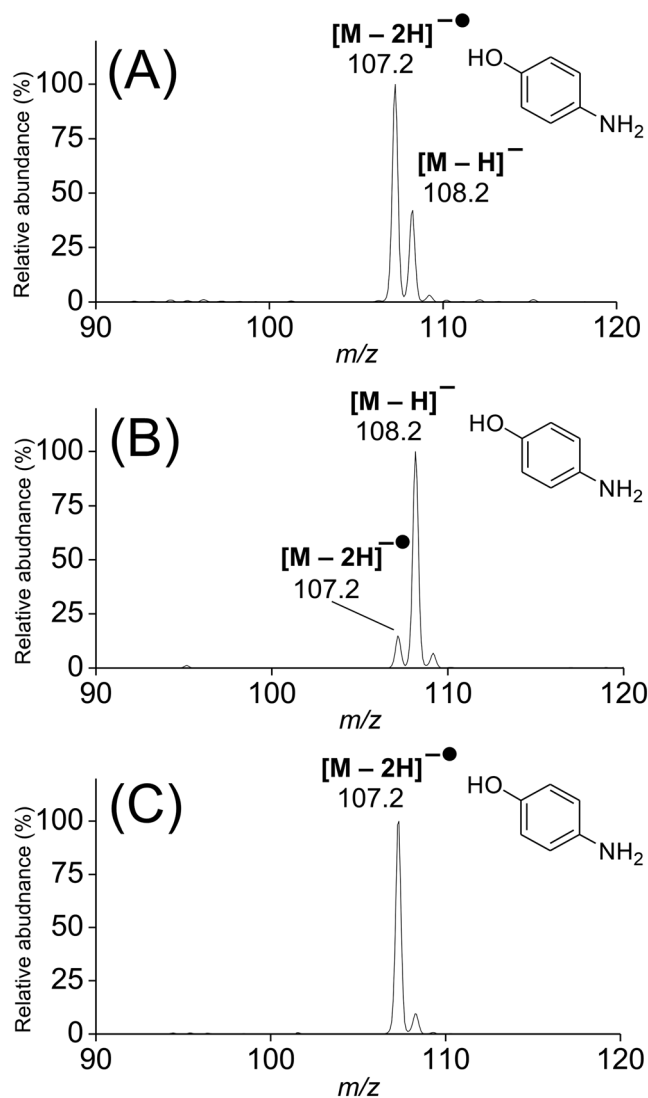


**FIGURE 5** APCI- mass spectra of 4-hydroxyaniline dissolved in methanol (1.0 mg/mL). The spectra were recorded in A, the open and B, the enclosed ion source operated with dry nitrogen as nebulizer gas, and C, in the enclosed ion source with dry synthetic air as nebulizer gas. The flow rate was 10  $\mu\text{L}/\text{min}$

### 3.3 | Hydration of alkynes

Chemical species from laboratory air or contaminated surfaces can enter alternative reaction channels in APCI to form new products. Such ions are usually considered artifacts and they may lead to misinterpretation of MS data. Tetradec-1-yne dissolved in *n*-hexane provided solvent-related adducts (Figure 6). In addition, an ion at  $m/z$  213.2 was formed solely in the open ion source (Figure 6B). Its elemental composition,  $\text{C}_{14}\text{H}_{29}\text{O}^+$  ( $m/z$  213.2210;  $-0.3$  ppm), suggested a product of water addition, probably ketone or aldehyde. The collision-induced dissociation (CID) spectrum of the ion at  $m/z$  213.2 closely resembled that of the synthetic standard of tetradecan-2-one (cf. Figures S11a and S11b, supporting information).

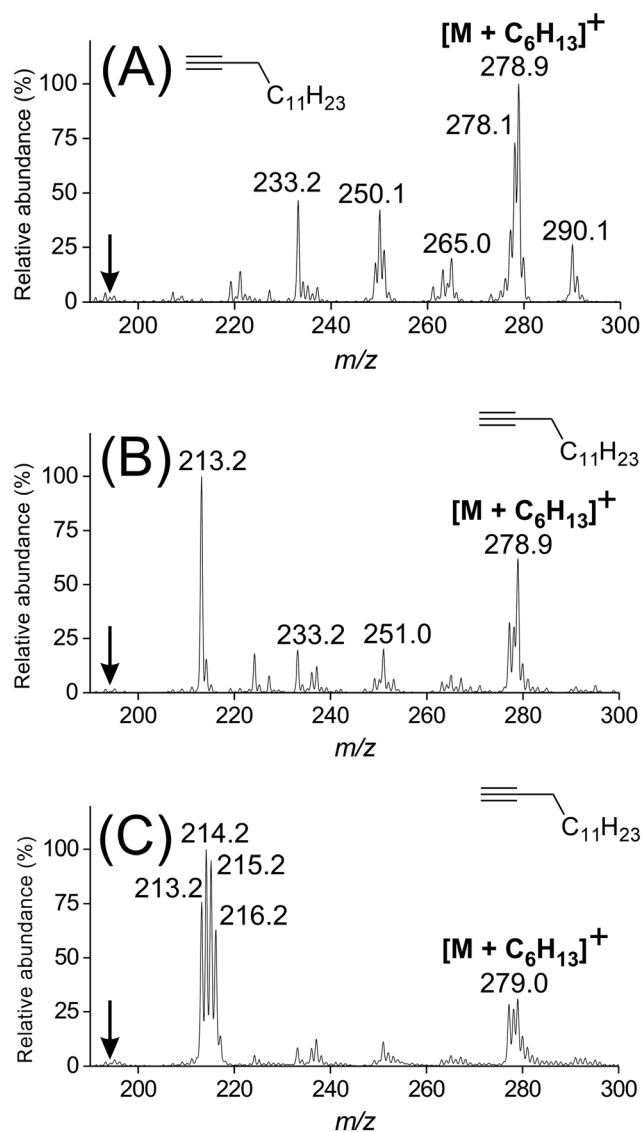


**FIGURE 6** APCI+ mass spectra of tetradec-1-yne dissolved in *n*-hexane (1.0 mg/mL). The spectra were recorded in A, the enclosed and B, the open ion source, and C, in the open ion source where liquid  $\text{D}_2\text{O}$  was allowed to evaporate. Dry nitrogen served as the nebulizer gas and the flow rate was 10  $\mu\text{L}/\text{min}$ . The composition of the adduct ions was deduced from high-resolution data as follows:  $m/z$  233.2 [ $\text{M} + \text{C}_3\text{H}_3$ ] $^+$ ,  $m/z$  251.3 [ $\text{M} + \text{C}_4\text{H}_9$ ] $^+$ ,  $m/z$  265.3 [ $\text{M} + \text{C}_5\text{H}_{11}$ ] $^+$ ,  $m/z$  277.3 [ $\text{M} + \text{C}_6\text{H}_{11}$ ] $^+$ ,  $m/z$  278.3 [ $\text{M} + \text{C}_6\text{H}_{12}$ ] $^{+*}$ ,  $m/z$  279.3 [ $\text{M} + \text{C}_6\text{H}_{13}$ ] $^+$ , and  $m/z$  290.3 [ $\text{M} + \text{C}_7\text{H}_{12}$ ] $^{+*}$ . The arrow shows a theoretical position of [ $\text{M}$ ] $^{+*}$  of tetradec-1-yne

Tetradecanal formation was ruled out because the spectrum did not show the  $\text{C}_n\text{H}_{(2n+1)}\text{O}^+$  series observed in the spectrum of the tetradecanal standard (Figure S11a, supporting information). Moreover, the water loss peak in the aldehyde spectrum was more pronounced than in the ketone spectrum. Therefore, protonated tetradecan-2-one was formed in the open ion source. This is in agreement with condensed phase chemistry, where terminal alkynes react with water to form methyl ketones.<sup>40</sup> To test the hypothesis

that  $m/z$  213.2 was formed by the reaction of tetradec-1-yne with water,  $D_2O$  vapors were introduced into the ion source. While the  $n$ -hexane-related adducts remained at the same  $m/z$  values, new ions were observed at  $m/z$  214.2, 215.2, and 216.2 (Figure 6C). These ions were consistent with  $[M + D]^+$  of tetradecan-2-one, and  $[M + H]^+$  and  $[M + D]^+$  of dideutero-tetradecan-2-one, respectively. This example showed that new compounds (i.e., artifacts) could be created in the open APCI source when the plasma region is exposed to ambient air.

### 3.4 | Addition of $C_3H_5N^{+*}$ to double bonds

Solvent-related adducts may sometimes be useful for structural elucidation. For instance, ions produced in APCI from acetonitrile are used to localize double bonds.<sup>41,42</sup> Unsaturated aliphatic compounds form  $[M + C_3H_5N]^+$ , probably via cycloaddition of  $C_3H_5N^{+*}$  to the C=C bond.<sup>42-44</sup> Upon CID, these ions provide product ions that are indicative of the original double-bond position. We investigated this reaction with palmityl oleate dissolved in acetonitrile/ethyl acetate (99/1, v/v). The expected adduct ( $m/z$  561.3) was formed in the enclosed ion source (Figure 7A) and provided two major CID ions at  $m/z$  194.2 and 448.3 that clearly indicated the  $n$ -9 double bond (Figure 7B). However, the formation of  $[M + C_3H_5N]^+$  was completely suppressed in the open ion source (Figure 7C). Water was not responsible for the suppression because the intensity of  $m/z$  561.3 remained the same even when 20% of water was added to the solvent (Figure S12, supporting information). It turned out that oxygen suppressed the ion formation. When dry synthetic air was

used in the enclosed ion source,  $m/z$  561.3 was not formed at all (Figure 7D). As discussed above, due to its low ionization energy, molecular oxygen probably entered charge transfer processes and thus altered the gas-phase chemistry of acetonitrile.<sup>29</sup> Consequently, the reaction useful for localizing double bonds proceeded only in the enclosed ion source.

### 3.5 | The extent of fragmentation in APCI

Some compounds fragment in APCI. The fragments are considered ionized products of thermal degradation, which takes place in heated nebulizers. For instance, triacylglycerols in APCI easily eliminate fatty acids, which can be used to elucidate their structures without a need for MS/MS.<sup>45-47</sup> Controlled thermal degradation can be utilized as a unique strategy in structural elucidation when common fragmentation techniques fail,<sup>48</sup> but, in most cases, fragment formation is undesirable. The APCI spectra of trielaidin dissolved in acetonitrile provided a protonated molecule at  $m/z$  885.5 and a neutral loss fragment ion at  $m/z$  603.5 ( $[M + H - FA_{18:1}]^+$ ) in both ion sources at 10  $\mu$ L/min, but the fragment ion intensity was significantly higher in the enclosed ion source (cf. Figures 8A and 8B). Since the vaporizer temperatures were set identically, the extent of thermal degradation in the heated probe was considered to be the same in both ion sources. An additional thermal degradation probably occurred after the trielaidin left the heated probe and before it reached the corona discharge region. More energetic  $[M + H]^+$  ions were possibly formed in the enclosed ion source. The internal energies of the ions formed in

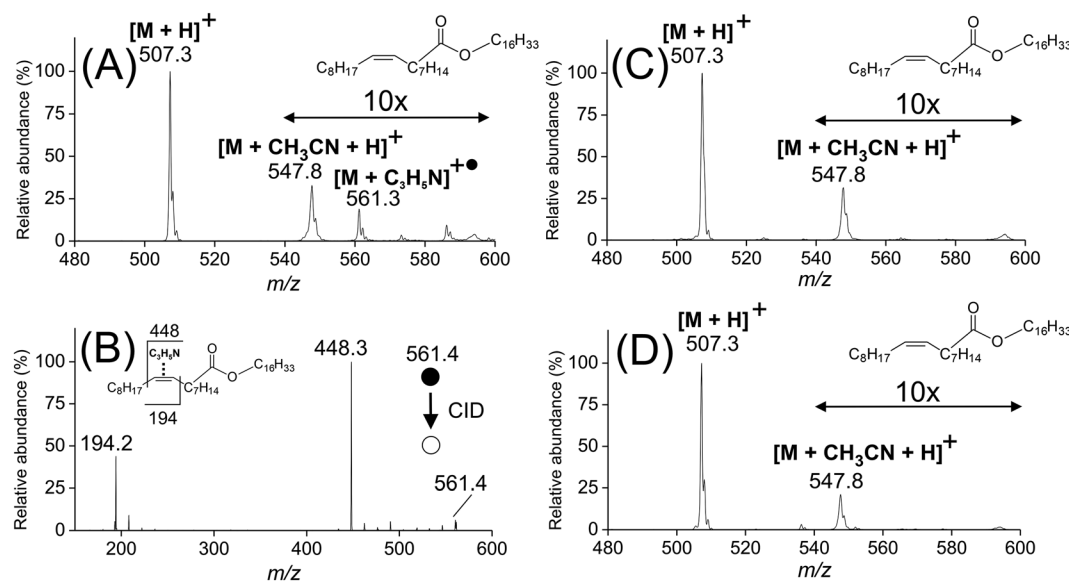


**FIGURE 7** APCI+ mass spectra of A, C, D, palmityl oleate and B, APCI+ CID MS/MS spectrum of palmityl oleate  $[M + C_3H_5N]^+$  ion. Palmityl oleate was dissolved in acetonitrile/ethyl acetate (99:1, v/v) at a concentration of 100  $\mu$ mol/L and delivered into the ion sources at 10  $\mu$ L/min. The spectra were recorded in A, B, the enclosed and C, the open ion source using dry nitrogen as the nebulizer gas and D, in the enclosed ion source with dry synthetic air as the nebulizer gas

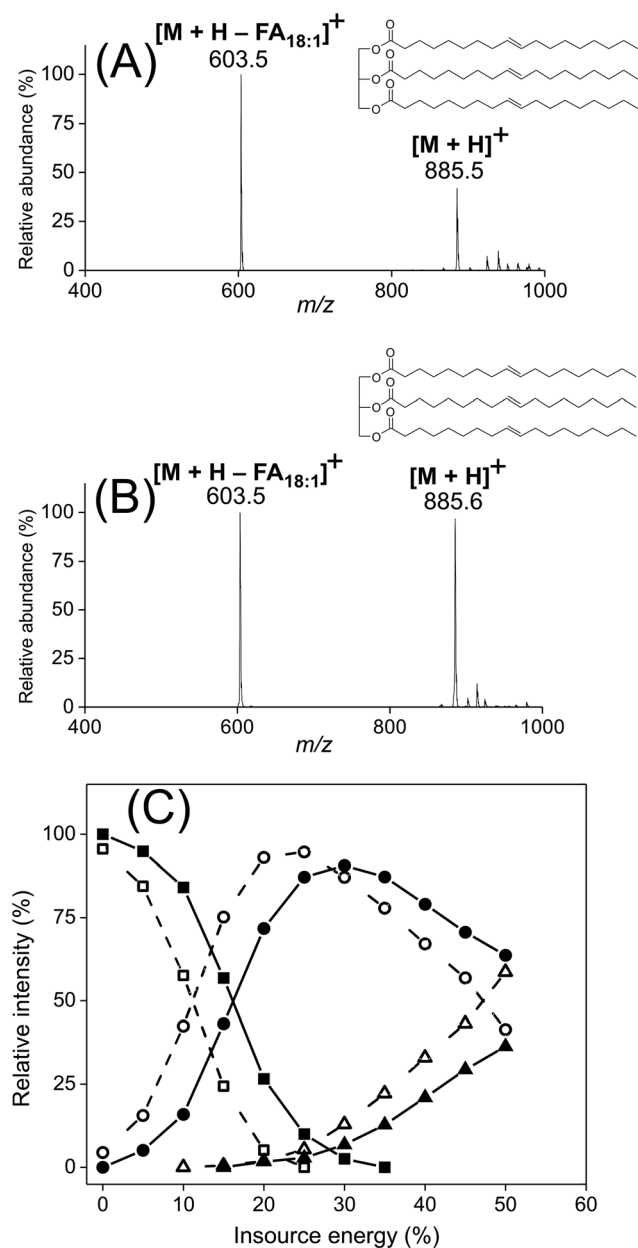


**FIGURE 8** APCI+ mass spectra of trielaidin dissolved in acetonitrile (50  $\mu\text{mol/L}$ ) recorded in A, the enclosed and B, the open ion source using dry nitrogen as the nebulizer gas. C, Breakdown curves of TEMPO dissolved in acetonitrile (50  $\mu\text{mol/L}$ ) obtained by in-source dissociation in the enclosed (dashed line) and open (solid line) ion sources. The symbols correspond to  $m/z$  157.0 (squares),  $m/z$  142.2 (circles), and  $m/z$  109.2 (triangles). The flow rates were 10  $\mu\text{L/min}$

the enclosed and open sources were compared using the acetonitrile solution of TEMPO, which provided protonated molecules in both ion sources with almost no fragmentation (Table 1). The ion energies were assessed from breakdown curves generated by source CID (in-source fragmentation). Protonated TEMPO ( $m/z$  157.0) dissociated to  $m/z$  142.2 (elimination of  $\text{CH}_3^{\bullet}$ ) and  $m/z$  109.2 (loss of  $\text{NH}_2\text{OH}$  from the  $m/z$  142.2 ion).<sup>49</sup> The breakdown curves recorded in the open source were consistently shifted towards higher fragmentation

energies (Figure 8C), which indicated higher internal energy of the ions in the enclosed ion source, consistent with the higher thermal energy of the molecule before ionization. We hypothesized that the nebulizer gas and the probe itself heated up the ion source housing, which radiated heat back to the enclosed ion source interior. Consequently, the molecules gained more internal energy, which resulted in increased thermal degradation and fragmentation. The temperature of the hot vapors inside the ion sources was measured using a digital thermometer. The sensor was placed where the discharge needle tip is normally located. Indeed, the temperature inside the enclosed ion source was about 40°C higher than in the open one (170°C and 130°C in the enclosed and open ion source, respectively, for the vaporizer temperature set to 250°C). Thus, the use of an ion source housing may result in increased fragmentation at a given probe temperature in low flow APCI.

## 4 | CONCLUSIONS

Ionization processes in the open source for APCI operating at a flow rate of 10  $\mu\text{L/min}$  were strongly influenced by ambient air. Water and oxygen entered the reaction sequences, which often led to unwanted or unexpected products and sometimes caused the desired ionization pathways to cease. Undesirable reactions could be avoided by using an enclosed ion source, where the plasma region is protected from external air by a source housing. Preventing outside air from entering the ion source is particularly important for processes leading to or involving odd-electron species. In some cases, the presence of water or oxygen in the open source could be considered beneficial. For example, protonation of some unsaturated or aromatic hydrocarbons in aprotic solvents can be achieved in this way, or the dissociative electron capture products in the negative ion mode can be suppressed. However, even in such cases, the use of the enclosed ion source is recommended. Water or oxygen can be supplied in the mobile phase or nebulizer gas, which provides better control over the reactants and thus ionization processes. Although not discussed in this article, another reason for using the enclosed APCI source is the elimination of negative effects related to ambient airflow. The jet of vapors at low flow rates is affected by draughts, which may have negative consequences on signal stability and reproducibility. The enclosed ion source produced ions with higher internal energy and generated more intense fragments for labile compounds such as triacylglycerols. This was explained by the higher temperature in the ion source interior caused by radiating heat from the hot ion source housing. It could probably be compensated for by lowering the nebulizer temperature or active cooling of the source housing.

The results of this work are also relevant for ambient ionization techniques that are based on chemical ionization like desorption atmospheric pressure chemical ionization (DAPCI),<sup>25,50</sup> atmospheric pressure thermal desorption chemical ionization (APTDCI),<sup>51</sup> or laser desorption atmospheric pressure chemical ionization (LD-APCI).<sup>52</sup> The air components can affect mass spectra in a similar way to that in the open APCI source.

## ACKNOWLEDGEMENTS

Financial support from the Czech Science Foundation (16-01639S) and Charles University in Prague (Project SVV260440) is hereby acknowledged with appreciation.

## ORCID

Josef Cvačka  <https://orcid.org/0000-0002-3590-9009>

## REFERENCES

- Saito Y, Jinno K, Greibrokk T. Capillary columns in liquid chromatography: Between conventional columns and microchips. *J Sep Sci*. 2004;27(17-18):1379-1390. <https://doi.org/10.1002/jssc.200401902>
- Chetwynd AJ, David A. A review of nanoscale LC-ESI for metabolomics and its potential to enhance the metabolome coverage. *Talanta*. 2018;182:380-390. <https://doi.org/10.1016/j.talanta.2018.01.084>
- Moriwaki H. Electrospray ionization mass spectrometric detection of low polar compounds by adding NaAuCl<sub>4</sub>. *J Mass Spectrom*. 2016; 51(11):1096-1102. <https://doi.org/10.1002/jms.3822>
- Tang K, Page JS, Smith RD. Charge competition and the linear dynamic range of detection in electrospray ionization mass spectrometry. *J Am Soc Mass Spectrom*. 2004;15(10):1416-1423. <https://doi.org/10.1016/j.jasms.2004.04.034>
- Schuhmacher J, Zimmer D, Tesche F, Pickard V. Matrix effects during analysis of plasma samples by electrospray and atmospheric pressure chemical ionization mass spectrometry: Practical approaches to their elimination. *Rapid Commun Mass Spectrom*. 2003;17(17):1950-1957. <https://doi.org/10.1002/rcm.1139>
- Klee S, Derpmann V, Wißdorf W, et al. Are clusters important in understanding the mechanisms in atmospheric pressure ionization? Part 1: Reagent ion generation and chemical control of ion populations. *J Am Soc Mass Spectrom*. 2014;25(8):1310-1321. <https://doi.org/10.1007/s13361-014-0891-2>
- Shahin MM. Ionic reactions in corona discharges of atmospheric gases. *Adv. Chem. Series: Chem. React. Electr Discharges*. 1969;80:48-58. <https://doi.org/10.1021/ba-1969-0080.ch004>
- Siegel MW, Fite WL. Terminal ions in weak atmospheric pressure plasmas. Applications of atmospheric pressure ionization to trace impurity analysis in gases. *J Phys Chem*. 1976;80(26):2871-2881. <https://doi.org/10.1021/j100567a013>
- Kostiainen R, Kauppila TJ. Effect of eluent on the ionization process in liquid chromatography-mass spectrometry. *J Chromatogr A*. 2009;1216(4):685-699. <https://doi.org/10.1016/j.chroma.2008.08.095>
- Terrier P, Desmazières B, Tortajada J, Buchmann W. APCI/APPI for synthetic polymer analysis. *Mass Spectrom Rev*. 2011;30(5):854-874. <https://doi.org/10.1002/mas.20302>
- Ervin KM, Anusiewicz I, Skurski P, Simons J, Lineberger WC. The only stable state of O<sub>2</sub><sup>-</sup> is the X<sup>2</sup>Π<sub>g</sub> ground state and it (still!) has an adiabatic electron detachment energy of 0.45 eV. *J Phys Chem AJ. Phys. Chem. A*. 2003;107(41):8521-8529. <https://doi.org/10.1021/jp0357323>
- Carroll DI, Dzidic I, Horning EC, Stillwell RN. Atmospheric pressure ionization mass spectrometry. *Appl Spectrosc Rev*. 1981;17(3):337-406. <https://doi.org/10.1080/05704928108060409>
- McEwen CN, Larsen BS. Ionization mechanisms related to negative ion APPI, APCI, and DART. *J Am Soc Mass Spectrom*. 2009; 20(8):1518-1521. <https://doi.org/10.1016/j.jasms.2009.04.010>
- Song Y, Cooks RG. Atmospheric pressure ion/molecule reactions for the selective detection of nitroaromatic explosives using acetonitrile and air as reagents. *Rapid Commun Mass Spectrom*. 2006;20(20): 3130-3138. <https://doi.org/10.1002/rcm.2714>
- Gao J, Owen BC, Borton DJ II, Jin Z, Kenttämää HI. HPLC/APCI mass spectrometry of saturated and unsaturated hydrocarbons by using hydrocarbon solvents as the APCI reagent and HPLC mobile phase. *J Am Soc Mass Spectrom*. 2012;23(5):816-822. <https://doi.org/10.1007/s13361-012-0347-5>
- Perazzolli C, Mancini I, Graziano G. Benzene-assisted atmospheric-pressure chemical ionization: A new liquid chromatography/mass spectrometry approach to the analysis of selected hydrophobic compounds. *Rapid Commun Mass Spectrom*. 2005;19(4):461-469. <https://doi.org/10.1002/rcm.1807>
- Nyholm LM, Sjöberg PJR, Markides KE. High-temperature open tubular liquid chromatography coupled to atmospheric pressure chemical ionisation mass spectrometry. *J Chromatogr A*. 1996;755(2): 153-164. [https://doi.org/10.1016/S0021-9673\(96\)00609-7](https://doi.org/10.1016/S0021-9673(96)00609-7)
- Takeda S, Tanaka Y, Yamane M, et al. Ionization of dichlorophenols for their analysis by capillary electrophoresis-mass spectrometry. *J Chromatogr A*. 2001;924(1-2):415-420. [https://doi.org/10.1016/S0021-9673\(01\)00899-8](https://doi.org/10.1016/S0021-9673(01)00899-8)
- Tanaka Y, Otsuka K, Terabe S. Evaluation of an atmospheric pressure chemical ionization interface for capillary electrophoresis-mass spectrometry. *J Pharm Biomed*. 2003;30(6):1889-1895. [https://doi.org/10.1016/S0731-7085\(02\)00532-0](https://doi.org/10.1016/S0731-7085(02)00532-0)
- Östman P, Marttila SJ, Kotiaho T, Franssila S, Kostianen R. Microchip atmospheric pressure chemical ionization source for mass spectrometry. *Anal Chem*. 2004;76(22):6659-6664. <https://doi.org/10.1021/ac049345g>
- Vrkoslav V, Rumlová B, Strmeň T, Nekvasilová P, Šulc M, Cvačka J. Applicability of low-flow atmospheric pressure chemical ionization and photoionization mass spectrometry with a microfabricated nebulizer for neutral lipids. *Rapid Commun Mass Spectrom*. 2018; 32(8):639-648. <https://doi.org/10.1002/rcm.8086>
- Strmeň T, Vrkoslav V, Pačes O, Cvačka J. Evaluation of an ion source with a tubular nebulizer for microflow atmospheric pressure chemical ionization. *Monatsh Chem*. 2018;149(6):987-994. <https://doi.org/10.1007/s00706-018-2172-4>
- Takáts Z, Wiseman JM, Gologan B, Cooks RG. Mass spectrometry sampling under ambient conditions with desorption electrospray ionization. *Science*. 2004;306(5695):471-473. <https://doi.org/10.1126/science.1104404>
- Haapala M, Pol J, Saarela V, et al. Desorption atmospheric pressure photoionization. *Anal Chem*. 2007;79(20):7867-7872. <https://doi.org/10.1021/ac071152g>
- Takats Z, Cotte-Rodriguez I, Talaty N, Chen H, Cooks RG. Direct, trace level detection of explosives on ambient surfaces by desorption electrospray ionization mass spectrometry. *Chem Commun*. 2005;15: 1950-1952. <https://doi.org/10.1039/b418697d>
- Thermo Fisher Scientific Inc., Ion Max and Ion Max-S API Source, Hardware Manual, 97055-97044 Revision D. November 2008, p. 60
- Marvin CH, Smith RW, Bryant DW, McCarty BE. Analysis of high-molecular-mass polycyclic aromatic hydrocarbons in environmental samples using liquid chromatography-atmospheric pressure chemical ionization mass spectrometry. *J Chromatogr A*. 1999;863(1):13-24. [https://doi.org/10.1016/S0021-9673\(99\)00955-3](https://doi.org/10.1016/S0021-9673(99)00955-3)
- Covey TR, Thomson BA, Schneider BB. Atmospheric pressure ion sources. *Mass Spectrom Rev*. 2009;28(6):870-897. <https://doi.org/10.1002/mas.20246>
- Kolakowski BM, Grossert JS, Ramaley L. Studies on the positive-ion mass spectra from atmospheric pressure chemical ionization of gases and solvents used in liquid chromatography and direct liquid injection. *J Am Soc Mass Spectrom*. 2004;15(3):311-324. <https://doi.org/10.1016/j.jasms.2003.10.019>
- Linstrom PJ, Mallard WG, eds. *NIST Chemistry WebBook, NIST Standard Reference Database Number 69*, December 2018, National Institute of Standards and Technology, Gaithersburg MD, 20899 (<http://webbook.nist.gov>)

31. Holmgren E, Carlsson H, Goede P, Crescenzi C. Determination and characterization of organic explosives using porous graphitic carbon and liquid chromatography-atmospheric pressure chemical ionization mass spectrometry. *J Chromatogr AJ. Chromatogr. A.* 2005;1099(1-2):127-135. <https://doi.org/10.1016/j.chroma.2005.08.088>
32. Astratov M, Preiß A, Levsen K, Wünsch G. Identification of pollutants in ammunition hazardous waste sites by thermospray HPLC/MS. *Int J Mass Spectrom Ion Processes.* 1997;167/168:481-502. [https://doi.org/10.1016/S0168-1176\(97\)00089-X](https://doi.org/10.1016/S0168-1176(97)00089-X)
33. Karthick T, Balachandran V, Perumal S, Nataraj A. Spectroscopic studies, HOMO-LUMO and NBO calculations on monomer and dimer conformer of 5-nitrosalicylic acid. *J Mol Struct.* 2011;1005(1-3):192-201. <https://doi.org/10.1016/j.molstruc.2011.08.050>
34. Xu B, Wu X, Li H, Tong H, Wang L. Selective detection of TNT and picric acid by conjugated polymer film sensors with donor-acceptor architecture. *Macromolecules.* 2011;44(13):5089-5092. <https://doi.org/10.1021/ma201003f>
35. Horning EC, Carroll DI, Dzidic I, Lin S-N, Stillwell RN, Thenot J-T. Atmospheric pressure ionization mass spectrometry: Studies of negative ion formation for detection and quantification purposes. *J Chromatogr.* 1977;142(NOV):481-495. [https://doi.org/10.1016/S0021-9673\(01\)92061-8](https://doi.org/10.1016/S0021-9673(01)92061-8)
36. Hayen H, Jachmann N, Vogel M, Karst U. LC-electron capture-APCI(2)-MS determination of nitrobenzoxadiazole derivatives. *Analyst.* 2003;128(11):1365-1372. <https://doi.org/10.1039/b308752b>
37. Dzidic I, Carroll DI, Stillwell RN, Horning EC. Gas phase reactions. Ionization by proton transfer to superoxide anions. *J Am Chem Soc.* 1974;96(16):5258-5259. <https://doi.org/10.1021/ja00823a045>
38. Hassan I, Pavlov J, Errabelli R, Attygalle AB. Oxidative ionization under certain negative-ion mass spectrometric conditions. *J Am Soc Mass Spectrom.* 2017;28(2):270-277. <https://doi.org/10.1007/s13361-016-1527-5>
39. Kauppila TJ, Kotiaho T, Kostianen R, Bruins AP. Negative ion-atmospheric pressure photoionization-mass spectrometry. *J Am Soc Mass Spectrom.* 2004;15(2):203-211. <https://doi.org/10.1016/j.jasms.2003.10.012>
40. Hintermann L, Labonne A. Catalytic hydration of alkynes and its application in synthesis. *Synthesis.* 2007;8(8):1121-1150. <https://doi.org/10.1055/s-2007-966002>
41. Xu Y, Brenna TJ. Atmospheric pressure covalent adduct chemical ionization tandem mass spectrometry for double bond localization in monoene- and diene-containing triacylglycerols. *Anal Chem.* 2007;79(6):2525-2536. <https://doi.org/10.1021/ac062055a>
42. Vrkoslav V, Háková M, Pecková K, Urbanová K, Cvačka J. Localization of double bonds in wax esters by high-performance liquid chromatography/atmospheric pressure chemical ionization mass spectrometry utilizing the fragmentation of acetonitrile-related adducts. *Anal Chem.* 2011;83(8):2978-2986. <https://doi.org/10.1021/ac1030682>
43. Vrkoslav V, Cvačka J. Identification of the double-bond position in fatty acid methyl esters by liquid chromatography/atmospheric pressure chemical ionization mass spectrometry. *J Chromatogr A.* 2012;1259:244-250. <https://doi.org/10.1016/j.chroma.2012.04.055>
44. Háková E, Vrkoslav V, Míková R, Schwarzová-Pecková K, Bosáková Z, Cvačka J. Localization of double bonds in triacylglycerols using high-performance liquid chromatography/atmospheric pressure chemical ionization ion-trap mass spectrometry. *Anal Bioanal Chem.* 2015;407(17):5175-5188. <https://doi.org/10.1007/s00216-015-8537-1>
45. Holčápek M, Jandera P, Zderadička P, Hrubá L. Characterization of triacylglycerol and diacylglycerol composition of plant oils using high-performance liquid chromatography-atmospheric pressure chemical ionization mass spectrometry. *J Chromatogr A.* 2003;1010(2):195-215. [https://doi.org/10.1016/S0021-9673\(03\)01030-6](https://doi.org/10.1016/S0021-9673(03)01030-6)
46. Byrdwell WC. Qualitative and quantitative analysis of triacylglycerols by atmospheric pressure ionization (APCI and ESI) mass spectrometry techniques. In: Byrdwell WC, ed. *Modern Methods for Lipid Analysis by Liquid Chromatography/Mass Spectrometry and Related Techniques 1.* New York, NY: AOCS Press; 2005:298-412.
47. Cvačka J, Hovorka O, Jiroš P, Kindl J, Stránský K, Valterová I. Analysis of triacylglycerols in fat body of bumblebees by chromatographic methods. *J Chromatogr A.* 2006;1101(1-2):226-237. <https://doi.org/10.1016/j.chroma.2005.10.001>
48. Kalužiková A, Vrkoslav V, Harazim E, et al. Cholesteryl esters of  $\omega$ -(O-acyl)-hydroxy fatty acids in vernix caseosa. *J Lipid Res.* 2017;58(8):1579-1590. <https://doi.org/10.1194/jlr.M075333>
49. Jahangiri S, Timerghazin QK, Jiang H, Peslherbe GH, English AM. Dramatic C-C bond activation on protonation of the persistent nitroxyl radical TEMPO\*. *Int J Mass Spectrom.* 2018;429(SI):182-188. <https://doi.org/10.1016/j.ijms.2017.08.007>
50. Chen HW, Zheng J, Zhang X, Luo MB, Wang ZC, Qiao XL. Surface desorption atmospheric pressure chemical ionization mass spectrometry for direct ambient sample analysis without toxic chemical contamination. *J Mass Spectrom.* 2007;42(8):1045-1056. <https://doi.org/10.1002/jms.1235>
51. Corso G, D'Apolito O, Garofalo D, Paglia G, Dello RA. Profiling of acylcarnitines and sterols from dried blood or plasma spot by atmospheric pressure thermal desorption chemical ionization (APTDCI) tandem mass spectrometry. *Biochim Biophys Acta Mol Cell Biol Lipids.* 2011;1811(11):669-679. <https://doi.org/10.1016/j.bbalip.2011.05.009>
52. Coon JJ, McHale KJ, Harrison WW. Atmospheric pressure laser desorption/chemical ionization mass spectrometry: A new ionization method based on existing themes. *Rapid Commun Mass Spectrom.* 2002;16(7):681-685. <https://doi.org/10.1002/rcm.626>
53. Silwal IKC, Rasaiah RC, Szulejko JE, Solouki T. Proton transfer reactions of halogenated compounds: Using gas chromatography/Fourier transform ion cyclotron resonance mass spectrometry (GC/FT-ICR MS) and ab initio calculations. *Int J Mass Spectrom.* 2010;293(1-3):1-11. <https://doi.org/10.1016/j.ijms.2010.03.003>
54. Vaikkinen A, Kauppila TJ, Kostianen R. Charge exchange reaction in dopant-assisted atmospheric pressure chemical ionization and atmospheric pressure photoionization. *J Am Soc Mass Spectrom.* 2016;27(8):1291-1300. <https://doi.org/10.1007/s13361-016-1399-8>
55. Morishima I, Yoshikawa K, Yonezawa T, Matsumoto H. Photoelectron spectra studies of organic free radicals. The nitroxide radical. *Chem Phys Lett.* 1972;16(2):336-339. [https://doi.org/10.1016/0009-2614\(72\)80287-2](https://doi.org/10.1016/0009-2614(72)80287-2)
56. Dávalos JZ, González J, Ramos R, Guerrero A, Lago AF. Intrinsic (gas-phase) acidity and basicity of paracetamol. *ARKIVOC.* 2014;2014(2):150-160. <https://doi.org/10.3998/ark.5550190.p008.249>
57. Stoica I, Angheluta E, Ivan M, Farcas A, Dorohoi DO. Electro-optical and morphological characterization of PVA foils with sulfathiazole. *Dig J Nanomater Biopstruct.* 2011;6(4):1667-1674. [http://www.chalcogen.ro/1667\\_Stoica.pdf](http://www.chalcogen.ro/1667_Stoica.pdf) Accessed September 4, 2019

## SUPPORTING INFORMATION

Additional supporting information may be found online in the Supporting Information section at the end of this article.

**How to cite this article:** Strmeň T, Vrkoslav V, Bosáková Z, Cvačka J. Atmospheric pressure chemical ionization mass spectrometry at low flow rates: Importance of ion source housing. *Rapid Commun Mass Spectrom.* 2020;34:e8722. <https://doi.org/10.1002/rcm.8722>

# SUPPORTING INFORMATION

*The list of contents:*

FIGURE S1 .....	2
SYNTHESIS OF TETRADECAN-2-ONE .....	3
DETERMINATION OF VOLUMETRIC FLOW RATES OF THE SHEATH AND AUXILIARY GASES .	3
FIGURE S2 .....	3
TABLE S1 .....	3
FIGURE S3 .....	4
FIGURE S4 .....	5
FIGURE S5 .....	6
FIGURE S6 .....	7
FIGURE S7 .....	8
FIGURE S8 .....	9
FIGURE S9 .....	9
FIGURE S10 .....	10
FIGURE S11 .....	10
FIGURE S12 .....	11
SI REFERENCES .....	12

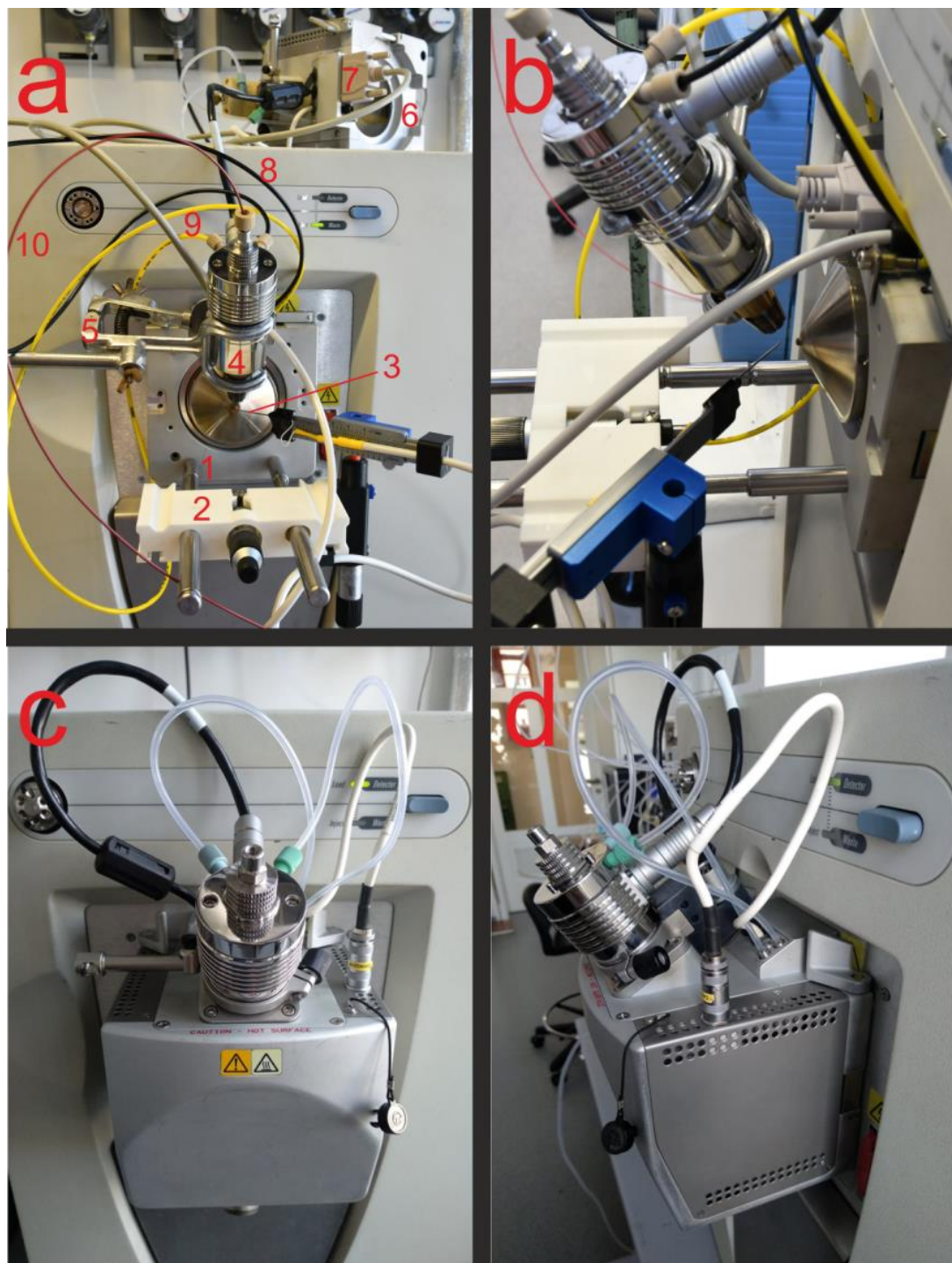


**Figure S1.** Photographs of the open (a, b) and enclosed (c, d) APCI source attached to LCQ Fleet ion trap mass spectrometer. Profiled aluminum flange (1), holder (2), corona discharge needle (3), APCI probe (4), clamp mounted on a stand (5), Ion Max-S API source housing (6), 15-pin D-SUB male/female connector (7), capillary for sheath gas delivery (8), capillary for auxiliary gas delivery (9), and capillary for liquid sample delivery (10).

### Synthesis of tetradecan-2-one

Tetradecan-2-one was prepared according to <sup>Ref. 1</sup> as follows: chromium trioxide ( $\geq 98\%$ , Sigma-Aldrich; 5.0 mg) and palladium dichloride (99 %, Sigma-Aldrich; 0.9 mg) were added to 1-tetradecene ( $\geq 97\%$ , Sigma-Aldrich; 19.5 mg) in 0.8 ml of acetonitrile and 0.2 ml of Milli-Q water. The mixture was stirred for 6.5 hours at 60 °C in a closed flask. The reaction mixture was filtered through silica gel, washed with ethyl acetate, and diluted in chloroform.

### Determination of volumetric flow rates of the sheath and auxiliary gases

The volumetric flow rates of the sheath and auxiliary gases were measured by the water displacement method. An Erlenmeyer flask filled with water was placed upside down in a tub. The sheath or auxiliary nitrogen from 1/8" OD PTFE tubing was fed under the flask until the flask was full of gas. The volumetric flow rates were calculated from the volume of the flask (5.4 l) and the time required to fill it. No corrections for vapor pressure of water were made.

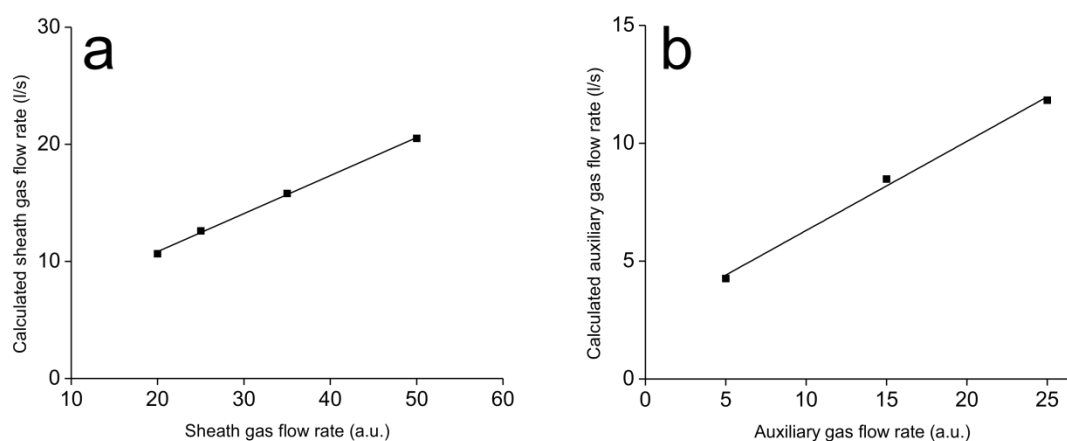


**Figure S2.** Graph showing the relationship between the set values of flow rate in arbitrary units and the actual values in liters per second for sheath (a) and auxiliary (b) gas (nitrogen).

**Table S1.** Contributions of nitrogen and solvent vapors to the total flow rate of gases in the APCI source (calculated for 180 °C; related to Figure 1).

Exp. no.	Gas-phase flow rate, l/s				
	N <sub>2</sub> Sheath gas	N <sub>2</sub> Aux. gas	Sum of N <sub>2</sub>	Toluene at 10 $\mu$ l/min	Toluene at 1 ml/min
1.	10.7	4.2	14.9	$5.8 \times 10^{-5}$	$5.8 \times 10^{-3}$
2.	10.7	11.7	22.4	$5.8 \times 10^{-5}$	$5.8 \times 10^{-3}$
3.	20.5	4.2	24.7	$5.8 \times 10^{-5}$	$5.8 \times 10^{-3}$
4.	20.5	11.7	32.2	$5.8 \times 10^{-5}$	$5.8 \times 10^{-3}$



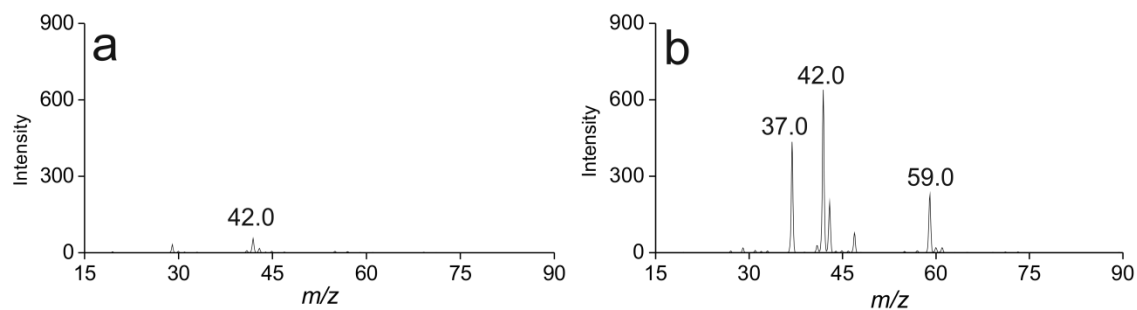


**Figure S3.** Blank APCI+ mass spectra (no sample solution introduced) recorded in the enclosed (a) and open ion sources (b) using dry nitrogen nebulizer gas. The ions were rationalized as follows:  $m/z$  37.0 ( $[(\text{H}_2\text{O})_2 + \text{H}]^+$ )<sup>a</sup> Ref. V, VI;  $m/z$  42.0 ( $[\text{CH}_3\text{CN} + \text{H}]^+$ )<sup>a</sup> Ref. V;  $m/z$  59.0 ( $[\text{C}_3\text{H}_6\text{O} + \text{H}]^+$ )<sup>HR, Ref. V</sup>.

<sup>a</sup> Exact mass could not be recorded because of the Orbitrap mass range from  $m/z$  50.

<sup>HR</sup> Based on high-resolution ESI measurement with Orbitrap XL (mass accuracy better than 5 ppm; for ions with  $m/z > 50$ ).

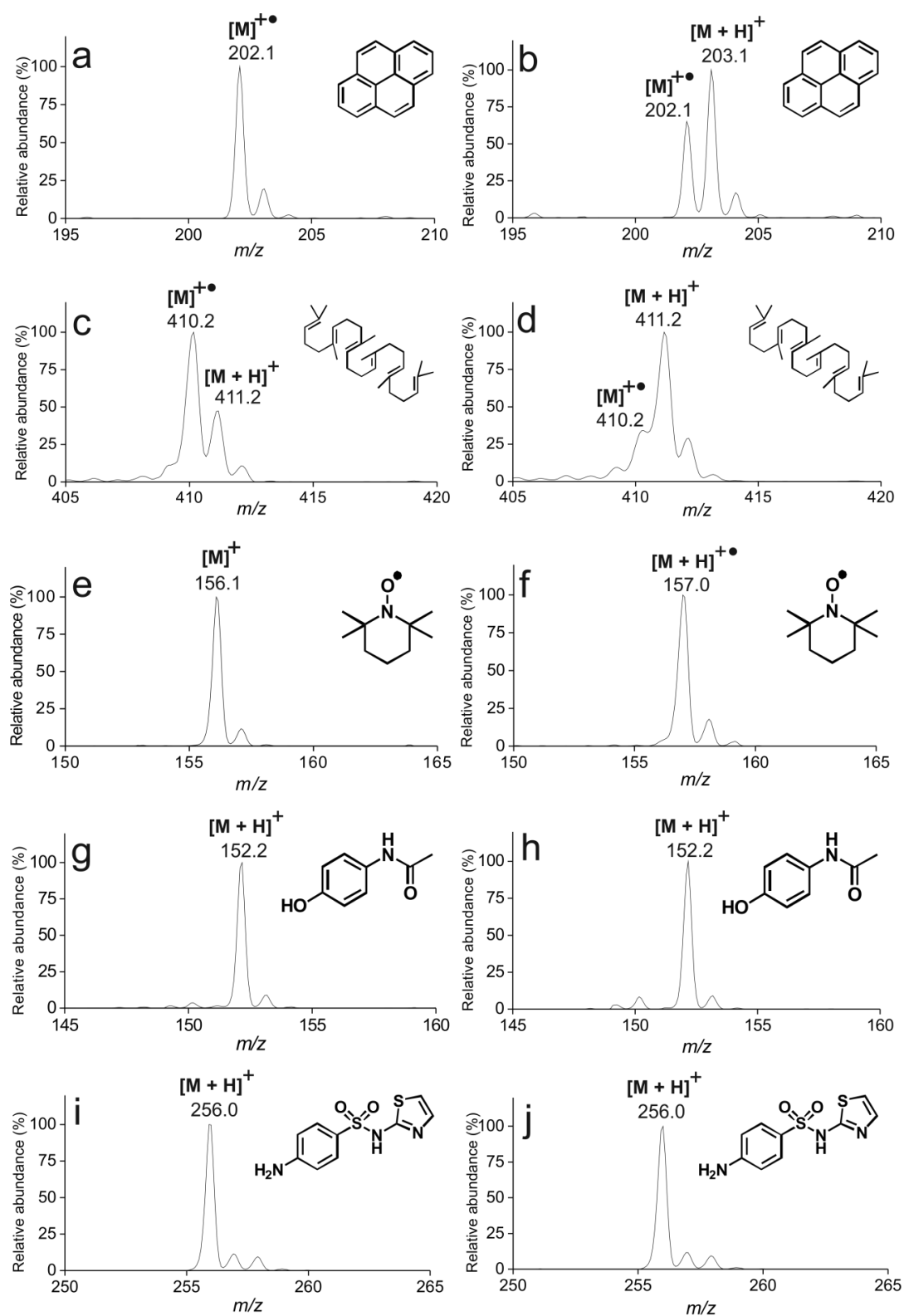


**Figure S4.** Selected APCI+ mass spectra of the tested compounds recorded in the enclosed (left column) and open (right column) ion sources using dry nitrogen nebulizer gas: pyrene in carbon disulfide (100  $\mu\text{mol/l}$ ; a, b), squalene in toluene (50  $\mu\text{mol/l}$ ; c, d), TEMPO in chloroform (50  $\mu\text{mol/l}$ ; e, f), paracetamol in acetonitrile (100  $\mu\text{mol/l}$ ; g, h), and sulfathiazole in methanol (100  $\mu\text{mol/l}$ ; i, j). The flow rate was 10  $\mu\text{l/min}$ .

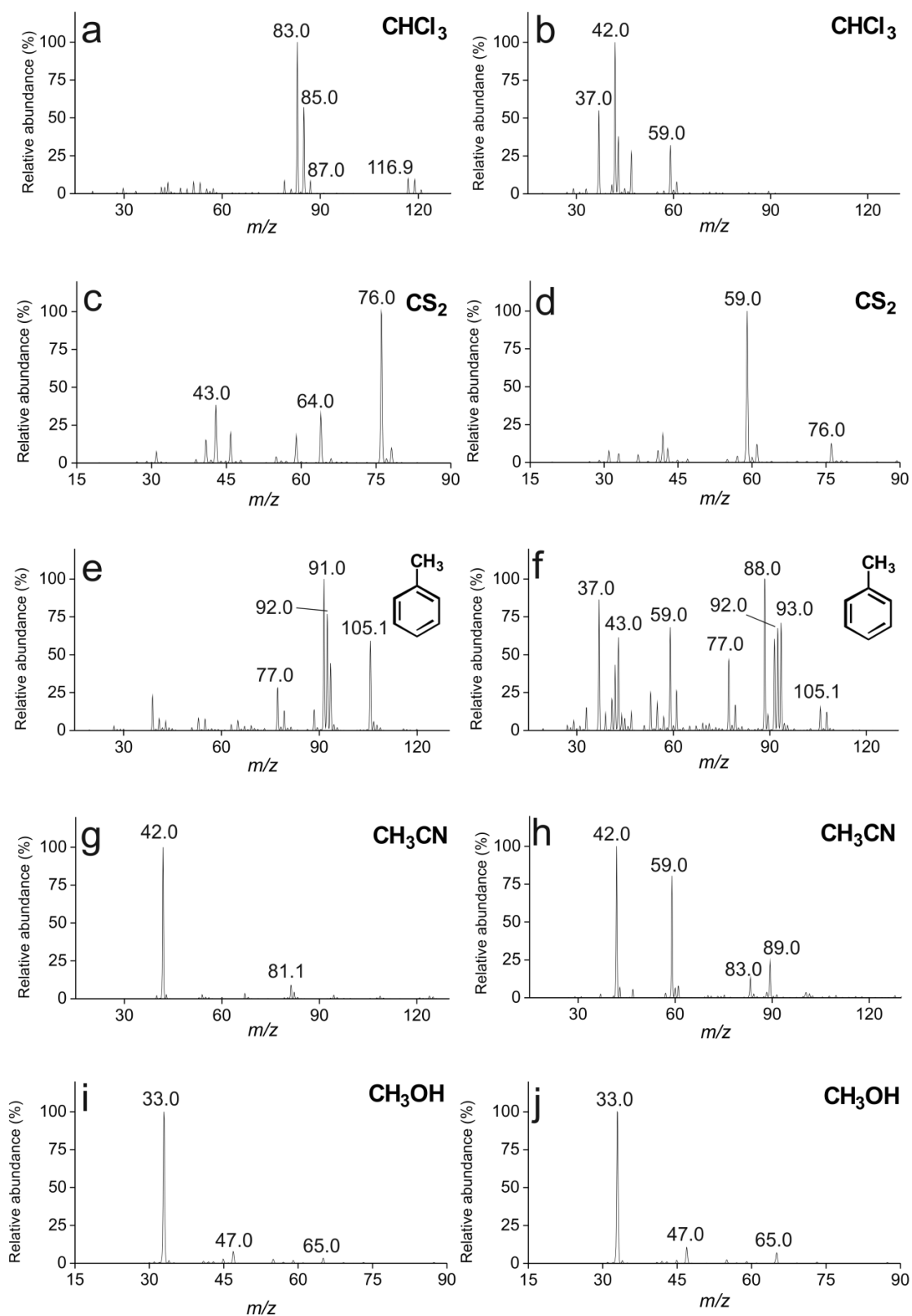


**Figure S5.** APCI+ mass spectra of solvents recorded in the enclosed (left column) and open (right column) ion sources at 10  $\mu\text{l}/\text{min}$  liquid flow rate using dry nitrogen nebulizer gas. Tentative ion identifications are given below.

Chloroform	$m/z$ 83.0 ( $[\text{CHCl}_2]^{++}$ ) <sup>Ref. II, HR</sup> ; 116.9 ( $[\text{CCl}_3]^{++}$ ) <sup>Ref. II, HR</sup>
Carbon disulfide	$m/z$ 64.0 ( $[\text{S}_2]^{++}$ ) <sup>HR</sup> ; $m/z$ 76.0 ( $[\text{CS}_2]^{++}$ ) <sup>Ref. III, HR</sup>
Toluene	$m/z$ 77.0 ( $[\text{C}_6\text{H}_5]^+$ ) <sup>HR</sup> ; $m/z$ 88.0 ( $[\text{C}_4\text{H}_{10}\text{NO}]^+$ ) <sup>HR</sup> ; $m/z$ 91.0 ( $[\text{C}_7\text{H}_7]^+$ ) <sup>Ref. IV, HR</sup> ; $m/z$ 92.0 ( $[\text{C}_7\text{H}_8]^{++}$ ) <sup>Ref. IV, HR</sup> ; $m/z$ 93.0 ( $[\text{C}_7\text{H}_9]^+$ ) <sup>HR</sup> ; $m/z$ 105.1 ( $[\text{C}_8\text{H}_9]^+$ ) <sup>HR</sup>
Acetonitrile	$m/z$ 42.0 ( $[\text{CH}_3\text{CN} + \text{H}]^+$ ) <sup>Ref. V</sup> ; $m/z$ 81.0 ( $[(\text{C}_4\text{H}_5\text{N}_2)^+]$ ) <sup>HR</sup> ; $m/z$ 83.0 ( $[(\text{CH}_3\text{CN})_2 + \text{H}]^+$ ) <sup>Ref. V, HR</sup> ; $m/z$ 89.0 ( $[\text{C}_4\text{H}_9\text{O}_2]^+$ ) <sup>HR</sup>
Methanol	$m/z$ 33.0 ( $[\text{CH}_3\text{OH} + \text{H}]^+$ ) <sup>Ref. II</sup> ; $m/z$ 47.0 ( $[(\text{CH}_3\text{OH})_2 + \text{H} - \text{H}_2\text{O}]^+$ ) <sup>Ref. II</sup> ; $m/z$ 65.0 ( $[(\text{CH}_3\text{OH})_2 + \text{H}]^+$ ) <sup>Ref. V, HR</sup>
Background ions	$m/z$ 37.0 ( $[(\text{H}_2\text{O})_2 + \text{H}]^+$ ) <sup>Ref. V, ref. VI</sup> ; $m/z$ 42.0 ( $[\text{CH}_3\text{CN} + \text{H}]^+$ ) <sup>Ref. V</sup> ; $m/z$ 59.0 ( $[\text{C}_3\text{H}_6\text{O} + \text{H}]^+$ ) <sup>Ref. V, HR</sup>

<sup>HR</sup> Based on high-resolution ESI measurement with Orbitrap XL (mass accuracy better than 5 ppm; for ions with  $m/z > 50$ ).

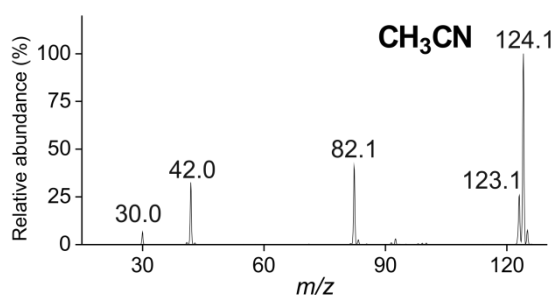


**Figure S6.** APCI+ mass spectrum of acetonitrile (10  $\mu\text{l}/\text{min}$ ) in the enclosed ion source using dry synthetic air nebulizer gas. The ions were rationalized as follows:  $m/z$  30.0 ( $[\text{NO}]^+$ )<sup>Ref. VII</sup>;  $m/z$  42.0 ( $[\text{CH}_3\text{CN} + \text{H}]^+$ )<sup>Ref. V</sup>;  $m/z$  82.0 ( $[(\text{CH}_3\text{CN})_2]^{++}$ )<sup>Ref. V, HR</sup>;  $m/z$  123.0 ( $[\text{C}_6\text{H}_9\text{N}_3]^{++}$ )<sup>Ref. V, HR</sup>;  $m/z$  124.0 ( $[\text{C}_6\text{H}_{10}\text{N}_3]^+$ )<sup>Ref. V, HR</sup>.

<sup>HR</sup> Based on high-resolution ESI measurement with Orbitrap XL (mass accuracy better than 5 ppm; for ions with  $m/z > 50$ ).

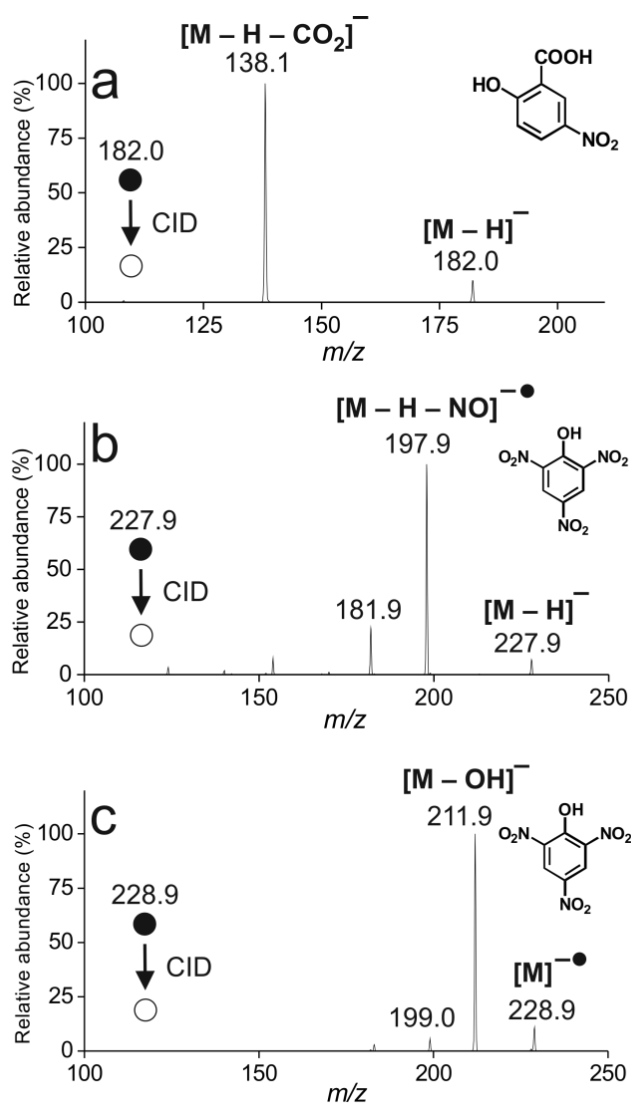


**Figure S7.** APCI- CID MS/MS spectra of 2-hydroxy-5-nitrobenzoic acid (a) and picric acid (b, c). Conditions for 2-hydroxy-5-nitrobenzoic acid: concentration 300  $\mu\text{mol/l}$ , solvent methanol, flow rate 10  $\mu\text{l/min}$ , normalized collision energy 23 %, isolation window 2.0 Da. Conditions for picric acid: concentration 200  $\mu\text{mol/l}$ , solvent 2% acetonitrile in methanol, flow rate 20  $\mu\text{l/min}$ , normalized collision energy 28 % (b) and 25 % (c), isolation window 2.0 Da.

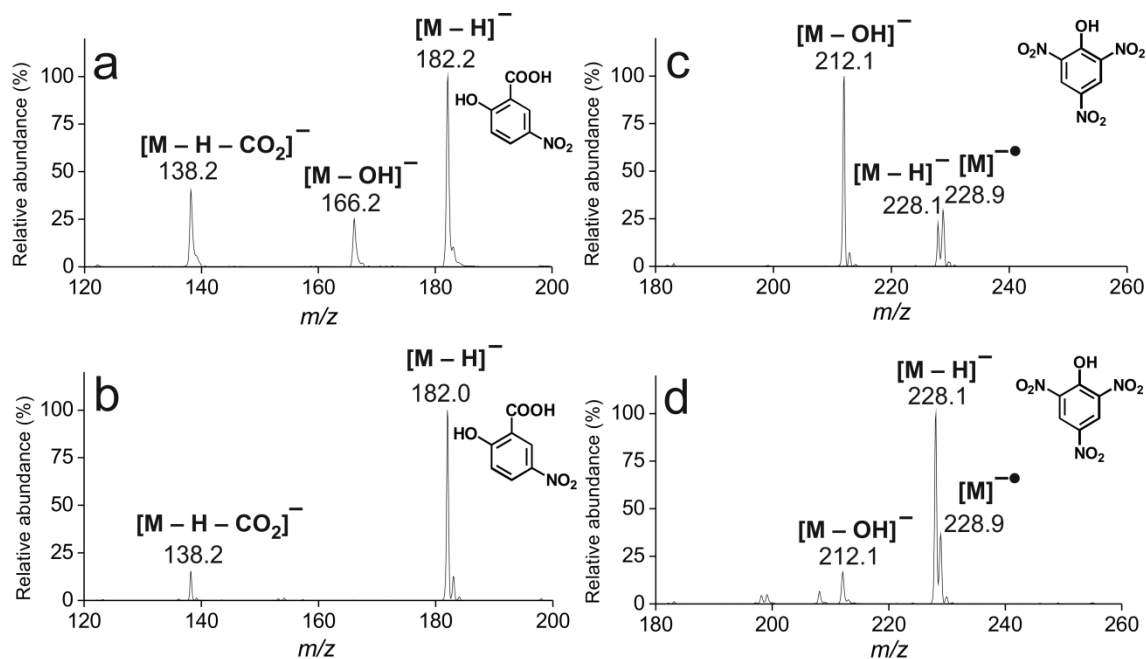


**Figure S8.** APCI- mass spectra of 2-hydroxy-5-nitrobenzoic acid (a, b) and picric acid (c, d) dissolved in acetonitrile and recorded in the enclosed ion source (a, c) and the open ion source (b, d) using dry nitrogen nebulizer gas. The flow rate was 10  $\mu\text{l}/\text{min}$ .

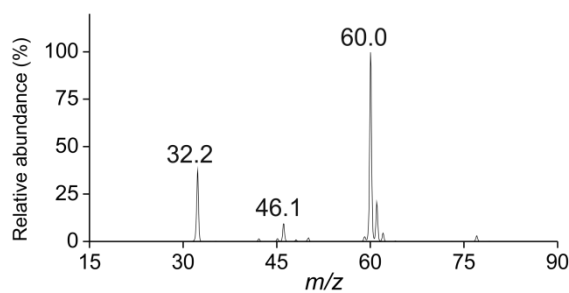


**Figure S9.** Blank APCI- mass spectrum (no sample solution introduced) recorded in the open ion source using dry nitrogen nebulizer gas. The ions were rationalized as follows:  $m/z$  32.2 ( $[O_2]^{-\bullet}$ )<sup>Ref. VIII</sup>;  $m/z$  46.1 ( $[NO_2]^-$ )<sup>Ref. VIII</sup>;  $m/z$  60.0 ( $[CO_3]^-$ )<sup>Ref. VIII, HR</sup>.

<sup>HR</sup> Based on high-resolution ESI measurement with Orbitrap XL (mass accuracy better than 5 ppm; for ions with  $m/z > 50$ ).

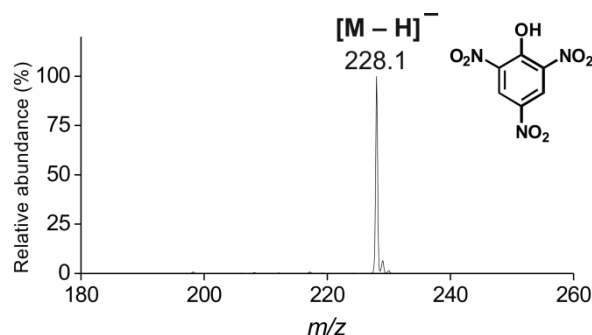


**Figure S10.** APCI- mass spectrum of picric acid dissolved in chloroform (300  $\mu\text{mol/l}$ ) and recorded in the enclosed ion source using dry nitrogen nebulizer gas. The flow rate was 20  $\mu\text{l/min}$ .

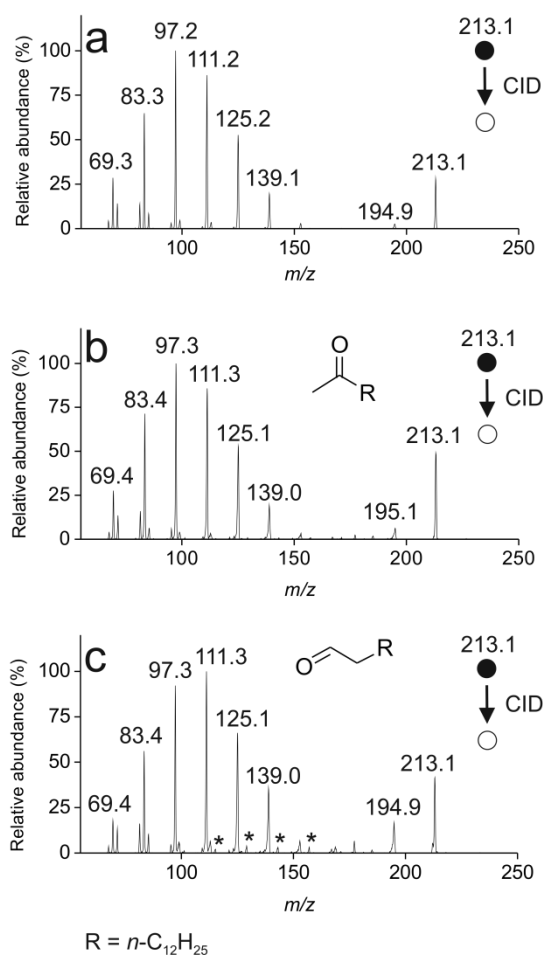


**Figure S11.** APCI+ CID MS/MS spectra of ion created by a gas-phase reaction of tetradec-1-yne with water recorded in the open ion source (a), standard of tetradecan-2-one (b), and standard of tetradecanal (c). The  $\text{C}_n\text{H}_{(2n+1)}\text{O}^+$  ion series in the spectrum of tetradecanal is labeled with asterisks. Conditions for (a): concentration unknown (generated in the ion source from tetradec-1-yne), solvent hexane, flow rate 10  $\mu\text{l/min}$ , normalized collision energy 20 %, isolation window 1.5 Da. Conditions for (b) and (c): concentration 300  $\mu\text{mol/l}$ , solvent chloroform, flow rate 10  $\mu\text{l/min}$ , normalized collision energy 20 %, isolation window 1.5 Da.

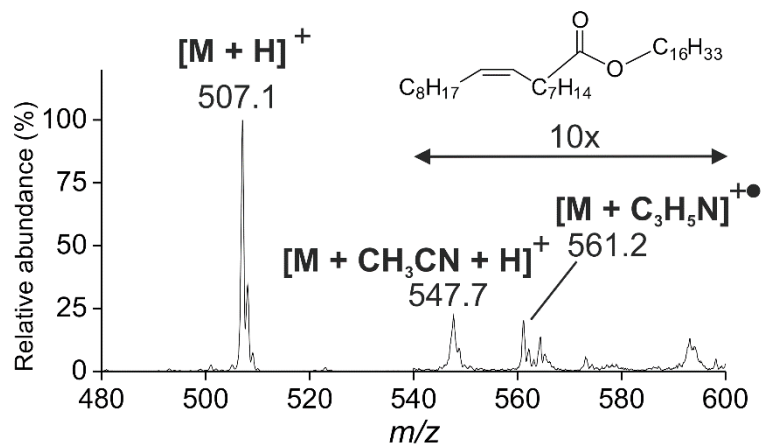


**Figure S12.** APCI+ mass spectrum of palmityl oleate dissolved in acetonitrile: ethyl acetate (99:1, by vol.) at the concentration of 100  $\mu\text{mol/l}$  delivered at 10  $\mu\text{l/min}$  and mixed in a T-union with acetonitrile: water (4:1; 400  $\mu\text{l/min}$ ). The mass spectrum was recorded in the enclosed ion sources using dry nitrogen as the nebulizer gas.



### SI References:

- I. Fernandes RA, Bethi V. Synthesis of methyl ketones from terminal olefins using PdCl<sub>2</sub>/CrO<sub>3</sub> system mimicking the Wacker process. *Tetrahedron* 2014; 70(32):4760-4767. doi: 10.1016/j.tet.2014.05.022
- II. Song L, Gibson SC, Bhandari D, Cook KD, Bartmess JE. Ionization mechanism of positive-ion direct analysis in real time: a transient microenvironment concept. *Anal Chem* 2009; 81(24):10080-10088. doi: 10.1021/ac901122b
- III. Owen BC, Gao J, Borton DJ 2nd, Amundson LM, Archibold EF, Tan X, Azyat K, Tykwinski R, Gray M, Kenttämäa HI. Carbon disulfide reagent allows the characterization of nonpolar analytes by atmospheric pressure chemical ionization mass spectrometry. *Rapid Commun Mass Spectrom* 2011;25(14):1924-1928. doi: 10.1002/rcm.5063
- IV. Badjagbo K, Picard P, Moore S, Sauvée S. Direct Atmospheric Pressure Chemical Ionization-Tandem Mass Spectrometry for the Continuous Real-Time Trace Analysis of Benzene, Toluene, Ethylbenzene, and Xylenes in Ambient Air. *J Am Soc Mass Spectrom* (2009);20(5):829-836. doi:10.1016/j.jasms.2008.12.021
- V. Kolakowski, BM, Grossert JS, Ramaley L. Studies on the positive-ion mass spectra from atmospheric pressure chemical ionization of gases and solvents used in liquid chromatography and direct liquid injection. *J Am Soc Mass Spectrom* 2004; 15(3):311-324 doi: 10.1016/j.jasms.2003.10.019
- VI. Horning EC, Horning MG, Carroll DI, Dzidic I, Stillwell RN. 1973 New Picogram Detection System Based on a Mass Spectrometer with an External Ionization Source at Atmospheric Pressure. *Anal Chem* 1973; 45(6):936-943. doi: 10.1021/ac60328a035
- VII. Sabo M, Matejčík Š. Corona discharge ion mobility spectrometry with orthogonal acceleration time of flight mass spectrometry for monitoring of volatile organic compounds. *Anal Chem* 2012; 84(12):5327-5334. doi: 10.1021/ac300722s
- VIII. Skalny, J.D., Mikoviny, T., Matejčík, S., Mason, N. J.: An analysis of mass spectrometric study of negative ions extracted from negative corona discharge in air. *Int J Mass Spectrom* 2004; 233(1-3):317-324 doi: 10.1016/j.ijms.2004.01.012

## Publikace II



# Evaluation of an ion source with a tubular nebulizer for microflow atmospheric pressure chemical ionization

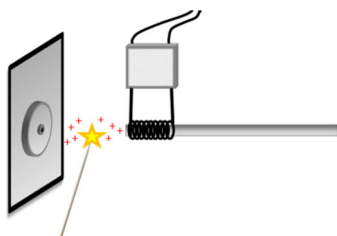
Timotej Strmeň<sup>1,2</sup> · Vladimír Vrkoslav<sup>2</sup> · Ondřej Pačes<sup>2</sup> · Josef Cvačka<sup>1,2</sup> 

Received: 4 October 2017 / Accepted: 2 February 2018 / Published online: 17 February 2018  
© Springer-Verlag GmbH Austria, part of Springer Nature 2018

## Abstract

An atmospheric pressure chemical ionization (APCI) source designed for microliter-per-minute flow rates (0.5–10.0 mm<sup>3</sup>/min) was constructed. A simple resistively heated 1/8 in. OD tube-based nebulizer, together with a corona-discharge electrode was positioned in front of the entrance capillary of a mass spectrometer. Working parameters of the ion source were optimized, and its performance was evaluated. The limit of detection for directly infused acridine was found to be lower for micro-APCI (10 fmol/s) than for conventional APCI (170 fmol/s), and the linear dynamic range was significantly wider for the micro-APCI source. The micro-APCI and conventional APCI sources provided similar, but not identical mass spectra. The micro-APCI source was used as a detector for high-performance liquid chromatography at 10 mm<sup>3</sup>/min; the limit of detection for acridine was 690 fmol, which was about ten times lower value than in conventional HPLC.

## Graphical abstract



**Keywords** Charge transfer · Hydrogen transfer · Mass spectroscopy · Micro-APCI · Tubular nebulizer

**Electronic supplementary material** The online version of this article (<https://doi.org/10.1007/s00706-018-2172-4>) contains supplementary material, which is available to authorized users.

✉ Josef Cvačka  
josef.cvacka@uochb.cas.cz

- <sup>1</sup> Department of Analytical Chemistry, Faculty of Sciences, Charles University in Prague, Hlavova 2030/8, Prague 2, Czech Republic
- <sup>2</sup> Institute of Organic Chemistry and Biochemistry of the Czech Academy of Sciences, Flemingovo nám. 2, Prague 6, Czech Republic

## Introduction

Atmospheric pressure chemical ionization (APCI) mass spectrometry is commonly used in LC/MS applications. In contrast to electrospray, the ions are generated from neutral species, which makes the method efficient at ionizing compounds of medium and low polarity [1]. It is best suited for relatively stable and small molecules like lipids [2–6], drugs and their metabolites, steroid derivatives, or pesticides [6]. APCI is considered less susceptible to ion suppression than electrospray and more tolerant to sample matrix and buffers [7].

The commercial APCI sources consist of a heated pneumatic nebulizer and an ionization region with a

corona-discharge electrode. The high-flow rate of carrier gas, usually nitrogen, is used to make a fine mist, which is quickly vaporized at high temperature. The mixture of sample vapors, carrier gas, and the residual air is carried along a corona-discharge electrode where the ionization takes place [1, 8]. The strong electric field near the electrode tip accelerates free electrons to high kinetic energies. The electrons ionize nearby molecules of the nebulizing gas, thus creating reactive primary ions [9]. In the positive ion mode, primary ions react with water or other solvents, creating protonated solvent molecules and subsequently clusters [10]. In the negative ion mode, oxygen anion radicals together with their water or nitrogen complexes are formed [11, 12]. Analytes are subsequently ionized by proton transfer [10, 13] or sometimes via charge exchange [12–14].

APCI has been commercially marketed in the late 1980s [15]. The ion source has been developed for high-flow rates of mobile phases compatible with standard-bore columns, and its design did not change much since then. Over the same period, chromatography has made a great progress towards miniaturization. Nano- and micro-bore chromatography columns used nowadays provide less dilution and, therefore, offer tremendously enhanced sensitivity and improved selectivity. When first introduced, these columns caused “omics revolution” and remained an important separation tool in these fields to these days [16]. Unfortunately, commercially available APCI sources still only work with high mobile phase flow rates, which prevents them to be coupled with nano- and micro-HPLC [17].

The idea of coupling APCI with low-flow rate separations appeared in the literature at the turn of the millennium [18–20]. The easiest way is to use a make-up liquid in the standard ion source to ensure sufficient flow rate of the mobile phase [18, 19]. For instance, an APCI interface from Hitachi was modified by the insertion of two stainless steel tubes to make co-axial sheath and gas flow system [18]. The ion source was tested for dichlorophenols in the direct injection mode at 10 mm<sup>3</sup>/min. A Thermo Fisher Scientific APCI source was adapted to accommodate a co-axial addition of sheath liquid flow using a stainless steel tube and a tee union. The device was successfully coupled to capillary electrophoresis [19]. Direct coupling of open-tubular liquid chromatography to APCI without sample dilution by make-up liquid was demonstrated for 50- $\mu$ m ID columns operated at flow rates of 0.1–1.6 mm<sup>3</sup>/min. The interface was made from three fused silica capillaries arranged concentrically, serving for delivery of sample (15- $\mu$ m ID), nebulizing gas (250- $\mu$ m ID), and auxiliary gas (700- $\mu$ m ID). The outermost capillary was wrapped in a heated resistance wire. This ion source has been used as an interface for reversed-phase (RP) nano-HPLC/MS of small organic molecules [20]. To the best of our knowledge, no

progress has been made in the development of this type of sources since then. Microchip-based interfaces have been later developed for coupling of micro- and nano-HPLC with MS. Microchip APCI source has been reported to be suitable for the flow rates down to 0.05 mm<sup>3</sup>/min. It was described as a two-dimensional version of the conventional APCI source consisting of a joined silicon and a glass wafer. The chip contained one channel for a liquid sample and two channels for nebulizing gas [17]. The heating was initially provided by the aluminum heater, but later, platinum one was introduced instead [17, 21]. The sample vaporized in a heated channel and exited the chip through a nozzle. The ionization was initiated with an external corona-discharge needle [17]. The source has been successfully used to hyphenate capillary reversed-phase HPLC with mass spectrometry as demonstrated on the analysis of steroids. [21].

In this work, a micro-APCI source based on a tube nebulizer was developed and tested. The nebulizer assembled from a PEEK cross, fused silica capillary, 1/8 in. OD corundum tube and a resistance heating wire was operated at flow rates ranging from 0.5 to 10 mm<sup>3</sup>/min. The performance of the ion source in direct infusion mode was compared to that of a commercial high-flow rate ion source. The micro-APCI source provided superior detection limits and linear dynamic range for acridine and it was tested as a detector for micro-HPLC.

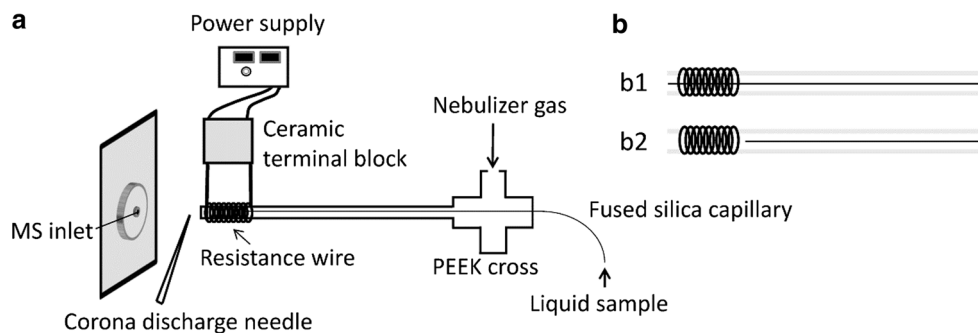
## Results and discussion

The tube nebulizer was assembled from a PEEK cross for 1/8 in. OD tubing, fused silica capillary (375- $\mu$ m OD, 25- $\mu$ m ID), quartz (3.0-mm OD, 1.5-mm ID), or corundum (2.1-mm OD, 1.3-mm ID) tube, and a resistance wire. The nebulizer was attached to a micromanipulator and positioned in front of the entrance capillary of Thermo Fisher Scientific LCQ Fleetion trap mass spectrometer as described in the “[Experimental](#)” section. The scheme of the device is shown in Fig. 1, and its photograph is in the Supplementary material (Fig. S-1). Initially, the fused silica capillary extended to the very end of the nebulizing quartz or corundum tube, as shown in Fig. 1b1. The ion source arrangement and its working parameters were optimized by the monitoring of the signal of acridine infused at a constant flow rate into the ion source.

### APCI needle position

The position of APCI needle in the ion source appeared to be very important. When the tip of the needle was too close to the MS inlet, undesirable and potentially harmful electric sparks were observed. The same was observed when

**Fig. 1** **a** Schematic view of a micro-APCI source, and **b** detailed view of the nebulizer outlet showing positions of fused silica capillary inside the quartz or corundum tube



the needle was placed in a short distance from the resistance wire. An optimal position was found to be 0.3 cm from the MS inlet and 0.7 cm from the resistance wire when the ionization was most efficient and no sparks were observed. The needle tip was positioned slightly off-axis. When it was directly in the way of the ions, the positive charge of the needle tip redirected part of the cations out of the MS inlet, which led to lower signal intensities.

### Tube nebulizer position

The optimum distance between the MS inlet and the outlet of the nebulizing tube was approximately 1.0 cm. Shorter distances did not create enough space to accommodate APCI needle, while longer distances prolonged the analyte trajectory, thus making the signal more susceptible to fluctuations. The distance of 1.0 cm was preserved in the experiments aiming at the optimum nebulizer tilt. No major impact on the signal intensity was observed for the nebulizer positioned at various angles. Therefore, the nebulizer was finally placed horizontally, pointing directly to the MS inlet.

### Resistance heating

High temperature served for evaporation of droplets leaving the fused silica capillary. As the polyimide coating of the capillary decomposed at high temperatures causing undesirable MS signals, it was intentionally burned off from the terminal part of the capillary. At low temperatures, the droplet desolvation was not efficient which resulted in poor or no signal of the analyte. On the other hand, excessively high temperatures caused analyte decomposition and its deposition inside the fused silica capillary, leading to a quick clogging. Moreover, high temperatures tended to weaken and ultimately damage the resistance wire. For these reasons, an optimum heating power was searched. The highest signal intensities were recorded at 2.1 W for the quartz tube and 10.5 W for the corundum tube (Fig. 2). The different values reflected various thermal conductivities of quartz and corundum, the

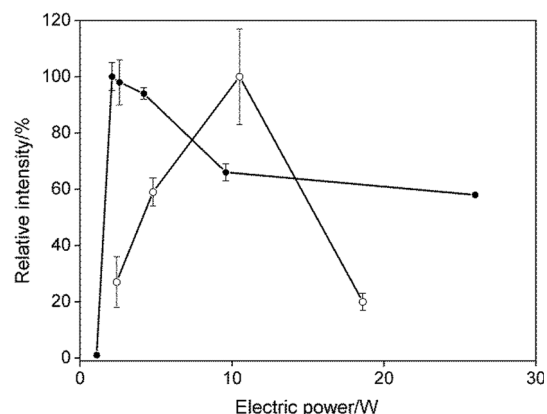


**Fig. 2** Relative signal intensities of acridine ( $50 \mu\text{mol}/\text{dm}^3$ ) infused into the micro-APCI source ( $3 \text{ mm}^3/\text{min}$ ) as a function of the electric power applied to the resistance heater for quartz tube (full circles) and corundum tube (empty circles). Nitrogen gas flow rate  $180 \text{ cm}^3/\text{min}$ , corona-discharge current  $1.0 \mu\text{A}$

tube wall thicknesses, and different lengths of the heated zones.

### Nebulizing gas flow rate

Just like in the conventional APCI, nebulizing gas affects both intensity and stability of the analyte signal. The nebulizing gas helps to transport the analyte molecules and ions into the mass spectrometer. While low gas flow rates make the analyte transport inefficient, high gas flow rates direct most of the analyte ions outside the inlet. Therefore, the best gas flow rate of nitrogen for both tube types was investigated. For the sample flow of  $3.0 \text{ mm}^3/\text{min}$ , the highest signal of acridine was observed at  $220 \text{ cm}^3/\text{min}$  (quartz) and  $100 \text{ cm}^3/\text{min}$  (corundum). This difference was likely caused by the smaller inner diameter of the corundum tube (Fig. 3).

During the above-mentioned experiments, the measured signal exhibited low stability. The instability was caused by the formation of gas bubbles from the solvent quickly evaporating inside the fused silica capillary. The problem was solved by retracting the capillary slightly back, so that its end was placed in front of the heating zone, as shown in

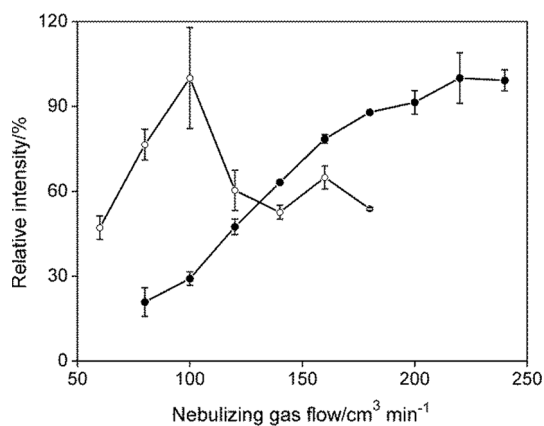


**Fig. 3** Relative signal intensities of acridine ( $50 \mu\text{mol}/\text{dm}^3$ ) infused into the micro-APCI source ( $3 \text{ mm}^3/\text{min}$ ) as a function of nebulizing gas flow rate for quartz tube (full circles) and corundum tube (empty circles). Electric power for the heater 2.6 W (quartz tube) or 10.5 W (corundum tube), corona-discharge current  $1.0 \mu\text{A}$

Fig. 1b2. As the corundum nebulizer exhibited significantly better signal stability, the quartz tube was not used for further investigations. The experiments aiming at the optimizing nitrogen flow rate were repeated with the corundum nebulizer having the fused silica capillary retracted. The nebulizer required higher gas flow rate ( $220 \text{ cm}^3/\text{min}$ ), likely because of prolonging the distance between the fused silica capillary and the MS inlet. A stable signal with the typical scan-to-scan RSD values of 7.5% was finally achieved (Fig. 4).

In conclusion, the corundum nebulizer with the fused silica capillary terminating in front of the heated area was used. The optimized gas flow rate of  $220 \text{ cm}^3/\text{min}$  and electric heating power of 10.5 W were used for the sample flow rate of  $3.0 \text{ mm}^3/\text{min}$ .

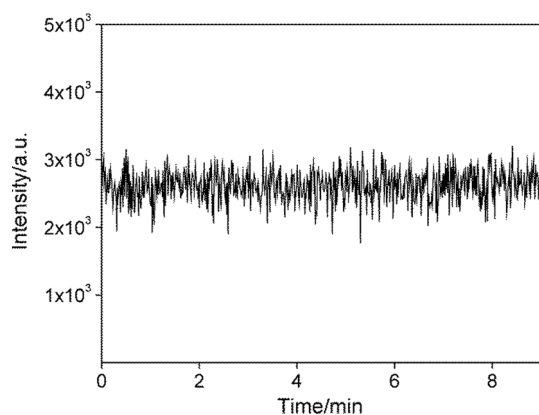


**Fig. 4** Stability of the signal of acridine ( $50 \mu\text{mol}/\text{dm}^3$ ) infused into the micro-APCI source ( $1 \text{ mm}^3/\text{min}$ ). Electric power for the heater 10.5 W, corona-discharge current  $1.0 \mu\text{A}$ , nitrogen gas flow rate  $220 \text{ cm}^3/\text{min}$

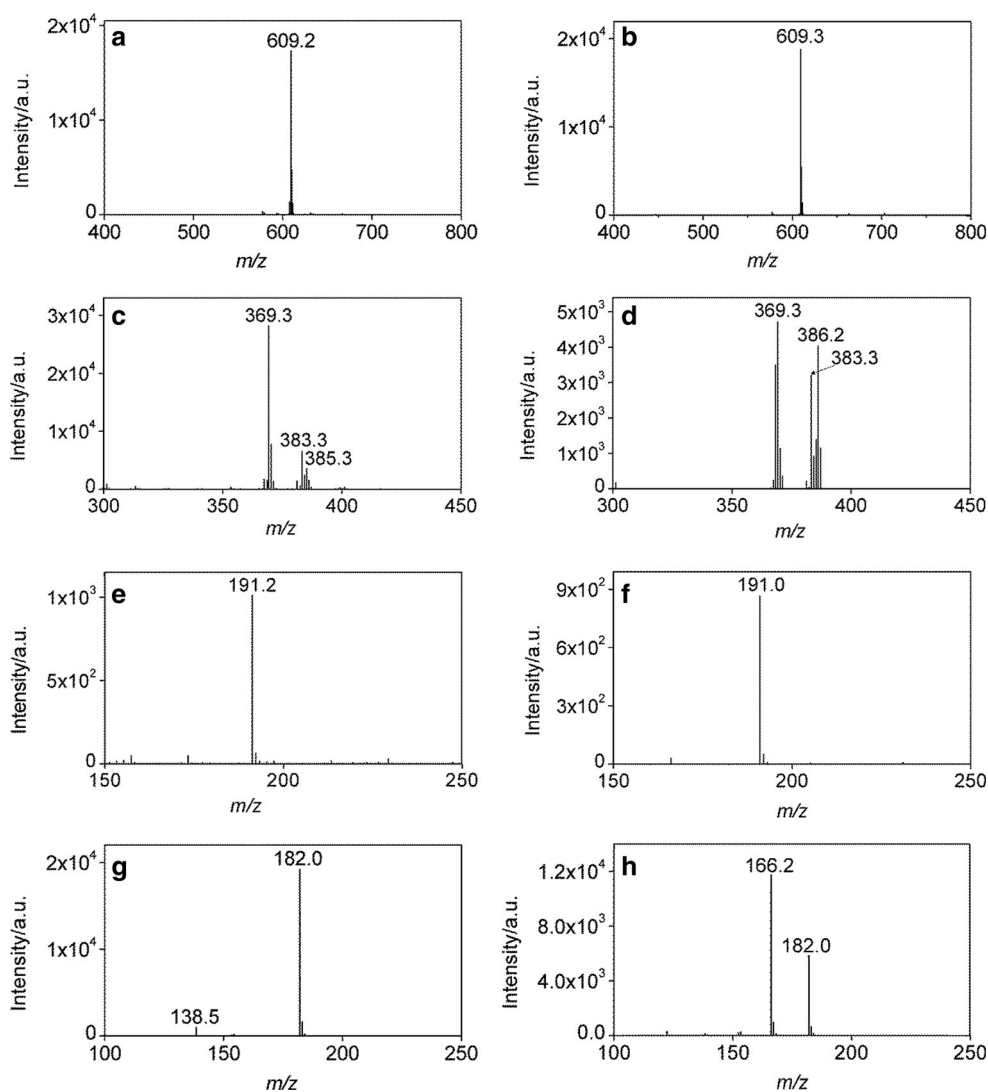
## Micro-APCI source performance

The performance of the micro-APCI source with optimized geometry and working parameters was compared to a commercial high-flow APCI source. Two model compounds for the positive ion mode (reserpine and cholesterol) and two for the negative ion mode (citric and 2-hydroxy-5-nitrobenzoic acid) were selected. Their mass spectra are shown in Fig. 5.

For both ion sources, reserpine provided  $[\text{M}+\text{H}]^+$  ions (Fig. 5a, b). In the mass spectrum of cholesterol (Fig. 5c, d), dehydrated protonated molecules  $[\text{M}-\text{H}_2\text{O}+\text{H}]^+$  ( $m/z$  369) were abundantly formed in both sources. However, in the conventional APCI,  $\text{M}^+$  ion ( $m/z$  386) was much more dominant than in micro-APCI, and the ions  $[\text{M}-3\text{H}]^+$  ( $m/z$  383) and  $[\text{M}-\text{H}]^+$  ( $m/z$  385) were prominently observed instead. It can be explained by a higher concentration of toluene, which is prone to undergo a charge-transfer reaction with cholesterol [22] (Fig. 4c, d). In the negative ion mode, both acids formed  $[\text{M}-\text{H}]^-$  ions ( $m/z$  191 and 182, respectively) in both sources (Fig. 5e–h). However, there was a striking difference between fragments. In micro-APCI, a fragment corresponding to the elimination of  $\text{CO}_2$  was detected ( $m/z$  138), whereas unexpected ion  $m/z$  166 was abundantly present in the spectrum from conventional APCI source. The  $m/z$  166 was not formed by collision activation, because MS/MS of the precursor ( $m/z$  182) showed only loss of  $\text{CO}_2$  ( $m/z$  138). We speculate that the fragment  $m/z$  166 ( $[\text{M}-\text{OH}]^-$ ) was formed by a dissociative electron capture process, which for unknown reason dominated in the high-flow ion source. The micro-APCI arrangement preferred proton transfer processes yielding mostly protonated or deprotonated molecules, while electron transfer processes took place in the conventional source in addition to proton transfer. Besides different operating parameters, the performance of the ion sources was likely affected by their design. The high-flow source was enclosed in a housing, while the micro-APCI operated in an open space, permitting diffusion of water into the ionization region. Nonetheless, preferential formation of even-electron species with a minimum degree of fragmentation is an advantage of micro-APCI, especially for quantitative analysis.

In the next step, calibration curves of acridine were recorded for both ion sources. The APCI-MS detector is known to be a mass-flow sensitive device, which responds to the mass of analyte passing through it per unit of time [23]. Therefore, the analyte mass-flow rates rather than concentration values were used to construct calibration curves. For these experiments, direct infusion of acridine calibration standards into the ion sources was used.

**Fig. 5** Mass spectra of reserpine in acetonitrile (**a, b**), cholesterol in toluene (**c, d**), citric acid in methanol (**e, f**), and 2-hydroxy-5-nitrobenzoic acid in methanol (**g, h**) recorded using micro-APCI (**a, c, e, and g**) and conventional APCI (**b, d, f, and h**). The micro-APCI conditions: sample flow rate 3.0 mm<sup>3</sup>/min (positive ion mode) and 5.0 mm<sup>3</sup>/min (negative ion mode), electric power for the heater 9.3 W, corona-discharge current 1.0 μA (positive ion mode) or 7.0 μA (negative ion mode). The conditions for the conventional APCI are stated in the “**Experimental**” section



The positive ion mass spectra were recorded for 1 min ( $m/z$  161–201), and the noise values were calculated from the intensity of the signals closest to  $m/z$  180 ( $[M+H]^+$  of acridine) in individual scans. The limits of detection (LOD) were calculated as a triple value of the background noise divided by the slope of the calibration curve (Fig. 6). The analytical figures of merit for acridine and both ion sources are summarized in Table 1.

The signals were higher for conventional APCI; however, lower LOD values were reached for micro-APCI. The background noise was approximately 100 times higher in conventional APCI than in micro-APCI. Moreover, the acridine response linearly increased in a wider range in case of micro-APCI. These results suggested the good performance of the micro-APCI source.

### Detection in micro-HPLC

As a proof of principle, the micro-APCI source was employed as a detector for HPLC. The test compound acridine was separated on a C18 column (0.5 mm ID) at the flow rate of 10 mm<sup>3</sup>/min using gradient elution. Using these conditions, acridine provided a tailing peak as shown in Fig. 7. Acridine is a basic compound, which can interact with residual silanols and thus exhibit excessive peak tailing. The limit of detection ( $S/N = 3$ ) was 0.69 pmol. A comparative measurement with conventional HPLC column (4.6 mm ID, flow rate 500 mm<sup>3</sup>/min) and high-flow APCI source revealed about ten times higher detection limit (6.5 pmol), which further confirmed superior performance of micro-APCI.

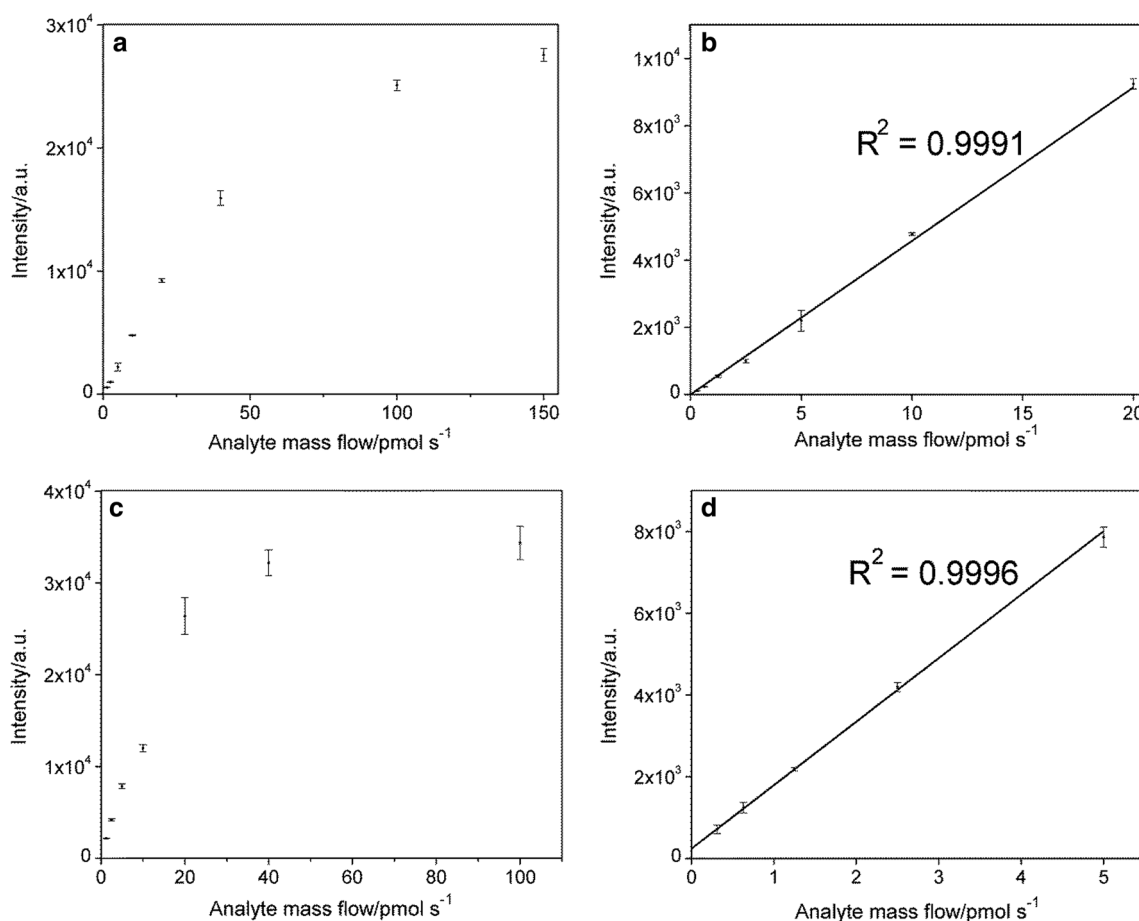


**Fig. 6** Calibration curves of acridine infused into the micro-APCI source (**a** detail of the linear part in **b** and conventional APCI source (**c** detail of the linear part in **d**). The micro-APCI conditions: sample flow rate  $3.0 \text{ mm}^3/\text{min}$ , nitrogen flow rate  $180 \text{ cm}^3/\text{min}$ , electric

power for the heater  $9.3 \text{ W}$ , and corona-discharge current  $1.0 \text{ }\mu\text{A}$ . The conditions for the conventional APCI are stated in the “[Experimental](#)” section

**Table 1** Analytical figures of merit for acridine infused into the conventional high-flow and in-house micro-APCI sources

Ion source	LOD/fmol $\text{s}^{-1}$	Dynamic range/pmole $\text{s}^{-1}$	Linear dynamic range/pmole $\text{s}^{-1}$
High-flow APCI	170	0.17 to $> 40$	0.17–5
Micro-APCI	10	0.01 to $> 150$	0.01–20

## Conclusion

In this work, an APCI source was developed for the sample flow rates  $0.5\text{--}10.0 \text{ mm}^3/\text{min}$ . Corundum was found to be a better material than quartz for the nebulizer construction. When compared to conventional APCI source, the in-house micro-APCI exhibited lower LOD and a wider linear dynamic range for direct infusion of acridine. Micro-APCI and conventional APCI provided similar, but not identical mass spectra. The differences were attributed to more efficient proton transfer reactions in the micro-APCI source, which is an important advantage of the micro-sources. The micro-APCI source was successfully hyphenated to micro-HPLC. The LOD of acridine was

$690 \text{ fmol}$  in the injected volume, which was about ten times lower amount than for conventional HPLC. When compared to microfluidic chip nebulizers for low-flow APCI-MS [17, 21], the tube nebulizer is simple and easy to assemble in common laboratories. The micro-APCI source developed in this work operated at  $0.5\text{--}10.0 \text{ mm}^3/\text{min}$  (capillary or micro-HPLC), while a similar source described earlier [20] was effective at significantly lower flow rates compatible with open-tubular LC. Despite its good performance, the micro-APCI described in this work was somewhat prone to variable performance due to a less firm mechanical connection of the key parts (heater, tube, and capillary). A further development is needed to make it more robust and applicable for routine detection in HPLC.



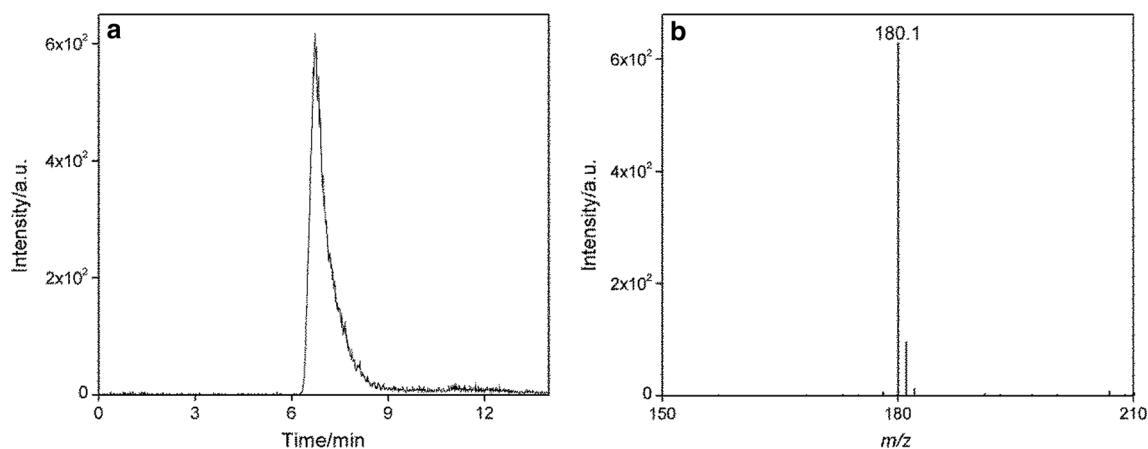


**Fig. 7** Basepeak chromatogram corresponding to the injection of 10 pmol of acridine onto HPLC column (a), and APCI spectrum taken across the peak (b). The micro-APCI conditions: sample flow

rate 10.0 mm<sup>3</sup>/min, nitrogen flow rate 400 cm<sup>3</sup>/min, electric power for the heater 17.0 W, and corona-discharge current 2.0 μA. For HPLC conditions, see the “[Experimental](#)” section

## Experimental

Acridine (97%), reserpine (≥ 99.0%), cholesterol (≥ 99.0%), 2-hydroxy-5-nitrobenzoic acid (99%), acetonitrile (for MS), and toluene (HPLC grade) were purchased from Sigma-Aldrich (St. Louis, MO, USA). Methanol (LC/MS grade) was obtained from VWR Chemicals (Radnor, PA, USA) and citric acid was obtained from Lachema (Brno, Czech Republic). Solutions of reserpine (50 μmol/dm<sup>3</sup>) and acridine were prepared in acetonitrile, whereas cholesterol was dissolved in toluene (260 μmol/dm<sup>3</sup>) and citric (500 μmol/dm<sup>3</sup>) and 2-hydroxy-5-nitrobenzoic acid (500 μmol/dm<sup>3</sup>) in methanol.

### High-performance liquid chromatography

The micro-HPLC was carried out using ExionLC AD System (Sciex, Framingham, MA, USA). The column was Zorbax XDB-C18 (0.5 mm i.d. × 150 mm, 3.5 μm particle size) from Agilent and it was kept at ambient temperature. The samples were injected by the ExionLC autosampler (0.1 mm<sup>3</sup>). The mobile phase was prepared from water (solvent A) and acetonitrile (solvent B). The gradient elution was programmed as follows: 0 min: 70% B; 8 min: 100% of B; the mobile phase flow rate was 10 mm<sup>3</sup>/min. After each analysis, the column was re-equilibrated at the initial conditions for 20 min. For the conventional HPLC, Rheos 2200 quaternary gradient pump (Flux Instruments, Reinach, Switzerland) and Accela autosampler (Thermo Fisher Scientific, Waltham, MA, United States) equipped with Nova-Pak C18 column (4.6 mm ID × 150 mm, 4 μm particle size) from Waters (Waters, Milford, MA, USA) were used. The column was kept at 30 °C and the injected volume of sample was 5 mm<sup>3</sup>. The solvent program was the same as used for

micro-HPLC and the mobile phase flow rate was 500 mm<sup>3</sup>/min.

### Micro-APCI source

The ion source was built on a platform consisting of a profiled aluminum flange for attaching the entire device to the mass spectrometer, and two steel rods for mounting the sprayer and corona-discharge needle on them. The position of the sprayer was adjusted using an MX10R 4-axis miniature micromanipulator (Siskiyou Corporation, Grand Pass, OR, USA). The sample solution was introduced into the ion source using a syringe pump (Fig. 1a).

The sprayer was constructed as a resistively heated quartz or corundum tube with a polyimide-coated fused silica capillary concentrically positioned inside. The fused silica capillary (375 μm OD, 25 μm ID) was inserted into and passed through a low-pressure polyether ether ketone (PEEK) cross for 1/8 in. OD tubing (IDEX Health & Science LLC, Oak Harbor, WA, USA). The cross served as a junction for the fused silica capillary and nebulizing gas flow. Nebulizing gas (nitrogen) was delivered from the mass spectrometer through a GFCS-011771 mass-flow controller (Aalborg, Orangeburg, NY, USA) which provided a precise regulation of nitrogen flow rate up to 500 cm<sup>3</sup>/min. The cross port opposite to the gas entrance was plugged. The fused silica capillary protruded into the nebulizing tube, which was fixed to the cross using a 1/8 inch nut. Two nebulizing tubes made of materials differing by their thermal conductivities were tested: (1) quartz tube (3.0 mm OD, 1.5 mm ID, length 118 mm, PeTra Turnov, Czech Republic) and (2) corundum tube (2.1 mm OD, 1.3 mm ID, length 100 mm). An iron wire spring was inserted into the nebulizing tubes to center the fused silica capillary. The polyimide coating was removed from the

terminal 4-cm part of the capillary. The end parts of the nebulizing tubes (3 cm) were heated with a Kanthal<sup>TM</sup> resistance wire (0.4 mm in diameter), which was tightly coiled around them. The number of wire threads was 27 for the quartz tube and 21 (for HPLC) or 41 (for other measurements) for the corundum tube. The heater was powered by an external voltage source Manson HCS-3202-000G (Manson Engineering Industrial Ltd, Hong Kong).

### Mass spectrometer

An ion trap mass spectrometer LCQ Fleet (Thermo Fisher Scientific; Waltham, MA, USA) was used. For the micro-APCI experiments, corona needle discharge current 1.0  $\mu$ A, capillary temperature 300 °C, capillary voltage 25.7 V, and tube lens voltage 120 V were used for the positive ion mode. The negative ions were detected with the capillary voltage – 25.0 V and tube lens voltage – 105 V. The high-flow conventional APCI was performed with the standard ion source equipped with APCI probe. In the positive ion mode, discharge current 2.0  $\mu$ A, sheath gas flow 30.0 a.u., auxiliary gas flow 10.0 a.u., sweep gas flow 10.0 a.u., capillary temperature 250 °C, and the vaporizer temperature 300 °C were used. The capillary voltage was set to 5.0 V and tube lens voltage was set to 120.0 V. In the negative ion mode, discharge current 6.5  $\mu$ A, sheath gas flow 20.0 a.u., auxiliary gas flow 5.0 a.u., capillary temperature 250 °C, and the vaporizer temperature 300 °C were used. Sweep gas was not used in the negative mode. The capillary and tube lens voltages were set to – 12.0 V and – 56.0 V, respectively.

For the calibration curve measurement in the high-flow ion source, the samples delivered from a syringe pump were mixed in a T-union with make-up solvent delivered by Rheos 2200 gradient pump (Flux Instruments, Reinach, Switzerland). The flow rates of the samples were always the same as in case of micro-APCI, making the mass-flow rates of acridine delivered to both sources identical. To determine background noise, acetonitrile was infused into the ion source (500 mm<sup>3</sup>/min for conventional APCI, 3 mm<sup>3</sup>/min for the micro-APCI).

All mass spectra were recorded for 1 min, with the exception of stability experiments, where the data were collected for 9 min. The error bars indicated in graphs are standard deviations calculated from three independent measurements.

**Acknowledgements** Financial support from the Czech Science Foundation (16-01639S) and Charles University in Prague (Project SVV260440) is hereby acknowledged with appreciation. The authors wish to thank Dr. Jindřich Houžvička (Crytur Ltd.) for providing them with the corundum tube.

### References

- Gross JH (2004) Mass spectrometry, a textbook, 1st edn. Springer, Berlin
- Vrkoslav V, Háková M, Pecková K, Urbanová K, Cvačka J (2011) *Anal Chem* 83:2978
- Vrkoslav V, Cvačka J (2012) *J Chromatogr A* 1259:244
- Háková E, Vrkoslav V, Míková R, Schwarzová-Pecková K, Bosáková Z, Cvačka J (2015) *Anal Bioanal Chem* 407:5175
- Kalužíková A, Vrkoslav V, Harazim E, Hoskovec M, Plavka R, Buděšínský M, Bosáková Z, Cvačka J (2017) *J Lipid Res* 58:1579
- Somogyi A (2008) Mass spectrometry instrumentation and techniques. In: Vékey K, Teleks A, Vertes A (eds) *Medical applications of mass spectrometry*. Elsevier, Amsterdam
- Dams R, Huestis MA, Lambert WE, Murphy CM (2003) *J Am Soc Mass Spectrom* 14:1290
- Cappiello A (2007) *Advances in LC-MS instrumentation*, vol 72. Elsevier, Amsterdam, p 67
- Andrade JF, Shelley TJ, Wetzel CW, Webb RM, Gamez G, Ray JS, Hieftje MG (2008) *Anal Chem* 80:2646
- Horning EC, Horning MG, Carroll DI, Dzidic I, Stillwell RN (1973) *Anal Chem* 45:936
- Mitchum RK, Moler GF, Korfmacher WA (1980) *Anal Chem* 52:2278
- Luosujärvi L, Karikko MM, Haapala M, Saarela V, Huhtala S, Franssila S, Kostianen R, Kotiaho T, Kauppila TJ (2008) *Rapid Commun Mass Spectrom* 22:425
- Niessen W, Correa R (2017) *Interpretation of MS-MS mass spectra of drugs and pesticides*. Wiley, Hoboken
- Kolakowski BM, Grossert JS, Ramaley L (2004) *J Am Soc Mass Spectrom* 15:311
- Niessen W (1999) *Liquid chromatography: mass spectrometry*, 2nd edn. Marcel Dekker Inc, New York
- Novotny MV (2017) *J Chromatogr A* 1523:3
- Östman P, Marttila SJ, Kotiaho T, Franssila S, Kostianen R (2004) *Anal Chem* 76:6659
- Takeda S, Tanaka Y, Yamane M, Siroma Z, Wakida S, Otsuka K, Terabe S (2001) *J Chromatogr A* 924:415
- Tanaka Y, Otsuka K, Terabe S (2003) *J Pharm Biomed Anal* 30:1889
- Nyholm LM, Sjöberg P, Markides KE (1996) *J Chromatogr A* 755:153
- Östman P, Jäntti S, Grigoras K, Saarela V, Ketola AR, Franssila S, Kotiaho T, Kostianen R (2006) *Lab Chip* 6:948
- Kim YH, Kim S (2010) *J Am Soc Mass Spectrom* 21:386
- Takino M, Daishima S, Nakahara T (2003) *J Chromatogr A* 1011:67

## Evaluation of an ion source with a tubular nebulizer for microflow atmospheric pressure chemical ionization

Timotej Strmeň<sup>1,2</sup> • Vladimír Vrkoslav<sup>2</sup> • Ondřej Pačes<sup>2</sup> • Josef Cvačka<sup>1,2</sup>

<sup>1</sup> Charles University in Prague, Faculty of Sciences, Department of Analytical Chemistry, Hlavova 2030/8 Prague 2, Czech Republic

<sup>2</sup> The Institute of Organic Chemistry and Biochemistry of the Czech Academy of Sciences, Flemingovo nám. 2, Prague 6, Czech Republic

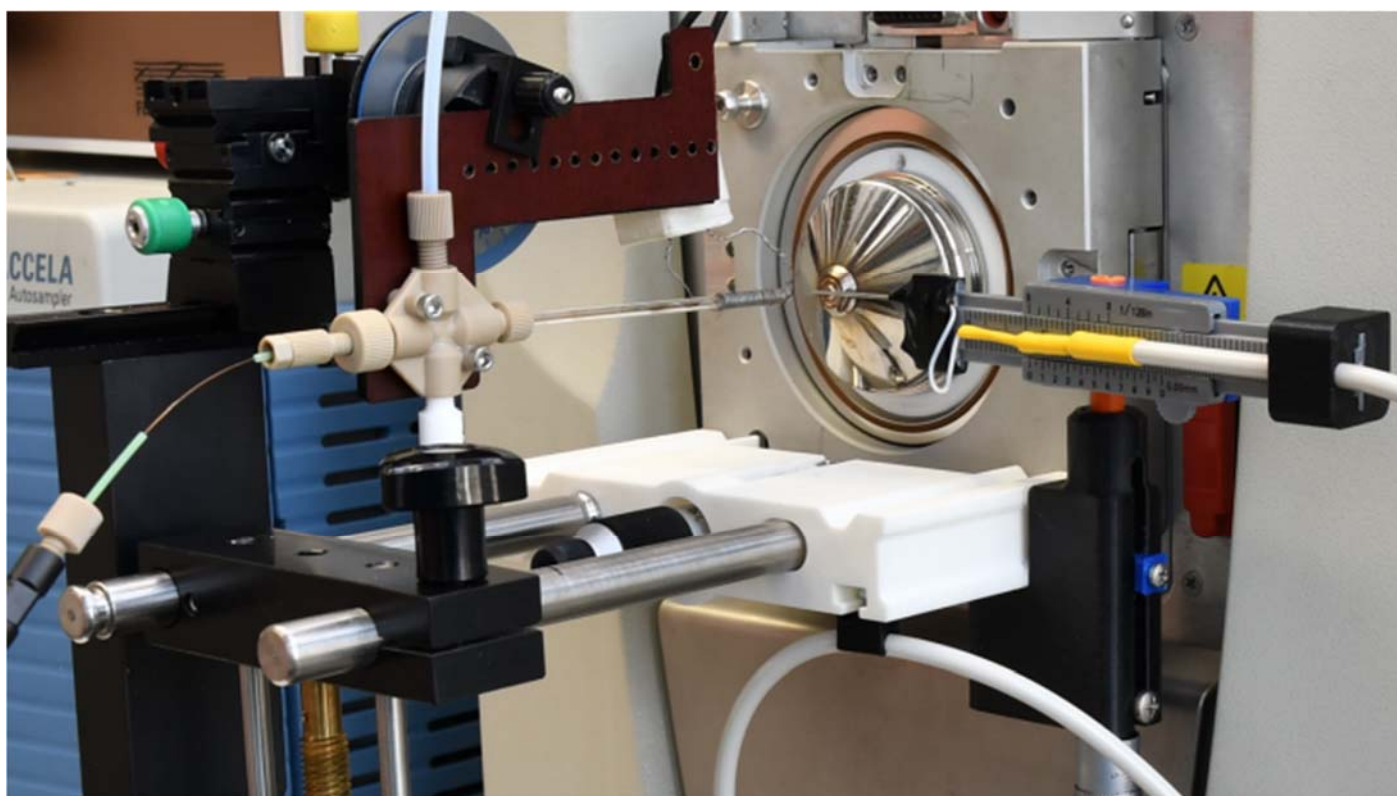



**Figure S-1** Photograph of the micro-APCI source with tube nebulizer.

## Publikace III

## RESEARCH ARTICLE

# Applicability of low-flow atmospheric pressure chemical ionization and photoionization mass spectrometry with a microfabricated nebulizer for neutral lipids

Vladimír Vrkoslav<sup>1</sup> | Barbora Rumlová<sup>2</sup> | Timotej Strmeň<sup>1,2</sup> | Pavlína Nekvasilová<sup>2</sup> |  
Miloslav Šulc<sup>3</sup> | Josef Cvačka<sup>1,2</sup> 

<sup>1</sup>Institute of Organic Chemistry and Biochemistry of the Czech Academy of Sciences, Flemingovo nám. 2, CZ-166 10 Prague 6, Czech Republic

<sup>2</sup>Department of Analytical Chemistry, Faculty of Science, Charles University in Prague, Hlavova 2030/8, CZ-128 43 Prague 2, Czech Republic

<sup>3</sup>Czech University of Life Sciences, Faculty of Agrobiological Sciences, Department of Chemistry, Kamýcká 129, CZ-165 00 Prague 6, Czech Republic

## Correspondence

J. Cvačka, Institute of Organic Chemistry and Biochemistry of the Czech Academy of Sciences, Flemingovo nám. 2, CZ-166 10 Prague, Czech Republic.  
Email: josef.cvacka@uochb.cas.cz

## Funding information

Grantová Agentura České Republiky, Grant/Award Number: 16-01639S; Univerzita Karlova v Praze, Grant/Award Number: SVV; Czech Science Foundation, Grant/Award Number: 16-01639S

**Rationale:** Mass spectrometry with atmospheric pressure chemical ionization (APCI) or photoionization (APPI) is widely used for neutral lipids involved in many fundamental processes in living organisms. Commercial APCI and APPI sources operate at high flow rates compatible with conventional high-performance liquid chromatography (HPLC). However, lipid analysis is often limited by a small amount of sample, which requires low flow rate separations like capillary or micro-HPLC. Therefore, APCI and APPI suitable for microliter-per-minute flow rates need to be developed and applied for neutral lipids.

**Methods:** A micro-APCI/APPI source with a heated chip nebulizer was assembled and mounted on a Thermo ion trap instrument. The ion source operated in APCI, APPI or dual mode was optimized for low microliter-per-minute sample flow rates. The source performance was investigated for squalene, wax esters, fatty acid methyl esters, triacylglycerols, and cholesterol.

**Results:** The ion source behaved as a mass-flow-sensitive detector. Direct infusion of methyl oleate showed superior analytical figures of merit when compared with high-flow ion sources. A detection limit of 200 pmol/mL and a linear dynamic range spanning three orders of magnitude were measured for micro-APCI. The mass spectra of most lipids differed from high flow rate spectra. Unlike micro-APCI, micro-APPI spectra were complicated by odd-electron species. Dual APCI/APPI mode did not show any benefits for neutral lipids. Applications for lipid samples were demonstrated.

**Conclusions:** Micro-APCI-MS is a useful detection technique for neutral lipids at microliter-per-minute flow rates. It offers high sensitivity and high quality of spectra in direct infusion mode and promises successful utilization in capillary and micro-HPLC applications.

## 1 | INTRODUCTION

Atmospheric pressure chemical ionization (APCI) and atmospheric pressure photoionization (APPI) are useful techniques for nonpolar and low-polar compounds.<sup>1-3</sup> In both ionization modes, the analytes in solution are introduced into a heated pneumatic nebulizer. A mixture of the analyte, solvent vapor, and nitrogen gas is generated and carried along a corona discharge electrode or a UV lamp. A strong electric field near the tip of the discharge electrode in APCI accelerates free electrons to high kinetic energies. The analytes are ionized by a sequence of charge and proton transfer reactions involving nitrogen and solvent molecules. The ionization in APPI is accomplished by high-energy photons, which are absorbed by the

analyte, solvent or dopant introduced into the ion source. An electron is ejected to form a radical cation and the ionization usually proceeds by proton transfer or charge exchange reactions. Unlike electrospray ionization (ESI), APPI and APCI are gas-phase processes. Protonated molecules, solvent adducts, radical species, and fragments can be found in the spectra of positively charged ions, and the ion formation depends on the proton and electron affinities of the analyte, solvent, and dopant. APCI and APPI sources operate under similar conditions which offer their simultaneous use for enhancing the detection sensitivity of some analytes.<sup>4</sup> APCI and APPI are not constrained by the solvent polarity, which is a great advantage for their coupling with high-performance liquid chromatography (HPLC) regardless of the separation system used. Unlike ESI, these ionization

methods can be easily used in normal-phase or non-aqueous reversed-phase chromatography. The application of APCI and, to a lesser extent of APPI, in HPLC/MS has gained much popularity for the sensitive detection of drugs and their metabolites, pesticides, neutral lipids, and other analytes.<sup>1,2,5,6</sup> As regards neutral lipids, APCI has been used for triacylglycerols (TGs),<sup>7-10</sup> fatty acid methyl esters (FAMES),<sup>11,12</sup> wax esters (WE),<sup>13-15</sup> diesters,<sup>16,17</sup> and sterols,<sup>18,19</sup> while APPI was found useful for polyunsaturated TGs and FAMES.<sup>20</sup>

Analytical HPLC separations are increasingly carried out at low flow rates, especially when high sensitivity is required for limited sample amounts. This is particularly relevant in the rapidly expanding field of bioanalytical analysis. Currently, nano-, capillary-, or micro-flow HPLC/MS rely on ESI, which offers sensitive detection for many analytes. Despite its widespread use, the ESI process suffers from some fundamental drawbacks; it works well for species that exist as ions in solution or those with acidic or basic functionality, but it is inefficient at ionizing compounds of low polarity. Moreover, ESI is susceptible to ion suppression as solutes at the droplet surface compete for a charge during the ionization process. Consequently, minor constituents with high charge affinity may dominate the ion current. Obviously, it would be highly beneficial to have an option for coupling low-flow HPLC to gas-phase ionization sources like APCI or APPI. Unfortunately, commercial ion sources are designed for high flow rates (hundreds to thousands of microliters per minute), thus preventing their direct connection to low-flow LC.

The feasibility of APCI and APPI at microliter-to-nanoliter-per-minute flow rates has been demonstrated for sources based on microfabricated nebulizing chips.<sup>21,22</sup> The original silicon/glass design<sup>21,22</sup> was replaced by all-glass chips,<sup>23</sup> which were later slightly modified.<sup>24</sup> All-glass chips offered higher nebulizing temperatures beneficial for higher boiling point solvents and less volatile analytes.<sup>23</sup> APCI and APPI with microfluidic chips have been successfully coupled to microliter-per-minute HPLC and provided better detection limits when compared to standard commercial high-flow sources. LC-microchip APPI-MS/MS has been used for the analysis of anabolic steroids,<sup>25</sup> pesticides,<sup>24</sup> and aromatic compounds,<sup>26,27</sup> while the utility of LC-microchip APCI-MS/MS has been demonstrated for neurosteroids.<sup>28</sup> To the best of our knowledge, micro-flow ion sources have never been systematically investigated for their application to neutral lipids, important compounds involved in many fundamental processes in living organisms. The successful introduction of low-flow APCI and/or APPI for sensitive analysis of neutral lipids would be highly beneficial for bioanalytical applications.

In this work, a micro-APCI/APPI source with a heated nebulizing chip was assembled and attached to a Thermo ion trap instrument. The ion source geometry and operating parameters were thoroughly adjusted for an optimum performance. The applicability of the ion source for neutral lipids like TGs, WEs, and FAMES was studied using direct infusion experiments in APCI, APPI, and dual APCI/APPI modes. Superior analytical figures of merit compared with high-flow sources are demonstrated, and examples of direct analysis of neutral lipid mixtures are given. The performance of the ion source is promising for future applications for low-flow HPLC of neutral lipids.

## 2 | EXPERIMENTAL

### 2.1 | Abbreviations

The composition of fatty acyls in lipids is described using number of carbons: number of double-bond convention with the first double bond from the chain terminus indicated in parentheses. For example, FAME18:1(n-9) means fatty acid methyl ester with 18 carbons and a double bond on the ninth carbon counted from the terminal methyl group (i.e., methyl oleate). The first part of WE abbreviations refers to the alcohol chain, whereas the second part indicates the fatty acid.

### 2.2 | Chemicals

Reserpine, cholesterol, 1,3-dipalmitoyl-2-oleoylglycerol (TG16:0/18:1(n-9)/16:0), palmityl oleate (WE16:0-18:1(n-9)), squalene, and Supelco 37 Component FAME Mix were purchased from Sigma-Aldrich (St Louis, MO, USA). The standards of stearyl stearate (WE18:0-18:0), lauryl myristoleate (WE12:0-14:1(n-5)), lauryl palmitoleate (WE12:0-16:1(n-7)), lauryl oleate (WE12:0-18:1(n-9)); myristyl oleate (WE14:0-18:1(n-9)), stearyl oleate (WE18:0-18:1(n-9)), arachidyl oleate (WE20:0-18:1(n-9)), behenyl oleate (WE22:0-18:1(n-9)), stearyl linoleate (WE18:0-18:2(n-6)), stearyl linolenate (WE18:0-18:3(n-3)), palmityl arachidonate (WE16:0-20:4(n-6)), methyl laurate (FAME12:0), and methyl oleate (FAME18:1(n-9)) were purchased from Nu-Chek-Prep (Elysian, MN, USA). The isolation of TGs from black currant oil,<sup>29</sup> WEs from jojoba oil,<sup>13</sup> and total lipid extract of vernix caseosa<sup>30</sup> was published earlier. Acetone ( $\geq 99.8\%$  Chromasolv® for HPLC, gradient grade), acetonitrile (LC-MS Chromasolv®), hexane (LC-MS Chromasolv®), methanol (LC-MS Chromasolv®), ethyl acetate ( $\geq 99.7\%$  LC-MS Chromasolv®, (GC)), chloroform (Chromasolv® Plus, for HPLC), 2-propanol (LC-MS, Chromasolv®), and toluene (Chromasolv® Plus, for HPLC) were purchased from Sigma-Aldrich.

### 2.3 | Ion source for micro-APCI/APPI

The in-house ion source (Figure S1, supporting information) was assembled on a platform consisting of a flange with two guiding rods. The flange made it possible to attach the whole device to the spectrometer, and the rods served as a support for a miniature micromanipulator (MX10R; Siskiyou, Grants Pass, OR, USA) holding the microfabricated chip and an adjustable holder for the corona discharge needle. These elements served to precisely and reproducibly adjust the position of the nebulizer chip and discharge needle relative to the inlet of the mass spectrometer. The low-pressure discharge krypton RF-excited VUV lamp (PKR 106, 58 mm  $\times$  12.7 mm, 10.0 and 10.6 eV; Heraeus Noblelight, Hanau, Germany) was mounted on a separate holder attached to a laboratory stand placed on the top of the mass spectrometer. The lamp was powered by a MANSION power supply (SDP-2405; Kwai Chung, N.T., Hong Kong). The microfabricated chip was obtained from the Division of Pharmaceutical Chemistry and Technology, Faculty of Pharmacy, University of Helsinki, Finland. The chip (33  $\times$  5  $\times$  1 mm) was an all-glass type with the nebulizing channel

cross section  $500 \times 250 \mu\text{m}$ , resistance platinum heater sputtered on the outer surface, and a fused-silica transfer capillary ( $50 \mu\text{m}$  i.d.,  $220 \mu\text{m}$  o.d.)<sup>24</sup> (see Figure S2, supporting information). The chip heater was powered by a IPS-603 power supply (ISO-TECH; Northamptonshire, UK). Nitrogen nebulizing gas was delivered from the mass spectrometer and regulated by a GFC5-011771 mass flow controller (Aalborg, Orangeburg, NY, USA). The discharge electrode was a standard APCI corona needle used in Thermo Fisher Scientific ion sources. The corona discharge was powered from the mass spectrometer. The optimized operating parameters of the ion source were as follows: nitrogen flow rate,  $60 \text{ mL/min}$ ; liquid sample flow rate,  $5 \mu\text{L/min}$ ; and microchip heating power,  $4.5 \text{ W}$ .

## 2.4 | Mass spectrometry

The mass spectra were acquired using an LCQ Fleet mass spectrometer (Thermo Fisher Scientific, San Jose, CA, USA) equipped with either the in-house micro-APCI/APPI source or the standard APCI/APPI source from Thermo Fisher Scientific. The capillary temperature was  $300^\circ\text{C}$  and the capillary and tube lens voltages were  $25.5 \text{ V}$  and  $80 \text{ V}$ , respectively. The standard APCI/APPI source was operated at the vaporizer temperature  $400^\circ\text{C}$  and the sheath and auxiliary gases set to 40 and 5 arbitrary units, respectively. The sample was directly infused into the micro-APCI/APPI source using an embedded syringe pump, or loop-injected ( $20 \mu\text{L}$ ) into the standard APCI/APPI source using a Rheos Allegro UHPLC pump (Flux Instruments, Basel, Switzerland) and Accela autosampler (Thermo Fisher Scientific). Data were measured and processed with Xcalibur software (Thermo Fisher Scientific).

## 2.5 | Calibration curves

The calibration curves were constructed from the signal intensities of methyl oleate ( $[\text{M}+\text{H}]^+$ ). The calibration standards were prepared in toluene in the concentration range of  $0.03\text{--}500 \mu\text{g/mL}$ . In the case of micro-APCI/APPI, the calibration standards were directly infused into the ion source at a flow rate of  $5 \mu\text{L/min}$ , and the signal was averaged from at least 100 scans. In case of high-flow APCI/APPI, the calibration standards were injected using a high-volume loop ( $20 \mu\text{L}$ ) into toluene flowing at  $100 \mu\text{L/min}$ . In this way, a wide zone rather than Gaussian peak was generated. The signal intensity in the zone plateau was averaged across at least 10 scans to obtain data equivalent to direct infusion at this flow rate. The noise signals were recorded for blank

toluene infused into ion sources at the same flow rates. The detection limits were calculated from the corresponding calibration curves for a signal-to-noise (S/N) ratio = 3.

## 3 | RESULTS AND DISCUSSION

### 3.1 | Ion source arrangement and working parameters

The arrangement of the micro-APCI/APPI source components was based on the original publications,<sup>21,22</sup> but the use of the newest version of the all-glass nebulizer and a mass spectrometer with different ion optics required verification of the optimum ion source geometry and working parameters. The chip was positioned close to the inlet capillary to maximize the ion collection efficiency, but far enough to accommodate a UV lamp and corona discharge needle as shown in Figure 1. The position of the needle was found to be crucial for efficient APCI. To avoid electric sparks, minimum distances between the needle tip and the inlet capillary and between the needle tip and the chip had to be maintained (distances ' $a_1$ ' and ' $a_2$ ' in Figure 1A). In our case, the minimum distances equaled  $3 \text{ mm}$  for the corona discharge voltage of  $1.5 \text{ kV}$ . The needle tip was positioned approximately  $1 \text{ mm}$  off-axis (distance ' $b$ ' in Figure 1A). When the corona discharge occurred directly in front of the inlet, no ions were recorded likely because of charge repulsing effects. The UV lamp was positioned from above, as close as possible to the spray (Figure 1B).

The chip position was optimized by monitoring the signal of reserpine recommended by the instrument manufacturers for tuning APCI and APPI sources. First, the distance of the terminal part of the chip with spraying nozzle to the inlet capillary (' $a_1$ ' plus ' $a_2$ ' in Figure 1A) was optimized separately for APCI and APPI. As evident from Figure 2A, the highest signal was recorded for the distance of  $10 \text{ mm}$  for both ionization modes, which was consistent with the published data for chip-based sources.<sup>21,24,25</sup> An effect of the chip tilt with respect to a horizontal plane hypothetically connecting the chip outlet and MS inlet was studied while keeping the optimum  $10\text{-mm}$  distance between the chip and mass spectrometer inlet. Interestingly, the charts obtained for APCI and APPI differed from each other (Figure 2B). The highest signal in APCI was observed for spraying on-axis and decreased with the increasing tilt angle. On the contrary, the signal in APPI showed two maxima, one for on-axis spraying ( $0^\circ$  tilt) and the second one for the chip tilted at  $40^\circ$ . The different shapes of the curves probably reflected diverse volumes and shapes

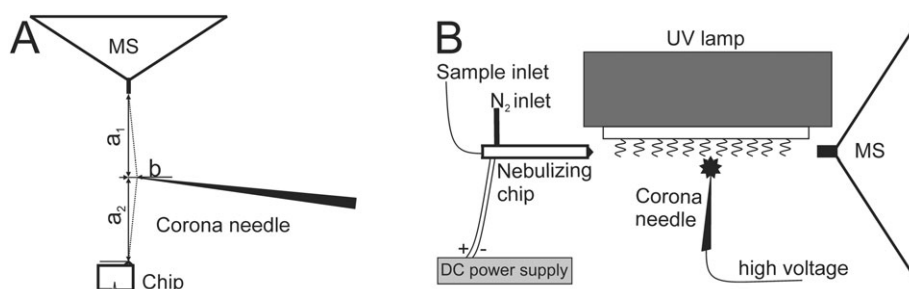


**FIGURE 1** Schema of the micro-APCI/APPI source arrangement. Top view of the needle position (A) and side view of the whole device (B)

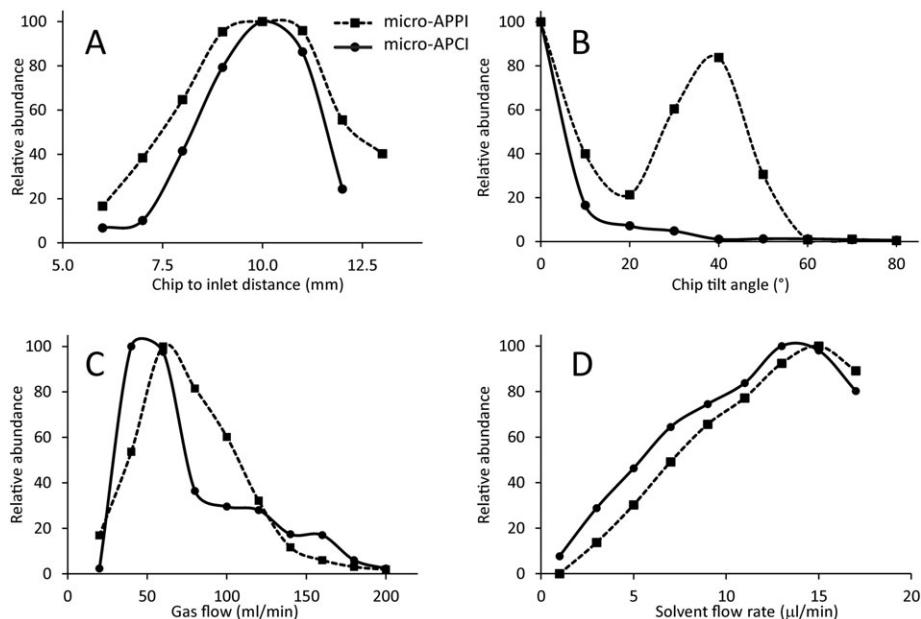


**FIGURE 2** Graphs showing the effects of the chip-to-inlet distance (A), chip tilt (B), nitrogen flow rate (C), and sample solution flow rate (D) on the signal intensity of reserpine ( $[M+H]^+$ ). The experimental conditions were as follows: A – 1  $\mu$ L/min of reserpine (10  $\mu$ g/mL) in 2-propanol/water (1:1), chip tilt 0°, nitrogen flow rate 180 mL/min; B – 1  $\mu$ L/min of reserpine (10  $\mu$ g/mL) in 2-propanol/water (1:1), chip-to-inlet distance 10 mm, nitrogen flow rate 180 mL/min; C – 1  $\mu$ L/min of reserpine (10  $\mu$ g/mL) in 2-propanol/water (1:1), chip-to-inlet distance 10 mm, chip tilt 0°; D – WE16:0-18:1(n-9) in toluene (62.5  $\mu$ g/mL), chip-to-inlet distance 10 mm, chip tilt 0°, nitrogen flow rate 60 mL/min

of the regions, where the ionizations take place. The chip tilt of 45° was previously used in micro-APCI arrangements.<sup>25,27</sup> For the next measurements, the chip sprayer was positioned on-axis to ensure optimum spraying for all three operating modes (APCI, APPI, and dual APCI/APPI).

The sample flow rate, nebulizing gas flow rate, and the vaporizer temperature settings depend on the analyte and mobile phase properties, which requires optimization of the source working parameters for each application. The chip platinum heater is known to have a limited lifetime at high electrical powers. For this reason, it was operated at the 'safe' limit of 4.5 W throughout this work. The vapor temperature at a distance of 10 mm from the chip was about 220°C.<sup>31</sup> The effect of the nebulizing gas flow rate on the signal intensity is demonstrated in Figure 2C. The maximum signal intensity of reserpine was observed at the nitrogen flow rates of 40 mL/min (micro-APCI) and 60 mL/min (micro-APPI). In general, the optimum nebulizing gas settings in this work were lower when compared with published values for pesticides and steroids,<sup>24,25,28</sup> ranging from 100 mL/min to 150 mL/min. Unlike ESI, mass spectrometers with APCI and APPI are considered mass-flow-sensitive detectors.<sup>32,33</sup> The response of such detectors is proportional to the amount of analyte reaching the detector in unit time. Consequently, the response increases with the sample flow rate. Such behavior has also been reported for chip-based micro-APCI and micro-APPI sources.<sup>21,22</sup> In our setup, mass-flow-sensitive behavior was observed for lipids. The intensity of WE16:0-18:1 ( $[M+H]^+$ ) linearly increased with the sample flow rate in the 1–15  $\mu$ L/min range for both micro-APCI and micro-APPI regimes (Figure 2D). Mass-flow-sensitive detectors are generally used at high sample flow rates as their application to low flows tends to be considered insensitive. However, it could not be necessarily the case for sources which maximize the efficiency of the ion generation and transport to a mass spectrometer.

### 3.2 | Solvents for micro-APCI/APPI of lipids

Neutral lipids are usually separated in non-aqueous reversed-phase, normal-phase or silver-ion chromatographic systems using low polarity solvents. Besides the effects on chromatography, the composition of the mobile phase has a great impact on the ionization process, and hence affects the detection sensitivity and mass spectra. Therefore, a sensitive detection in micro-APCI and/or micro-APPI requests solvents efficiently promoting ionization. For this reason, a set of experiments was performed (see section II, supporting information). Toluene significantly enhanced ionization of neutral lipids and exhibited a low level of background ions (high S/N ratios). Hence, it was selected for further experiments with the micro-APCI/APPI source.

### 3.3 | Mass spectra of neutral lipids

Micro-APCI/APPI spectra of selected lipids were compared with conventional high-flow source spectra to learn how they are influenced by the source design and its working parameters. As regards APCI, similar spectra were recorded for FAMES and WEs (Figures 3A and 3B and Figures S3A, S3B and S3C, S3D, supporting information), but certain differences were noticed in the spectra of squalene (Figures 3C and 3D), cholesterol (Figures 3E and 3F), and TG16:0/18:1/16:0 (Figures S3E and S3F, supporting information). Squalene in micro-APCI provided almost exclusively the  $[M+H]^+$  ( $m/z$  411) ion, while the high-flow spectrum showed also  $[M]^+$  ( $m/z$  410) and a fragment  $m/z$  341 consistent with allylic cleavage of the terminal C<sub>5</sub>H<sub>9</sub> from the molecular ion. Cholesterol exhibited an abundant water loss peak in both ion sources, but high-flow APCI provided also  $[M]^+$  ( $m/z$  386) and  $[M-H_2O]^+$  ( $m/z$  368), cf. Figures 3E and 3F. TG16:0/18:1/16:0 mostly fragmented by the elimination of fatty acids



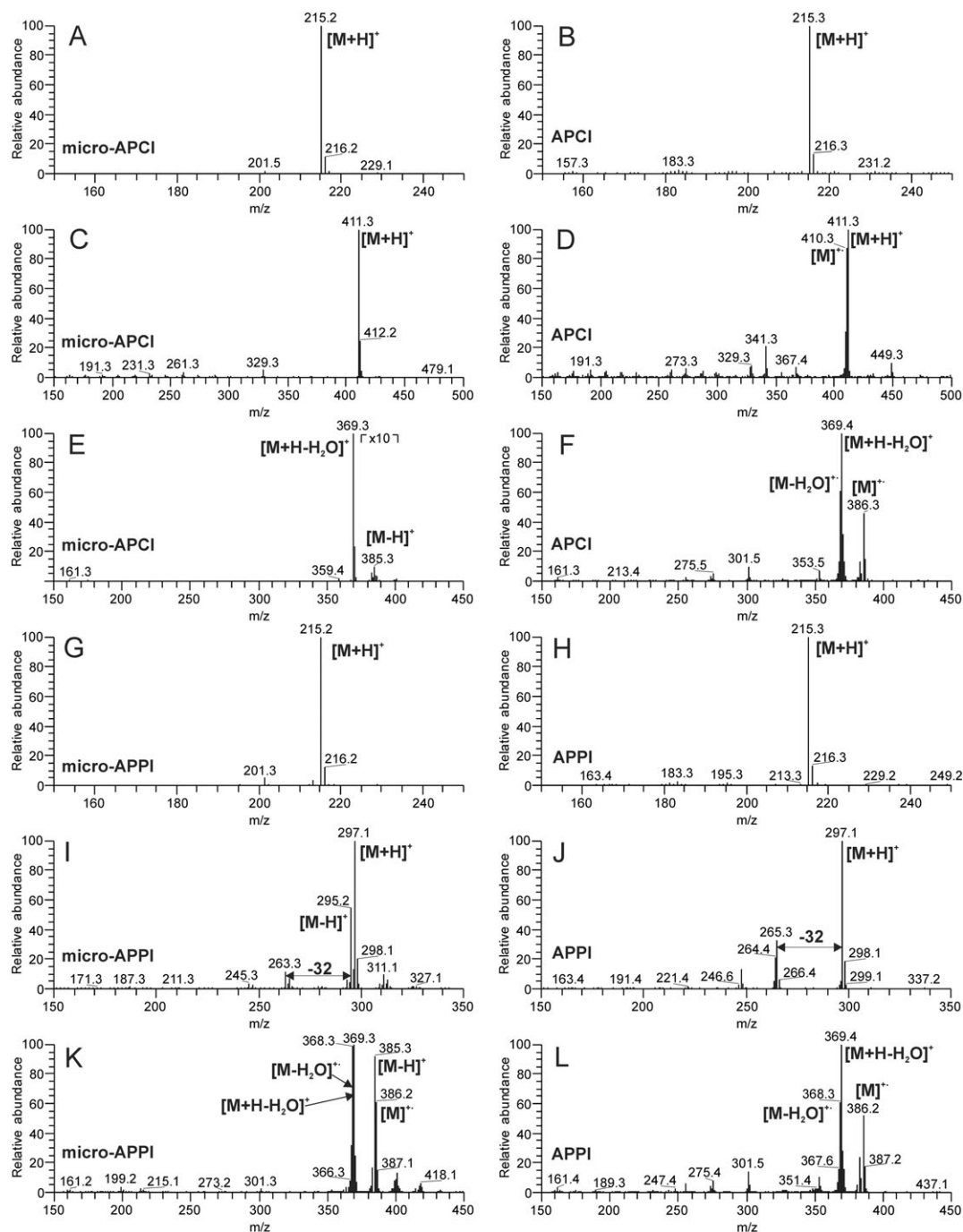


**FIGURE 3** Micro-APCI spectra (A, C, E) and conventional high-flow APCI spectra (B, D, F) of methyl laurate (A, B), squalene (C, D), and cholesterol (E, F). Micro-APPI spectra (G, I, K) and conventional high-flow APPI spectra (H, J, L) of methyl laurate (G, H), methyl oleate (I, J), and cholesterol (K, L). The compounds were dissolved in toluene (12.5  $\mu\text{g/mL}$ ). The spectra were recorded at the sample flow rate of 5  $\mu\text{L/min}$  (micro-APCI/APPI source) or 100  $\mu\text{L/min}$  (conventional high-flow APCI/APPI source)

(cf. Figures S3E and S3F, supporting information). The intensity of these fragments is commonly used for a disclosing fatty acid linked to the *sn*-2 position on glycerol.<sup>2</sup> Whereas in the micro-APCI spectra the fragment intensity ratio corresponded to the expected value, it was not the case for the high-flow source. Radical species corresponding to eliminations of palmitic acid ( $m/z$  576) and water ( $m/z$  814) from fully fragmented  $[\text{M}]^{\bullet+}$  were detected in the conventional high-flow APCI spectra. Clearly, all these lipids showed enhanced signals of radical cations in high-flow spectra, indicating more charge transfer and fewer proton transfer reactions. Proton transfer in micro-APCI is likely more efficient

because of the open design of the ion source and a smaller jet of vapors permitting water to diffuse in and be involved in the ionization processes.

In APPI, saturated methyl laurate was the only compound which exclusively provided  $[\text{M}+\text{H}]^+$  both in micro-APPI and high-flow APPI (Figures 3G and 3H). The APPI spectra of all other lipids showed a certain degree of fragmentation or simultaneous formation of radical species, particularly in micro-APPI. This can be illustrated by methyl oleate ( $m/z$  295) which eliminated methanol ( $m/z$  265) (see Figures 3I and 3J). In addition, the micro-APPI spectrum showed also  $[\text{M}-\text{H}]^+$

**TABLE 1** Analytical figures of merit for methyl oleate

Ionization mode	Detection limit		Dynamic range	Linear dynamic range
	pmol/s	nmol/mL	nmol/mL	nmol/mL
Micro-APCI	0.02	0.19	0.13–1986*	0.13–116
APCI	1.55	0.93	0.62–843	0.62–15
Micro-APPI	0.07	0.80	0.53–105	0.53–29
APPI	2.26	1.35	0.90–53	0.90–15
Micro-APCI/APPI	0.03	0.35	0.23–1686*	0.23–29
APCI/APPI	0.56	0.34	0.22–210	0.22–15

\*The highest concentration measured.

and its fragment after neutral loss of methanol ( $m/z$  263). Mass spectra of cholesterol (Figures 3K and 3L) showed  $[M+H]^+$ ,  $[M]^+$ ,  $[M+H_2O]^+$ , and  $[M-H_2O]^+$  as in APCI with the even-electron species more pronounced in micro-APPI. The high-flow APPI spectrum of TG16:0/18:1/16:0 (Figure S4F, supporting information) showed fragments of the protonated molecule with the intensity ratio reflecting oleic acid in the *sn*-2 position. In micro-APPI, the fragment intensity ratio was skewed; the protonated molecule showed multiple eliminations of hydrogen, and odd-electron fragments were detected (Figure S4E, supporting information). The micro-APPI spectra also provided signals above the  $m/z$  values of protonated molecules, likely products of oxidation (Figures 3I and 3K, Figure S4E, supporting information). It was concluded that micro-APPI provided more complex and poorly interpretable spectra, likely because of efficient direct photoionization of the analytes and their photochemical reactions.

When the ion sources were operated in dual APCI/APPI mode, the spectra showed mixtures of ions originated from APCI and APPI processes (Figure S5, supporting information). The dual mode had no advantage over the measurement in the individual ionization modes.

### 3.4 | Analytical figures of merit

Limit of detection, linear dynamic range, dynamic range, and signal repeatability were determined for the micro- and high-flow ion sources operated in the APCI, APPI and dual APCI/APPI modes for methyl oleate (see section 2). As discussed above, mass spectrometers with APCI and APPI sources are mass-flow-sensitive detectors and their response should be given in units of signal per mass flow rate of the sample. For practical reasons, the analytical figures of merit are presented here also in the concentration units. As evident from Table 1, the micro sources provided significantly lower detection limits than conventional high-flow counterparts. Enhanced performance of the micro sources could be explained by efficient ionization and better ion transport to the mass spectrometer. In addition, a low amount of solvent in the ion source led to a reduction in chemical noise and thus a better S/N ratio. The APCI mode proved to be more sensitive than APPI for both the micro- and the high-flow regimes. The limit of detection of methyl oleate established in this work was somewhat higher when compared with previous reports dealing with chip-based micro-APCI or micro-APPI.<sup>21,25</sup> However, the published data are difficult to compare with our results because they were measured using a triple quadrupole instrument for relatively easily ionizable steroids or acridine. As regards dynamic ranges and their linear portions, they were significantly wider for micro sources, particularly for micro-APCI spanning three orders of magnitude. Signal repeatability calculated as relative standard deviation (RSD) values from individual data points in the calibration curves were 2.5–5.5% for micro sources and 2.5–6.5% for conventional ionization sources. The analytical figures of merit for the micro source operated in dual APCI/APPI mode did not show any benefits justifying its application for quantitative analysis.

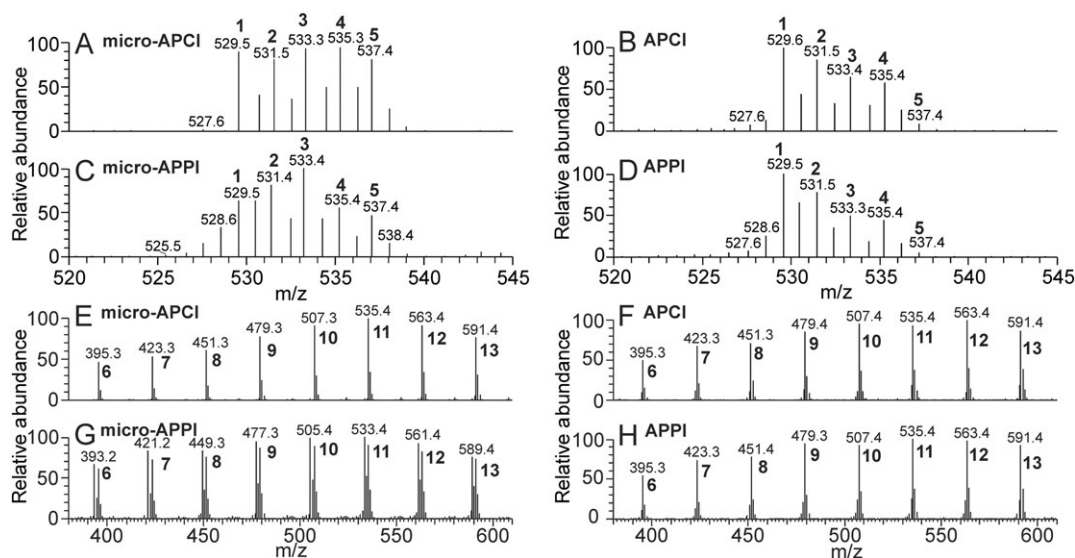


**FIGURE 4** Micro-APCI (A, E), conventional high-flow APCI (B, F), micro-APPI (C, G) and conventional high-flow APPI (D, H) spectra of wax esters differing by the number of double bonds (A–D) and differing by the number of carbon atoms (E–H). The compounds were dissolved in toluene (25  $\mu\text{mol/L}$ ). The spectra were recorded at the sample flow rate of 5  $\mu\text{L/min}$  (micro-APCI/APPI source) or 100  $\mu\text{L/min}$  (conventional high-flow APCI/APPI source). Compound identification: WE16:0-20:4(n-6) (1), WE18:0-18:3(n-3) (2), WE18:0-18:2(n-6) (3), WE16:0-18:1(n-9) (4), WE16:0-18:0 (5), WE12:0-14:1(n-5) (6), WE12:0-16:1(n-7) (7), WE12:0-18:1(n-9) (8), WE14:0-18:1(n-9) (9), WE16:0-18:1(n-9) (10), WE18:0-18:1(n-9) (11), WE20:0-18:1(n-9) (12), WE22:0-18:1(n-9) (13)

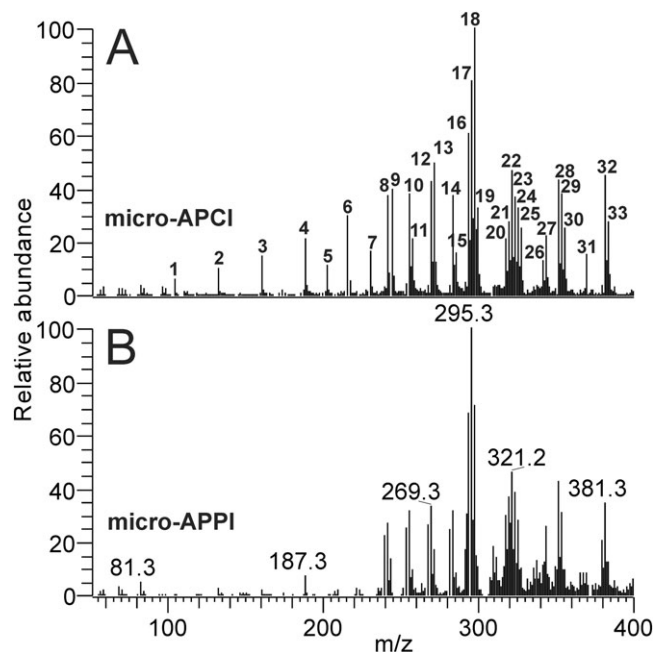


**FIGURE 5** Micro-APCI (A) and micro-APPI (B) spectra of Supelco 37 Component FAME Mix. The compounds were dissolved in toluene (0.1 mg/mL) and the spectra were recorded at the sample flow rate of 5  $\mu$ L/min. Compound identification: FAME4:0 (1), FAME6:0 (2), FAME8:0 (3), FAME10:0 (4), FAME11:0 (5), FAME12:0 (6), FAME13:0 (7), FAME14:1(n-5) (8), FAME14:0 (9), FAME15:1(n-5) (10), FAME15:0 (11), FAME16:1(n-7) (12), FAME16:0 (13), FAME17:1(n-5) (14), FAME17:0 (15), FAME18:3(n-6) + FAME18:3(n-3) (16), FAME18:2(n-6c) + FAME18:2(n-6 t) (17), FAME18:1(n-9c) + FAME18:1(n-9 t) (18), FAME18:0 (19), FAME20:5(n-3) (20), FAME20:4(n-6) (21), FAME20:3(n-6) + FAME20:3(n-3) (22), FAME20:2(n-6) (23), FAME20:1(n-9) (24), FAME20:0 (25), FAME21:0 (26), FAME22:6(n-3) (27), FAME22:2(n-6) (28), FAME22:1(n-9) (29), FAME22:0 (30), FAME23:0 (31), FAME24:1(n-9) (32), FAME24:0 (33)

### 3.5 | Effects of lipid structure on signal intensity

In conventional APCI of lipids, the intensity of the  $[M+H]^+$  ion depends on the number of double bonds and the alkyl chain length.<sup>7,13</sup> As in the case of other neutral lipids, the ionization efficiency of WEs increases with the number of double bonds and carbon atoms in their aliphatic chain.<sup>13</sup> To investigate these effects in micro sources, equimolar

mixtures of WEs were probed using micro- and high-flow APCI/APPI sources (Figure 4). The signal intensities gradually increased with the number of double bonds in high-flow APCI (Figure 4B), but, surprisingly, the responses in micro-APCI were almost equal (Figure 4A). In the case of APPI, the effect was not so clear, but the relative intensities of more saturated WEs were closer to unsaturated WEs than in high-flow APPI (Figures 4C and 4D). The equality of response factors is very attractive for quantitative analysis of neutral lipids because it circumvents the need for a standard of each molecular species within a lipid class. As regards the effect of chain length, insignificant differences between the high-flow and micro source were found in APCI (Figures 4E and 4F). The micro-APPI spectra (Figure 4G) were complicated by a series of  $[M-H]^+$  ions, as in the case of methyl oleate discussed above.

### 3.6 | Applications

Although the micro-APCI/APPI source is being developed mostly for HPLC/MS, its direct use for infusion experiments might be of interest for rapid and high-throughput applications. For this reason, several lipid samples were probed by their direct infusion into the micro source. The first sample was a commercial mixture of FAME standards. Of the 37 FAMES in this sample, 33 had a unique molecular weight, and the signals for all of them ( $[M+H]^+$ ) were clearly detected in the micro-APCI spectrum (Figure 5A). On the other hand, the micro-APPI spectrum (Figure 5B) was found to discriminate saturated FAMES and the spectra were complicated by the signals of  $[M-H]^+$ . The second sample was a mixture of wax esters (WEs) from jojoba oil. The oil is produced in the seeds of *Simmondsia chinensis* and used in cosmetics and personal care products. The abundant ions in the spectra (Figures 6A and 6B) were related to protonated molecules of doubly unsaturated WEs (WE38:2,  $m/z$  561; WE40:2,  $m/z$  589; WE42:2,  $m/z$  617; WE44:2,  $m/z$  645, WE46:2,  $m/z$  673).<sup>13</sup> Whereas the micro-APCI spectrum showed almost exclusively  $[M+H]^+$ , the micro-APPI spectrum also provided  $[M-H]^+$  ions, which made the data interpretation difficult. A mixture of TGs isolated from black currant seeds was selected as the third sample of neutral lipids (Figures 6C and 6D). Two groups of protonated molecules were observed in the

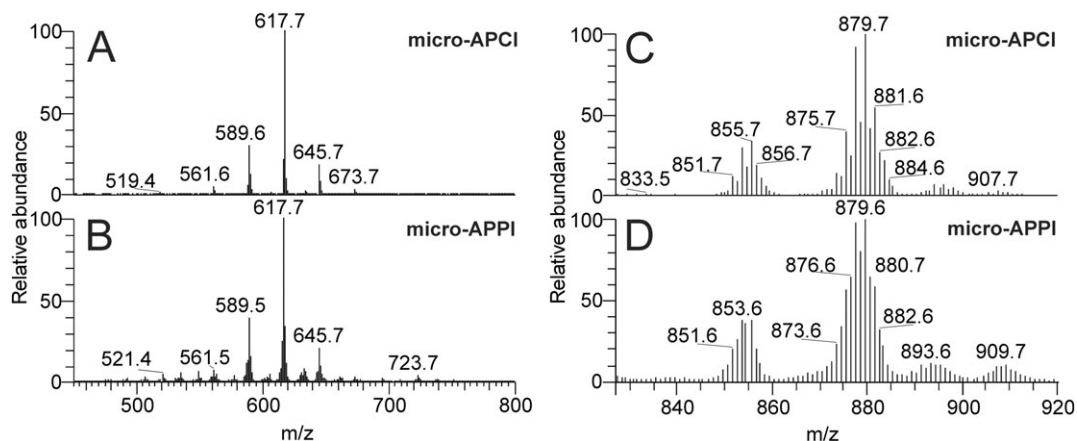


**FIGURE 6** Micro-APCI (A) and micro-APPI (B) spectra of jojoba oil wax esters. Micro-APCI (C) and micro-APPI (D) spectra of blackcurrant seed oil. The samples were dissolved in toluene (0.5 mg/mL) and the spectra were recorded at the sample flow rate of 5  $\mu$ L/min

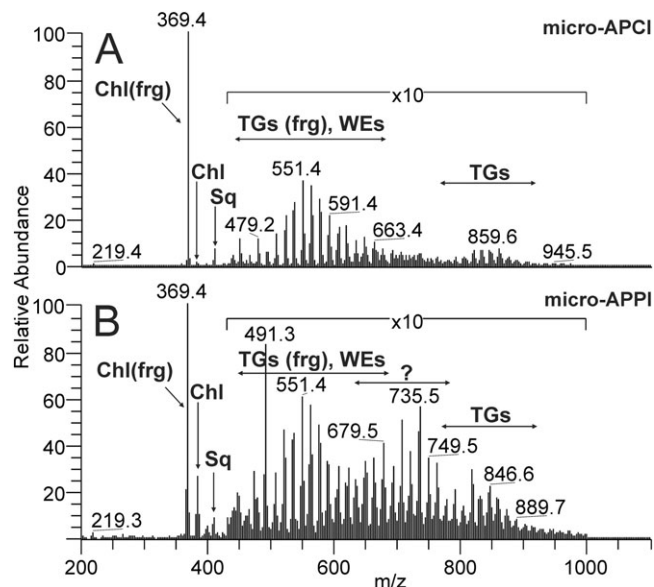


**FIGURE 7** Micro-APCI (A) and micro-APPI (B) spectra of lipids isolated from vernix caseosa. The sample was dissolved in toluene (0.2 mg/mL) and the spectra were recorded at the sample flow rate of 5  $\mu$ L/min

ranges  $m/z$  851–857 and  $m/z$  873–883. These signals were consistent with TGs having 55 carbons and 3–6 double bonds, and 57 carbons and 4–9 double bonds, respectively, and corresponded well to the known composition of blackcurrant seed oil.<sup>32</sup> The micro-APPI spectrum was difficult to interpret because of the formation of radical cations and hydrogen eliminations. The last sample was a total lipid extract from vernix caseosa, which is a cheese-like substance coating the skin of newborn human babies. Squalene, WEs, sterol esters, diol diesters, TGs, sterols, and ceramides are among the main components of vernix caseosa lipids.<sup>34</sup> The basepeak in the micro-APCI and micro-APPI spectra (Figure 7) was a cholesterol fragment ( $m/z$  369) originating from cholesterol and its esters.<sup>16,19,35–37</sup> Other signals were consistent with protonated squalene ( $m/z$  411), protonated TGs ( $m/z$  650–800), protonated WEs ( $m/z$  450–600), and other lipids. The micro-APPI spectrum was more crowded in the  $m/z$  625–800 range, likely because of the radical species and fragments generated by photoionization. Some of these signals might also represent polyunsaturated or polar lipids efficiently ionized by APPI. As regards the dual mode of the micro-APCI/APPI source, the spectra contained a mixture of ions generated by APCI and APPI processes, as shown in Figure S7 (supporting information).

## 4 | CONCLUSIONS

The micro-APCI/APPI source with a heated chip nebulizer was assembled and connected to an ion trap mass spectrometer. Data showed that the ion source could be used for the sensitive detection of neutral lipids like FAMES, WEs, TGs, squalene, or cholesterol. The ion source was found to behave as a mass-flow-sensitive detector in both APCI and APPI modes. The best analytical figures of merit were obtained in micro-APCI mode; the detection limit of methyl oleate infused into the ion source was 200 fmol/ $\mu$ L, and the linear dynamic range spanned three orders of magnitude. Among the tested solvents,

toluene made it possible to detect tested lipids with the highest sensitivity. Besides its ability to promote ionization of lipids, toluene also exhibited low background. The high sensitivity of micro sources was suggested to be due to efficient generation and transfer of ions into the instrument. The mass spectra of lipids like methyl laurate were not affected by the ionization mode (APCI vs. APPI) or sample flow rate (micro vs. conventional source). However, the spectra of most lipids exhibited substantial differences reflecting different processes taking place during ionization. The micro-APCI spectra were easy to interpret; they mostly showed even-electron ions like protonated molecules and expected neutral loss fragments. The signal intensity of the molecular species within a lipid class as demonstrated for WEs was found to be independent of the number of double bonds. The efficient protonation in micro-APCI of samples dissolved in toluene was explained by easy diffusion of ambient moisture into the ionization region of the source due to its small dimensions and open design. On the other hand, the micro-APPI spectra were complicated by a number of other ions in addition to even-electron species. These ions were odd-electron fragments, products of multiple hydrogen eliminations, and oxidation products. Their formation was explained by direct photoionization processes facilitated by low amounts of solvent acting as a dopant. The dual mode of the APCI/APPI source was tested in the hope of increased detection sensitivity, but it was not the case for the investigated lipids. The APCI/APPI spectra showed features reflecting both APCI and APPI processes, which rather complicated data interpretation. Finally, the usefulness of the micro source, particularly in the micro-APCI regime, was demonstrated for several lipid samples.

Micro-APCI-MS thus seems to be a promising analytical technique for neutral lipids. It offers high sensitivity and high-quality spectra. Reduced sample flow rate brings benefits such as the use of small sample volumes and low consumption of expensive and toxic solvents. Our further research will be focused on the applications of the micro-APCI/APCI source as a detector of neutral lipids in capillary and micro-HPLC.

## ACKNOWLEDGEMENTS

This project was financially supported by the Czech Science Foundation (Project No. 16-01639S) and Charles University in Prague (Project SVV). The authors are indebted to Markus Haapala (Mass Spectrometry and Metabolomics Group, Faculty of Pharmacy, University of Helsinki) for the microchips, and the Development Center Workshops of IOCB, Prague, for indispensable assistance on this project.

## ORCID

Josef Cvačka  <http://orcid.org/0000-0002-3590-9009>

## REFERENCES

- Kaupilla TJ, Syage JA, Benter T. Recent developments in atmospheric pressure photoionization-mass spectrometry. *Mass Spectrom Rev.* 2017;36(3):423–449. <https://doi.org/10.1002/mas.21477>
- Byrdwell WC. Atmospheric pressure chemical ionization mass spectrometry for analysis of lipids. *Lipids.* 2001;36(4):327–346. <https://doi.org/10.1007/s11745-001-0725-5>

3. Byrdwell WC. *Modern Methods for Lipid Analysis by Liquid Chromatography/Mass Spectrometry and Related Techniques*. 1st ed. Champaign, IL: AOCS Publishing; 2005.
4. Syage JA, Hanold KA, Lynn TC, Horner JA, Thakur RA. Atmospheric pressure photoionization II. Dual source ionization. *J Chromatogr A*. 2004;1050(2):137-149. <https://doi.org/10.1016/j.chroma.2004.08.033>
5. Marchi I, Rudaz S, Veuthey JL. Atmospheric pressure photoionization for coupling liquid-chromatography to mass spectrometry: A review. *Talanta*. 2009;78(1):1-18. <https://doi.org/10.1016/j.talanta.2008.11.031>
6. Cai SS, Syage JA. Comparison of atmospheric pressure photoionization, atmospheric pressure chemical ionization, and electrospray ionization mass spectrometry for analysis of lipids. *Anal Chem*. 2006;78(4):1191-1199. <https://doi.org/10.1021/ac0515834>
7. Holčápek M, Lísá M, Jandera P, Kabátová N. Quantitation of triacylglycerols in plant oils using HPLC with APCI-MS, evaporative light-scattering, and UV detection. *J Sep Sci*. 2005;28(12):1315-1333. <https://doi.org/10.1002/jssc.200500088>
8. Lísá M, Netušilová K, Franěk L, Dvořáková H, Vrkoslav V, Holčápek M. Characterization of fatty acid and triacylglycerol composition in animal fats using silver-ion and non-aqueous reversed-phase high-performance liquid chromatography/mass spectrometry and gas chromatography/ flame ionization detection. *J Chromatogr A*. 2011;1218(42):7499-7510. <https://doi.org/10.1016/j.chroma.2011.07.032>
9. Háková E, Vrkoslav V, Míková R, Schwarzová-Pecková K, Bosáková Z, Cvačka J. Localization of double bonds in triacylglycerols using high-performance liquid chromatography/atmospheric pressure chemical ionization ion-trap mass spectrometry. *Anal Bioanal Chem*. 2015;407(17):5175-5188. <https://doi.org/10.1007/s00216-015-8537-1>
10. Kofroňová E, Cvačka J, Vrkoslav V, et al. A comparison of HPLC/APCI-MS and MALDI-MS for characterising triacylglycerols in insects: Species-specific composition of lipids in the fat bodies of bumblebee males. *J Chromatogr B*. 2009;877(30):3878-3884. <https://doi.org/10.1016/j.jchromb.2009.09.040>
11. Vrkoslav V, Cvačka J. Identification of the double-bond position in fatty acid methyl esters by liquid chromatography/atmospheric pressure chemical ionisation mass spectrometry. *J Chromatogr A*. 2012;1259:244-250. <https://doi.org/10.1016/j.chroma.2012.04.055>
12. Řezanka T. Analysis of polyunsaturated fatty acids using high performance liquid chromatography - Atmospheric pressure chemical ionization mass spectrometry. *J High Resolut Chromatogr*. 2000;23(4):338-342.
13. Vrkoslav V, Urbanová K, Cvačka J. Analysis of wax ester molecular species by high performance liquid chromatography/atmospheric pressure chemical ionisation mass spectrometry. *J Chromatogr A*. 2010;1217(25):4184-4194. <https://doi.org/10.1016/j.chroma.2009.12.048>
14. Vrkoslav V, Háková M, Pecková K, Urbanová K, Cvačka J. Localization of double bonds in wax esters by high-performance liquid chromatography/atmospheric pressure chemical ionization mass spectrometry utilizing the fragmentation of acetonitrile-related adducts. *Anal Chem*. 2011;83(8):2978-2986. <https://doi.org/10.1021/ac1030682>
15. Butovich IA, Wojtowicz JC, Molai M. Human tear film and meibum. Very long chain wax esters and (O-acyl)-omega-hydroxy fatty acids of meibum. *J Lipid Res*. 2009;50(12):2471-2485. <https://doi.org/10.1194/jlr.M900252-JLR200>
16. Kalužiková A, Vrkoslav V, Harazim E, et al. Cholesteryl esters of omega-(O-acyl)-hydroxy fatty acids in vernix caseosa. *J Lipid Res*. 2017;58(8):1579-1590. <https://doi.org/10.1194/jlr.M075333>
17. Šubčíková L, Hoskovec M, Vrkoslav V, et al. Analysis of 1,2-diol diesters in vernix caseosa by high-performance liquid chromatography-atmospheric pressure chemical ionization mass spectrometry. *J Chromatogr A*. 2015;1378:8-18. <https://doi.org/10.1016/j.chroma.2014.11.075>
18. Kim D, Park JB, Choi WK, Lee SJ, Lim I, Bae SK. Simultaneous determination of beta-sitosterol, campesterol, and stigmasterol in rat plasma by using LC-APCI-MS/MS: Application in a pharmacokinetic study of a titrated extract of the unsaponifiable fraction of Zea mays L. *J Sep Sci*. 2016;39(21):4060-4070. <https://doi.org/10.1002/jssc.201600589>
19. Palmgren JJ, Toyras A, Mauriala T, Monkkonen J, Auriola S. Quantitative determination of cholesterol, sitosterol, and sitostanol in cultured Caco-2 cells by liquid chromatography-atmospheric pressure chemical ionization mass spectrometry. *J Chromatogr B*. 2005;821(2):144-152. <https://doi.org/10.1016/j.jchromb.2005.04.029>
20. Cai SS, Syage JA. Atmospheric pressure photoionization mass spectrometry for analysis of fatty acid and acylglycerol lipids. *J Chromatogr A*. 2006;1110(1-2):15-26. <https://doi.org/10.1016/j.chroma.2006.01.050>
21. Östman P, Marttila SJ, Kotiaho T, Franssila S, Kostianen R. Microchip atmospheric pressure chemical ionization source for mass spectrometry. *Anal Chem*. 2004;76(22):6659-6664. <https://doi.org/10.1021/ac049345g>
22. Kauppila TJ, Östman P, Marttila S, et al. Atmospheric pressure photoionization-mass spectrometry with a microchip heated nebulizer. *Anal Chem*. 2004;76(22):6797-6801. <https://doi.org/10.1021/ac049058c>
23. Saarela V, Haapala M, Kostianen R, Kotiaho T, Franssila S. Glass microfabricated nebulizer chip for mass spectrometry. *Lab Chip*. 2007;7(5):644-646. <https://doi.org/10.1039/b700101k>
24. Krueve A, Haapala M, Saarela V, et al. Feasibility of capillary liquid chromatography-microchip-atmospheric pressure photoionization-mass spectrometry for pesticide analysis in tomato. *Anal Chim Acta*. 2011;696(1-2):77-83. <https://doi.org/10.1016/j.aca.2011.04.006>
25. Ahonen LL, Haapala M, Saarela V, Franssila S, Kotiaho T, Kostianen R. Feasibility of capillary liquid chromatography/microchip atmospheric pressure photoionization mass spectrometry in analyzing anabolic steroids in urine samples. *Rapid Commun Mass Spectrom*. 2010;24(7):958-964. <https://doi.org/10.1002/rcm.4468>
26. Haapala M, Luosujarvi L, Saarela V, et al. Microchip for combining gas chromatography or capillary liquid chromatography with atmospheric pressure photoionization-mass spectrometry. *Anal Chem*. 2007;79(13):4994-4999. <https://doi.org/10.1021/ac070157a>
27. Haapala M, Saarela V, Pól J, et al. Integrated liquid chromatography-heated nebulizer microchip for mass spectrometry. *Anal Chim Acta*. 2010;662(2):163-169. <https://doi.org/10.1016/j.aca.2010.01.005>
28. Östman P, Jantti S, Grigoras K, et al. Capillary liquid chromatography-microchip atmospheric pressure chemical ionization-mass spectrometry. *Lab Chip*. 2006;6(7):948-953. <https://doi.org/10.1039/b601290f>
29. Vacek M, Zarevúcka M, Wimmer Z, et al. Lipase-mediated hydrolysis of blackcurrant oil. *Enzyme Microb Technol*. 2000;27(7):531-536. [https://doi.org/10.1016/s0141-0229\(00\)00239-8](https://doi.org/10.1016/s0141-0229(00)00239-8)
30. Míková R, Vrkoslav V, Hanus R, et al. Newborn boys and girls differ in the lipid composition of vernix caseosa. *PLoS One*. 2014;9(6). <https://doi.org/10.1371/journal.pone.0099173>
31. Parshintsev J, Vaikkinen A, Lipponen K, et al. Desorption atmospheric pressure photoionization high-resolution mass spectrometry: a complementary approach for the chemical analysis of atmospheric aerosols. *Rapid Commun Mass Spectrom*. 2015;29(13):1233-1241. <https://doi.org/10.1002/rcm.7219>
32. Cavaliere C, Foglia P, Pastorini E, Samperi R, Lagana A. Liquid chromatography/tandem mass spectrometric confirmatory method for determining aflatoxin M1 in cow milk - Comparison between electrospray and atmospheric pressure photoionization sources. *J Chromatogr A*. 2006;1101(1-2):69-78. <https://doi.org/10.1016/j.chroma.2005.09.060>
33. Takino M, Daishima S, Nakahara T. Liquid chromatography/mass spectrometric determination of patulin in apple juice using atmospheric pressure photoionization. *Rapid Commun Mass Spectrom*. 2003;17(17):1965-1972. <https://doi.org/10.1002/rcm.1136>

34. Karkkainen J, Nikkari T, Ruponen S, Haahti E. Lipids of vernix caseosa. *J Invest Dermatol.* 1965;44(5):333-338. <https://doi.org/10.1038/jid.1965.58>
35. Proitsi P, Kim M, Whiley L, et al. Plasma lipidomics analysis finds long chain cholesteryl esters to be associated with Alzheimer's disease. *Transl Psychiatry.* 2015;5:8. <https://doi.org/10.1038/tp.2014.127>
36. Rejšek J, Vrkoslav V, Vaikkinen A, et al. Thin-layer chromatography/desorption atmospheric pressure photoionization orbitrap mass spectrometry of lipids. *Anal Chem.* 2016;88(24):12279-12286. <https://doi.org/10.1021/acs.analchem.6b03465>
37. Butovich IA. Cholesteryl esters as a depot for very long chain fatty acids in human meibum. *J Lipid Res.* 2009;50(3):501-513. <https://doi.org/10.1194/jlr.M800426-JLR200>

## SUPPORTING INFORMATION

Additional Supporting Information may be found online in the supporting information tab for this article.

**How to cite this article:** Vrkoslav V, Rumlová B, Strmeň T, Nekvasilová P, Šulc M, Cvačka J. Applicability of low-flow atmospheric pressure chemical ionization and photoionization mass spectrometry with a microfabricated nebulizer for neutral lipids. *Rapid Commun Mass Spectrom.* 2018;32:639-648. <https://doi.org/10.1002/rcm.8086>

Supporting material.

## **Applicability of low-flow APCI and APPI mass spectrometry with a microfabricated nebulizer for neutral lipids**

Vladimír Vrkoslav<sup>1</sup>, Barbora Rumlová<sup>2</sup>, Timotej Strmeň<sup>1,2</sup>, Pavlína Nekvasilová<sup>2</sup>, Miloslav Šulc<sup>3</sup>, Josef Cvačka<sup>1,2,1</sup>

<sup>1</sup> *Institute of Organic Chemistry and Biochemistry of the Czech Academy of Sciences, Flemingovo nám. 2, CZ-166 10 Prague 6, Czech Republic*

<sup>2</sup> *Department of Analytical Chemistry, Faculty of Science, Charles University in Prague, Hlavova 2030/8, CZ-128 43 Prague 2, Czech Republic*

<sup>3</sup> *Czech University of Life Sciences, Faculty of Agrobiological Sciences, Department of Chemistry, Kamýcká 129, CZ-165 00 Prague 6, Czech Republic*

### Table of contents:

I. Supporting figures . . . . .	2
Figure S1. Photograph of the microAPCI/APCI ion source . . . . .	2
Figure S2. Photograph of the all-glass heated chip nebulizer . . . . .	3
Figure S3. Micro-APCI spectra and conventional high-flow APCI spectra . . . . .	4
Figure S4. Micro-APPI spectra and conventional high-flow APPI spectra . . . . .	5
Figure S5. Dual micro-APCI/APPI spectra and conventional high-flow dual APCI/APPI spectra . . . . .	6
Figure S6. Dual micro-APCI/APPI spectra and conventional high-flow dual APCI/APPI spectra of wax esters . . . . .	7
Figure S7. Dual micro-APCI/APPI spectra of lipid mixtures . . . . .	8
II. Solvents for micro-APCI/APPI of lipids . . . . .	9

---

<sup>1</sup> Correspondence to: Josef Cvačka, Institute of Organic Chemistry and Biochemistry of the Czech Academy of Sciences, Flemingovo nám. 2, CZ-166 10 Prague, Czech Republic  
E-mail: josef.cvacka@uochb.cas.cz

## I. Supporting figures

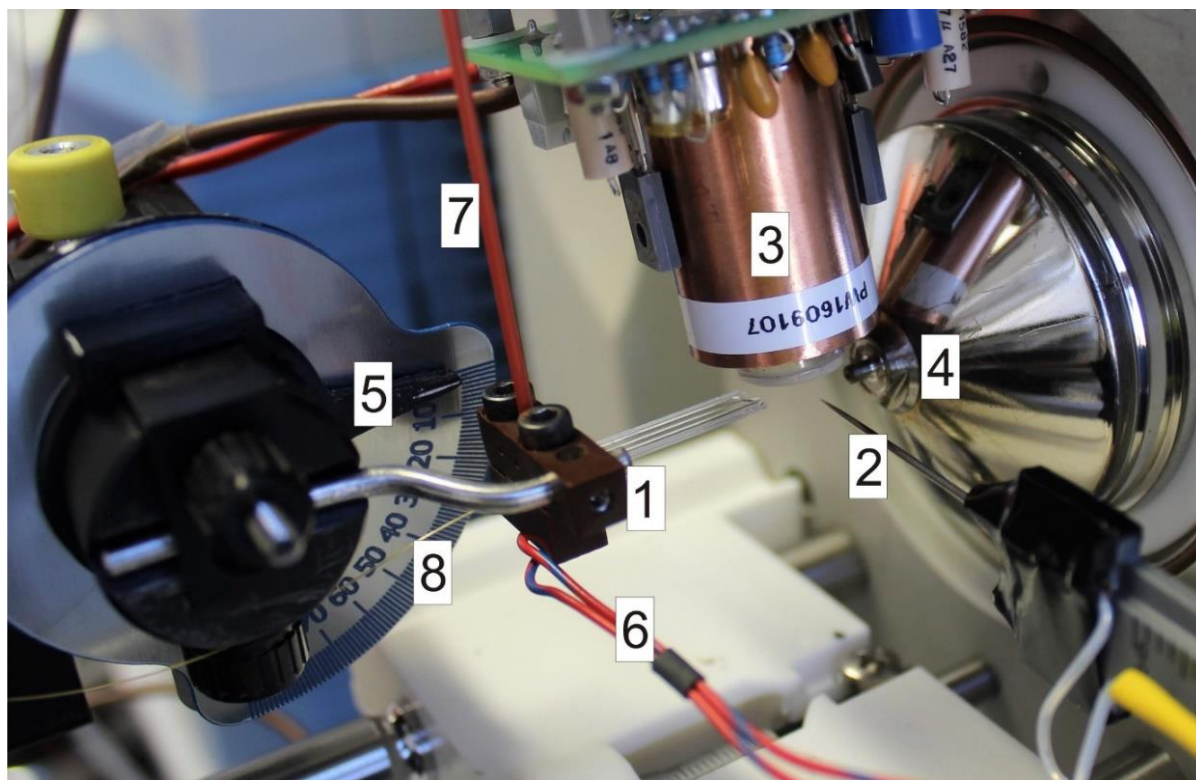


**Figure S1.** Photograph of the microAPCI/APCI ion source. 1 – nebulizing microchip in a holder, 2 – corona discharge needle, 3 – UV lamp, 4 – mass spectrometer inlet, 5 – micromanipulator, 6 – connecting cables for microchip heater, 7 – inlet capillary for nitrogen, 8 – inlet capillary for sample. For the micro-APCI and micro-APPI modes, the ion source was operated without UV lamp and corona discharge needle, respectively.



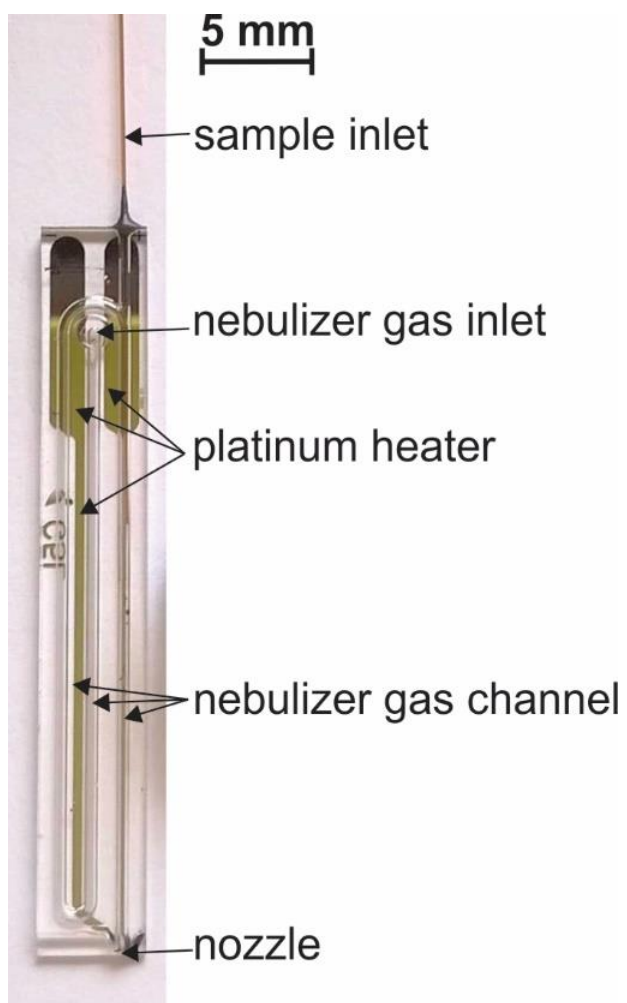


**Figure S2.** Photograph of the all-glass heated chip nebulizer.

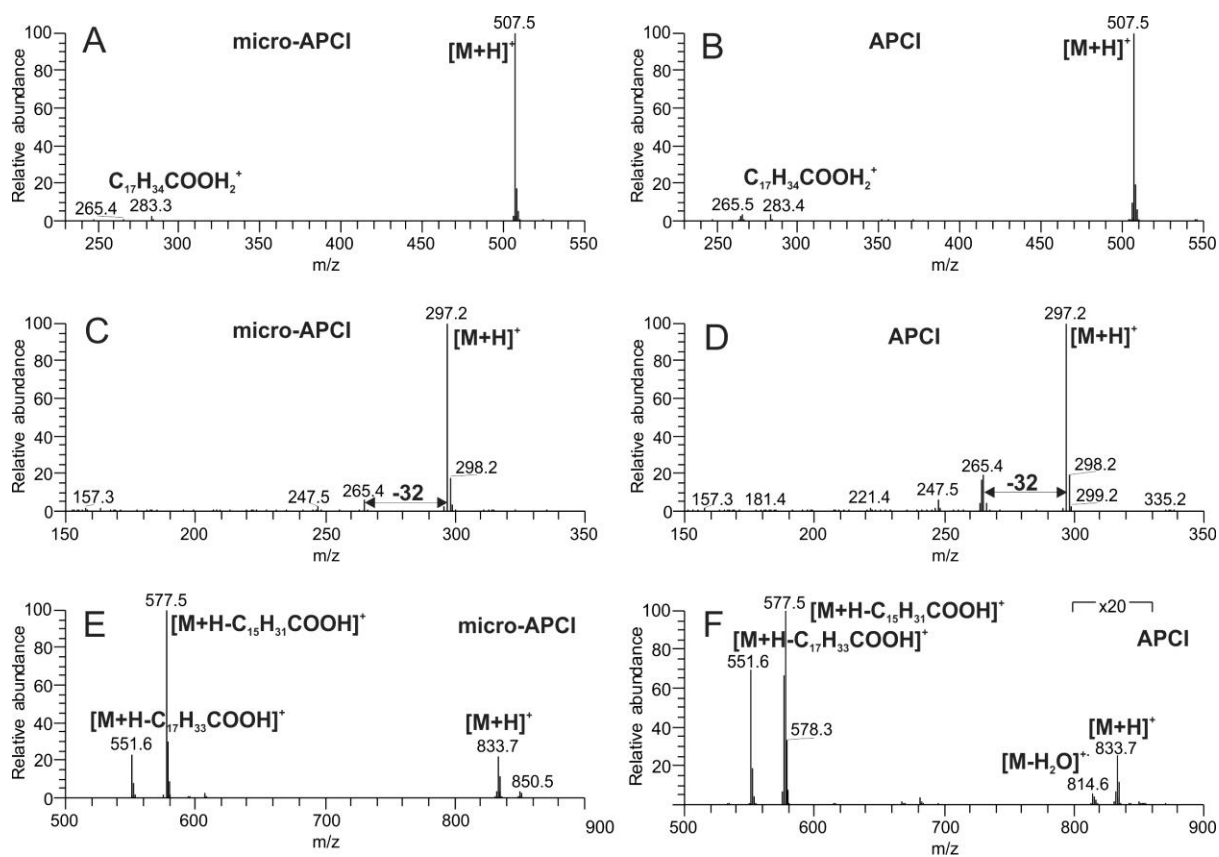


**Figure S3.** Micro-APCI spectra and conventional high-flow APCI spectra of WE16:0-18:1(n-9) (A, B) FAME18:1(n-9) (C, D), and TG16:0/18:1/16:0 (E, F). The compounds were dissolved in toluene (12.5  $\mu\text{g/mL}$ ). The spectra were recorded at the sample flow rate of 5  $\mu\text{L/min}$  (micro-APCI/APPI source) or 100  $\mu\text{L/min}$  (conventional high-flow APCI/APPI source).

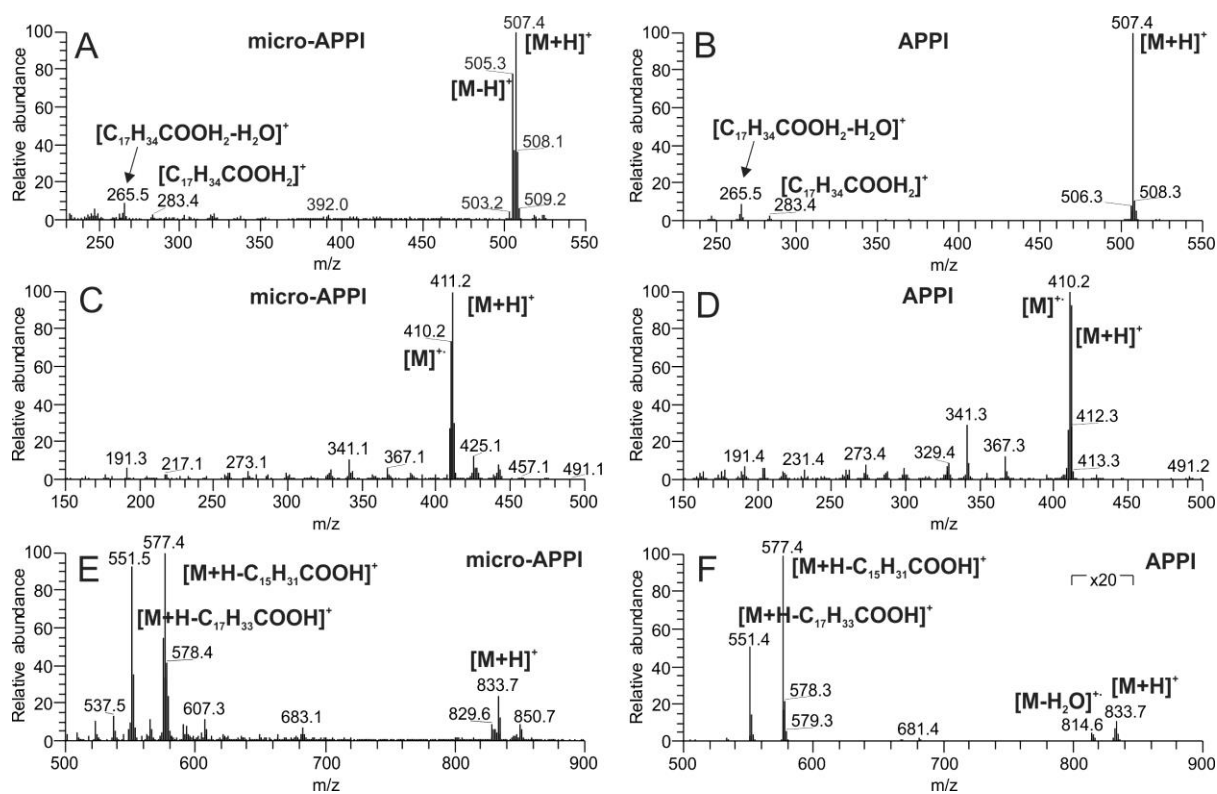


**Figure S4.** Micro-APPI spectra and conventional high-flow APPI spectra of WE16:0-18:1(n-9) (A, B) squalene (C, D), and TG16:0/18:1/16:0 (E, F). The compounds were dissolved in toluene (12.5  $\mu\text{g/mL}$ ). The spectra were recorded at the sample flow rate of 5  $\mu\text{L/min}$  (micro-APCI/APPI source) or 100  $\mu\text{L/min}$  (conventional high-flow APCI/APPI source).

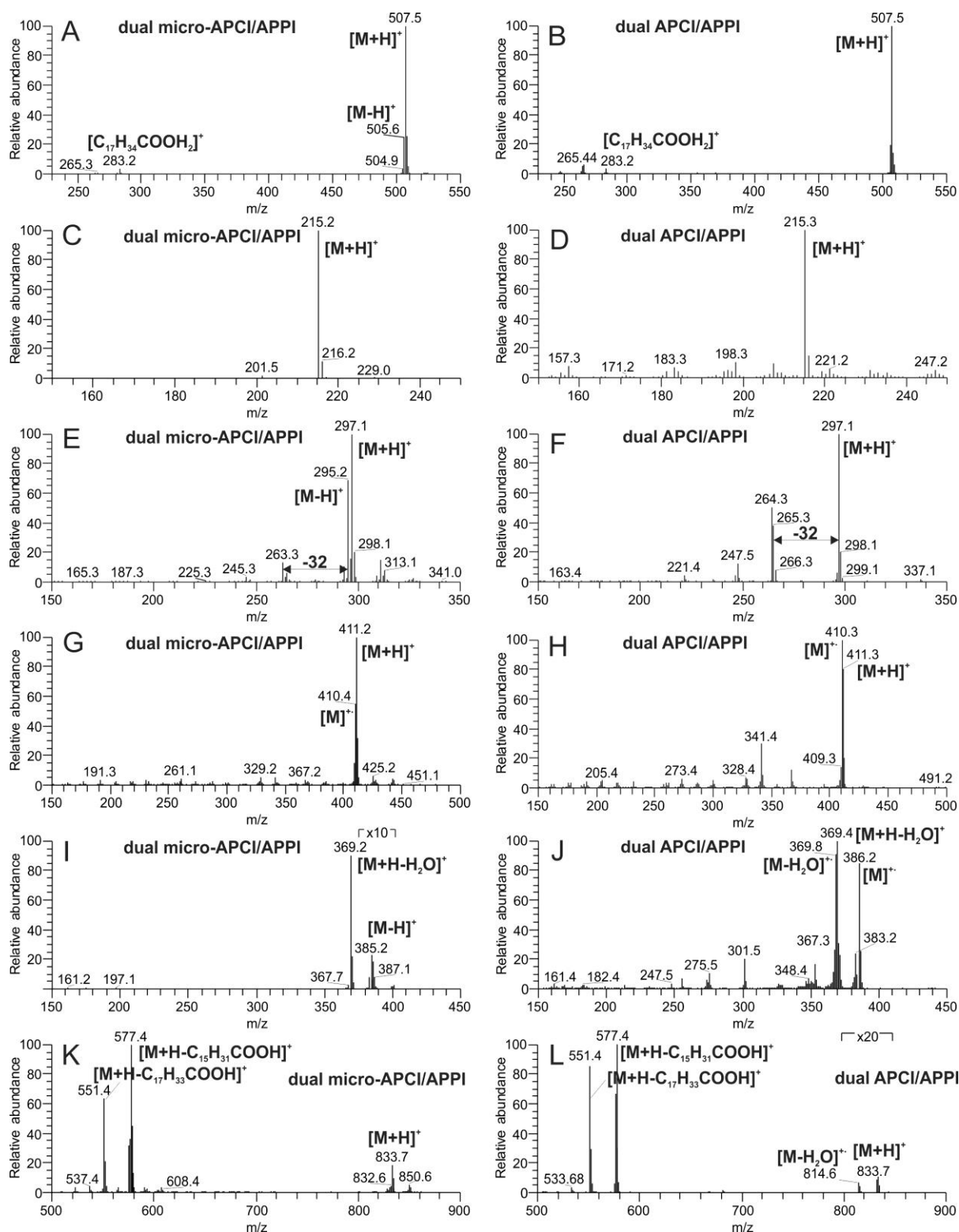


**Figure S5.** Dual micro-APCI/APPI spectra and conventional high-flow dual APCI/APPI spectra of WE16:0-18:1(n-9) (A, B), FAME12:0, (C, D), FAME18:1(n-9) (E, F), squalene (G, H), cholesterol (I, J), and TG16:0/18:1/16:0 (K, L). The compounds were dissolved in toluene (12.5  $\mu\text{g/mL}$ ). The spectra were recorded at the sample flow rate of 5  $\mu\text{L/min}$  (micro-APCI/APPI source) or 100  $\mu\text{L/min}$  (conventional high-flow APCI/APPI source).

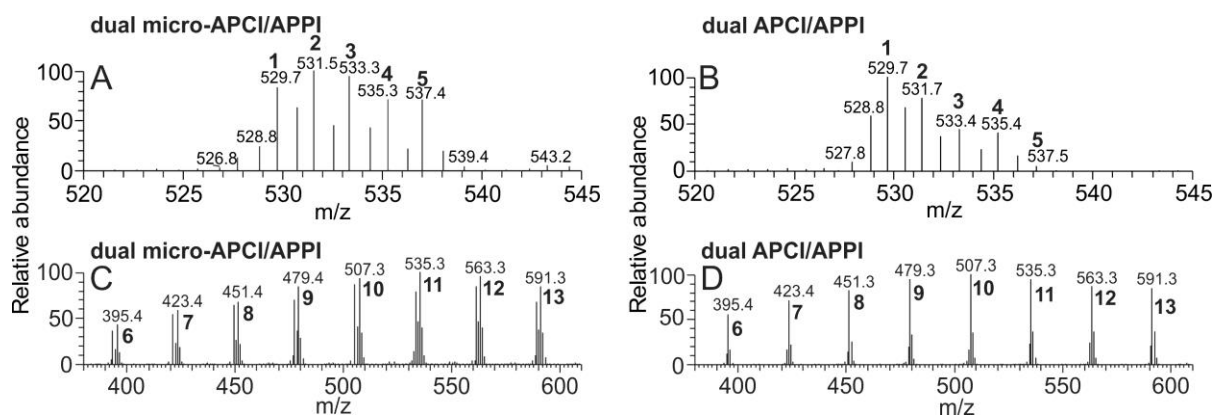


**Figure S6.** Dual micro-APCI/APPI spectra and conventional high-flow dual APCI/APPI spectra of wax esters differing by the number of double bonds (A, B) and differing by the number carbon atoms (C, D). The compounds were dissolved in toluene (25  $\mu\text{mol/L}$ ). The spectra were recorded at the sample flow rate of 5  $\mu\text{L/min}$  (micro-APCI/APPI source) or 100  $\mu\text{L/min}$  (conventional high-flow APCI/APPI source). Compound identification: 16:0-20:4(n-6) (1), WE18:0-18:3(n-3) (2), WE18:0-18:2(n-6) (3), WE16:0-18:1(n-9) (4), WE16:0-18:0 (5), WE12:0-14:1(n-5) (6), WE12:0-16:1(n-7) (7), WE12:0-18:1(n-9) (8), WE14:0-18:1(n-9) (9), WE16:0-18:1(n-9) (10), WE18:0-18:1(n-9) (11), WE20:0-18:1(n-9) (12), WE22:0-18:1(n-9) (13).

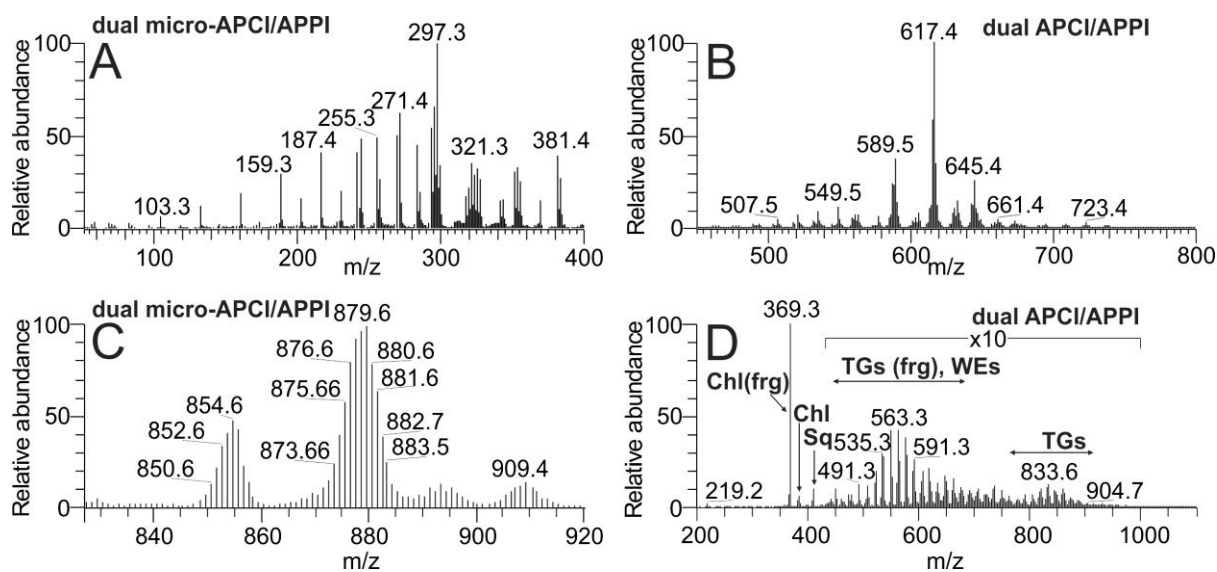


**Figure S7.** Dual micro-APCI/APPI spectra of Supelco 37 Component FAME Mix (0.1 mg/mL) (A), jojoba oil wax esters (0.5 mg/mL) (B), black currant seeds oil (0.5 mg/mL) (C), and lipids isolated from vernix caseosa (0.2 mg/mL) (D). The compounds were dissolved in toluene and the spectra were recorded at the sample flow rate of 5  $\mu$ L/min.

## II. Solvents for micro-APCI/APPI of lipids

Two lipid standards, methyl laurate (saturated, nonpolar compound) and cholesterol (unsaturated compound of higher polarity) were dissolved in toluene, hexane, chloroform, acetone, ethyl acetate, methanol, or acetonitrile and infused into the micro ion source operated in APCI, APPI, and dual APCI/APPI modes. The intensities of base peaks ( $[M+H]^+$  for methyl laurate and  $[M+H-H_2O]^+$  for cholesterol) were compared across the solvents and the ionization modes (Figure S8). For both analytes, the highest signals were observed in toluene. Toluene is known to readily form radical cations and it is a popular dopant widely used for APPI<sup>1</sup>. Toluene radical cations likely reacted with residual water to form protonated clusters, which subsequently transferred a proton to the analyte. Other tested solvents turned out to be significantly less effective or even ineffective. The lowest signals were observed for all three ionization modes in ethyl acetate and acetone. Both of them are photoionizable, but at the same time, they have relatively high proton affinities. These solvents likely efficiently competed with the analyte for protons. The order of the solvents in terms of ionization efficiency differed from data for high-flow conventional APPI published earlier<sup>2</sup>. It could be attributed to different analytes used for the experiments, different levels of impurities in the solvents, and possibly different conditions during the ionization, for instance, a lower concentration of solvent vapors or easier penetration of moisture into the ionization region of the micro-APCI/APPI source. No major increase of signal intensity was detected when the micro source was operated in dual APCI/APPI mode. Conversely, signal significantly decreased for both analytes in toluene and chloroform in dual mode. Only the signal of cholesterol dissolved in acetone increased to some extent. Therefore, dual APCI/APPI mode did not provide higher sensitivity for neutral lipids, similarly to the majority of aromatic compounds and drugs in conventional high-flow source<sup>3</sup>.

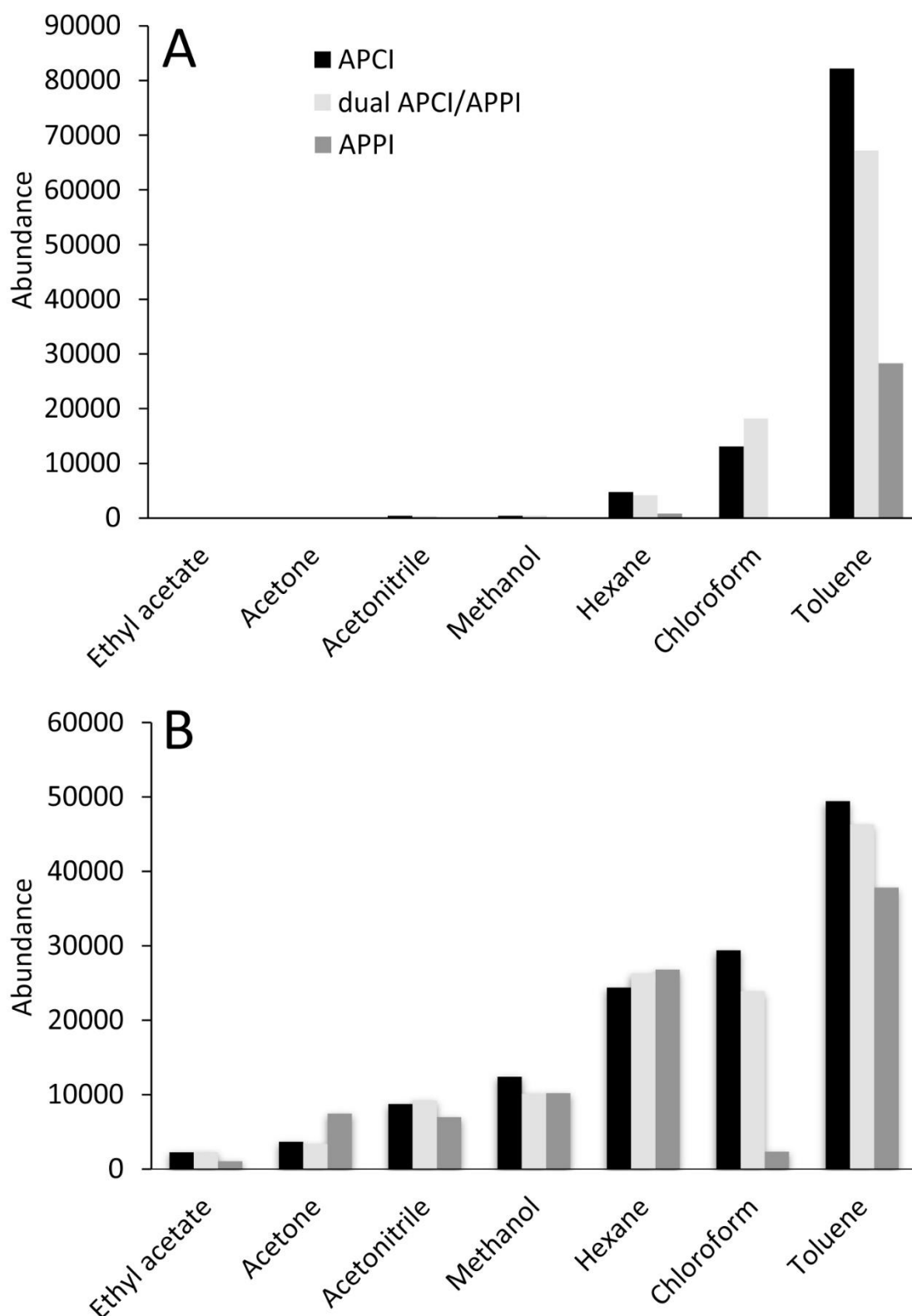


**Figure S8.** The signal intensities of methyl laurate ( $[M+H]^+$ ) (A) and cholesterol ( $[M+H-H_2O]^+$ ) (B) in different solvents as measured by the micro source operated in APCI, APPI and dual APCI/APPI modes. The analyte concentration was 12.5  $\mu\text{g/mL}$ . The sample flow rate was 5  $\mu\text{L/min}$ .




## References

1. Robb DB, Blades MW. State-of-the-art in atmospheric pressure photoionization for LC/MS. *Anal Chim Acta* 2008;627(1):34-49. doi: 10.1016/j.aca.2008.05.077
2. Cai SS, Syage JA. Atmospheric pressure photoionization mass spectrometry for analysis of fatty acid and acylglycerol lipids. *J Chromatogr A* 2006;1110(1-2):15-26. doi: 10.1016/j.chroma.2006.01.050
3. Syage JA, Hanold KA, Lynn TC, Horner JA, Thakur RA. Atmospheric pressure photoionization II. Dual source ionization. *J Chromatogr A* 2004;1050(2):137-149. doi: 10.1016/j.chroma.2004.08.033

## Publikace IV

## RESEARCH ARTICLE

# Temperature-programmed capillary high-performance liquid chromatography with atmospheric pressure chemical ionization mass spectrometry for analysis of fatty acid methyl esters

Vladimír Vrkoslav<sup>1</sup> | Barbora Rumlová<sup>1,2</sup> | Timotej Strmeň<sup>1,2</sup> | Josef Cvačka<sup>1,2</sup> 

<sup>1</sup>Institute of Organic Chemistry and Biochemistry, Czech Academy of Sciences, Prague 6, Czech Republic

<sup>2</sup>Department of Analytical Chemistry, Faculty of Science, Charles University in Prague, Prague 2, Czech Republic

## Correspondence

Dr. Josef Cvačka, Institute of Organic Chemistry and Biochemistry of the Czech Academy of Sciences, Flemingovo nám. 2, CZ-166 10 Prague 6, Czech Republic.  
Email: josef.cvacka@uochb.cas.cz

## Funding information

Czech Science Foundation, Grant/Award Number: 16-01639S; Charles University in Prague, Grant/Award Number: SVV; European Regional Development Fund, Grant/Award Number: CZ.02.1.01/0.0/0.0/16\_019/0000729

A new capillary high-performance liquid chromatography method with atmospheric pressure chemical ionization mass spectrometry was developed for the analysis of fatty acid methyl esters and long-chain alcohols. The chromatographic separation was achieved using a Zorbax SB-C18 HPLC column (0.3 × 150 mm, 3.5 μm) with a mobile phase composed of acetonitrile and formic acid and delivered isocratically at a flow rate of 10 μL/min. The column temperature was programmed simply, using a common column oven. Good reproducibility of the temperature profile and retention times were achieved. The temperature programming during the isocratic high-performance liquid chromatography run had a similar effect as a solvent gradient; it reduced retention times of later eluting analytes and improved their detection limits. Two atmospheric pressure chemical ionization sources of the mass spectrometry detector were compared: an enclosed conventional ion source and an in-house made ion source with a glass microchip nebulizer. The enclosed source provided better detectability of saturated fatty acid methyl esters and made it possible to determine the double bond positions using acetonitrile-related adducts, while the open chip-based source provided better analytical figures of merit for unsaturated fatty acid methyl esters. Temperature-programmed capillary high-performance liquid chromatography is a promising method for analyzing neutral lipids in lipidomics and other applications.

## KEYWORDS

double bonds, high-performance liquid chromatography, lipidomics, lipids, temperature programming

## 1 | INTRODUCTION

The separation temperature is seldom optimized in HPLC, although it can be used to influence the chromatographic resolution, speed of analysis, and column backpressure. It offers a convenient way to adjust the selectivity of the chromatographic system without changing the mobile or stationary phase [1–3]. Temperature affects the diffusion coefficient and changes the shape of the van Deemter curve [4]. Therefore, one can use higher linear velocities of the

mobile phase at higher temperatures without a significant loss of efficiency. Temperature also changes the viscosity and dielectric properties of the mobile phase. In most solvents, the static permittivity, which is a relative measure of solvent polarity, decreases with temperature. The solvent strength in reversed-phase systems thus increases with the temperature. This is utilized for temperature programming, which can yield similar results as solvent programming in HPLC [3,5,6]. Temperature-programmed HPLC is best performed using dedicated systems allowing for mobile phase preheating, fast equilibration of column temperature, cooling of the mobile phase before detection, and backpressure regulation to avoid solvent phase transition [1,7].

Article-Related Abbreviations: Alc, alcohol; APCI, atmospheric pressure chemical ionization; FAME, fatty acid methyl ester.

When compared to standard-bore columns, those of smaller inner dimensions are better suited for temperature programming because much less material needs to be heated and thus the temperature equilibration is fast [7,8]. In this case, heat transfer can be mediated by air using a gas chromatograph oven [9–11], in-house [12], or commercial devices [13,14]. Working with narrow-bore columns brings additional benefits including increased separation efficiency, low solvent consumption, and a higher peak concentration at the detector. There is a variety of stationary phases available for narrow-bore columns, including monolithic materials [15,16]. Narrow-bore columns are easily coupled to ESI-MS, a versatile and sensitive method for detecting the majority of compounds. Despite the obvious benefits, temperature programming is still not commonly used.

HPLC-MS offers a quantitative and qualitative characterization of lipids in targeted and untargeted lipidomics. Depending on the lipid mixture to be analyzed, various separation systems are employed [17,18]. Electrospray is widely used for lipids but it does not work optimally for nonpolar molecules, which are difficult to protonate or deprotonate. Therefore, gas-phase ionization methods such as atmospheric pressure chemical ionization (APCI) or atmospheric pressure photoionization are preferred for detecting nonpolar lipids. Currently, conventional APCI sources operate best at  $\approx 1$  mL/min and accept flow rates between hundreds of microliters and 2–3 mL/min [19], which complicates their use in nano- and microflow HPLC. Several concepts for low flow rate APCI sources have been proposed [20–25], including those operated at ambient conditions (no ion source housing used) with a heated nebulizer based on concentrically arranged capillaries [20,21] or a microchip [23–25]. Despite their promising performance, additional development is needed to design a more robust, sensitive, and reliable APCI source for low sample flow rates. To quantify lipids, response factors reflecting different ionization efficiency in an MS detector are often used. Since the ionization efficiency strongly depends on the composition of the mobile phase, the actual response of compounds eluting at various points of the solvent gradient can change dramatically, causing erroneous quantification [26]. In this respect, it is preferable to use isocratic conditions, but they may not be convenient for the separation. Temperature-programmed HPLC can be a simple and elegant solution because the mobile phase composition does not change during the analysis and the temperature has a similar effect as the solvent gradient [6]. The beneficial effects of sub-ambient or high temperature on the HPLC analysis of lipids including carotenoids [27,28], fatty acid methyl esters (FAMES), squalene, ceramides, cholesterol, and triacylglycerol have been demonstrated [4] but, to the best of our knowledge, temperature programming has not been applied to neutral lipids so far.

FAMES are among the most frequently analyzed neutral lipids. They are often generated from more complex lipids and lipid mixtures by a transesterification reaction. FAMES are usually analyzed by GC-MS detection, which provides high sensitivity and allows identification. However, the method has limited use for extremely long-chain FAMES and does not provide direct information on the double bond position(s). Alternatively, FAMES can be analyzed using HPLC in reversed-phase [29,30] or silver ion systems [31–33]. APCI mass spectra provide abundant signals of protonated molecules. If the mobile phase contains acetonitrile, unsaturated lipids form  $[M + C_3H_5N]^+$  ions, which provide fragments indicative of the original double bond(s) [34–36]. The HPLC-MS methods for FAMES developed so far utilize conventional HPLC systems with standard-bore columns [30].

In this work, changing the column temperature during an isocratic HPLC was used to improve the separation of FAMES. Strongly retained esters eluted faster while maintaining good resolution of the earlier eluting components. The column temperature was controlled by a common column oven. The lipids were detected by APCI-MS using either a conventional high flow rate source or an in-house ion source based on a heated microchip nebulizer. To the best of our knowledge, this is the first application of temperature programming in lipid analysis.

## 2 | MATERIALS AND METHODS

### 2.1 | Chemicals

Supelco 37 Component FAME Mix and acetyl chloride (p.a.,  $\geq 99\%$ ) were purchased from Sigma-Aldrich (St. Louis, MO, USA). Silver carbonate was obtained from Lachema (Brno, Czech Republic). The standards of methyl stearate (18:0), methyl oleate (18:1n-9), methyl linoleate (18:2n-6), and  $\gamma$ -methyl linolenate (18:3n-6) were from Nu-Chek-Prep (Elysian, MN, USA). Acetonitrile (Chromasolv, LC-MS), ethyl acetate (Chromasolv, LC-MS), chloroform (Chromasolv Plus, for HPLC), 2-propanol (Chromasolv, LC-MS), toluene (Chromasolv® Plus, for HPLC), and methanol (Chromasolv, LC-MS) were purchased from Honeywell/Riedel-de Haën (Seelze, Germany). Formic acid (99.0+%, LC-MS) was from Fisher Chemical (Hampton, NH, USA).

### 2.2 | Transesterification

The samples of seed oil FAMES were obtained by transesterification of triacylglycerols isolated from blackcurrant oil [37] and wax esters isolated from jojoba oil [38] according to Stránský et al. [39]. Briefly, lipids were dissolved in methanol:chloroform (3:2, by vol.) in a small glass ampoule. After adding acetyl chloride, the ampoule was sealed and

placed in a water bath (70°C) for 90 min. After opening the vials, the reaction mixture was neutralized by adding silver carbonate and separated from solid precipitate of silver chloride.

### 2.3 | Liquid chromatography–mass spectrometry

The capillary HPLC system was assembled from Teledyne ISCO M65 manual valve gradient pump (Lincoln, NE, USA), VICI CI4W.06 injector with internal volume of 60 nL (VICI AG International, Schenkon, Switzerland), Zorbax SB-C18 HPLC column (0.3 × 150 mm, 3.5 μm; Agilent, Santa Clara, CA, USA), a built-in column oven of Accela autosampler (5–95°C; Thermo Fisher Scientific, San Jose, CA, USA), and an LCQ Fleet ion trap mass spectrometer (Thermo Fisher Scientific). The mass spectrometer was equipped with either Ion Max-S API source with an APCI probe or a chip-based ion source (see below). In the final method, an isocratic elution of FAMES was carried out using acetonitrile with 0.1% of formic acid. The temperature program was performed by an abrupt change of the temperature from 5 to 50°C in the sixth min of the HPLC run. The IR-1200-50D USB thermometer (Votcraft, Hirschau, Germany) was used to monitor the temperature inside the column compartment. The temperature slowly increased from 8.5 (0–6 min) to 49.6°C; the maximum value was reached in 17 min. The column temperature was equilibrated for at least 25 min before each HPLC run.

### 2.4 | Atmospheric pressure chemical ionization sources

The conventional Ion Max-S API source with the APCI probe was operated at 10 μL/min sample flow rate. The working parameters of the ion source were set as follows: vaporizer temperature 180°C, sheath and auxiliary gas flow rates 40 and 5 arbitrary units, respectively, capillary temperature 300°C, capillary voltage 25.5 V, tube lens voltage 80 V, and corona discharge current 3 μA. Alternatively, a chip-based ion source described recently [25] was used. Briefly, the source components were mounted onto LCQ-Fleet compatible flange with two guiding rods. The rods supported an adjustable holder for a corona discharge needle and a micromanipulator MX10R (Siskiyou, Grants Pass, OR, USA) holding a chip-based nebulizer. The nebulizer consisted of a glass microfabricated chip [40] kindly provided by Prof. Risto Kostianen from the University of Helsinki, Finland. Its platinum resistance heater was powered by ISO-TECH power supply IPS-603 (Corby, Great Britain). The GFCS-011771 mass flow controller (Aalborg, Orangeburg, NY, USA) was used to deliver nitrogen nebulizer gas. High voltage for the corona discharge electrode was taken from the mass spectrometer. The operating parameters of the chip-APCI source were set as follows: the nitrogen flow

rate 60 mL/min, the liquid sample flow rate 10 μL/min, the microchip heating power 4.5 W, capillary temperature 300°C, capillary voltage 25.5 V, tube lens voltage 80 V, and corona discharge current 1 μA. Data were collected and processed with Xcalibur software (Thermo Fisher Scientific).

### 2.5 | Calibration curves

FAME 18:2n-6 calibration standards were prepared in chloroform:methanol (1:3, v/v) at the concentrations of 1–10 000 μg/mL. The analyte signal was measured in the selected reaction monitoring (SRM) mode using  $m/z$  295.2 > 263.2 transition with the normalized collision energy of 30%. Peak areas and peak heights were used for the construction of the calibration curves. The noise level was established from the signal of the blank solvent infused into the capillary HPLC–APCI–MS at the same flow rate (10 μL/min). It was determined as the peak-to-peak envelope of all contributions to background signal (i.e., random noise plus possible chemical interferences). The LOD values (instrumental detection limit values) were calculated for  $S/N = 3$  using the calibration curve constructed from the peak heights. Sensitivity values correspond to the slope of the calibration curves constructed from the peak areas.

## 3 | RESULTS AND DISCUSSION

### 3.1 | Capillary chromatography of fatty acid methyl esters

The separation of FAMES was optimized using a Zorbax SB-C18 capillary column (0.3 mm × 150 mm, 3.5 μm) operated at the flow rate of 10 μL/min. The analytes were detected with conventional APCI source, which has been designed for substantially higher sample flow rates than suitable for capillary HPLC. It turned out that the ion source can be operated at 10 μL/min if the nebulizer temperature is reduced to 180°C. The lower nebulizing temperature was required to prevent excessive baseline noise due to the solvent evaporation inside the probe capillary. A negative consequence of operating the ion source at the low flow rate was lower detection sensitivity. The composition of the mobile phase was first optimized for isocratic and isothermal conditions (25°C). Inspired by our previous work [30], acetonitrile and its mixtures with various solvents were tested as mobile phases. Tailing peaks were detected in acetonitrile with no modifier added. Although the addition of toluene slightly improved detection sensitivity [25], it did not help to improve the tailing. The addition of ethyl acetate or 2-propanol did not improve the peak shape either. Moreover, ethyl acetate and 2-propanol suppressed the ionization. The best results were achieved using acetonitrile containing 0.1% of formic acid. FAMES provided narrow

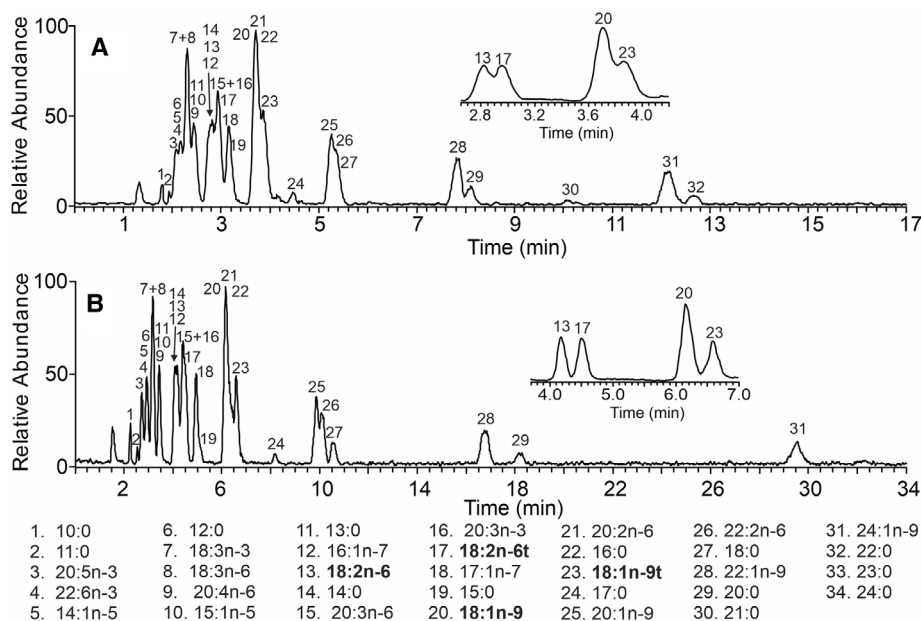


**FIGURE 1** Capillary HPLC-APCI-MS chromatogram of the mixture of FAMES (total concentration 1 mg/mL) obtained at the column temperature of 25°C (A) and 5°C (B); inset: separation of 18:2n-6, 18:2n-6t, 18:1n-9, and 18:1n-9t; experimental conditions: flow rate 10  $\mu$ L/min, acetonitrile with 0.1% FA, conventional APCI source; for other conditions, see Section 2

symmetrical peaks and the chromatograms were reproducible (Figure 1A). As expected, the elution order of FAMES reflected the number of carbons and double bonds in their aliphatic chains. The retention increased with the chain length and decreased with the number of double bonds. The separation of isobaric FAMES was improved by lowering the column temperature to 5°C. Almost baseline separation of cis/trans isomers of 18:2n-6 and 18:1n-9 was achieved (Figure 1B). However, the retention times of long-chain saturated FAMES were too high at such a low temperature. Therefore, temperature-programmed chromatography was used. Since a temperature-programmed column oven was not available, a common column thermostat was used. The analysis started at 5°C and after 6 min, the temperature was abruptly set to 50°C. The temperature in the column compartment gradually increased and reached the final value of 50°C in about 17 min (Figure 2A). The repeated experiments showed that the temperature gradient generated in this way was highly reproducible. As shown in Figure 2B, the analysis time was reduced significantly, while the resolution of the early-eluting peaks was preserved. The temperature had a similar effect as a solvent gradient. The total analysis time was reduced roughly by half and the peaks of late-eluting FAMES were narrow, exhibiting improved S/N ratio. In this way, we were able to detect all FAMES in the standard mixture.

Good repeatability of the retention times was achieved (Supporting Information Figure S1). Within 1 week, the average RSD of the retention times was <2%. This result not only confirmed the excellent reproducibility of the temperature profile in the column compartment but also illustrated the

thermal stability of the column. No ions related to the column bleed were detected even after prolonged use of the column.

### 3.2 | Mass spectrometric detection of fatty acid methyl esters

Since the conventional ion source has been designed for higher flow rates, the in-house chip-based APCI source was tested to increase detection sensitivity. The optimized temperature-programmed method was used to separate FAMES. Although the retention times of the FAMES were the same, the chromatogram looked differently (cf. Figure 2B and C). The total signal was higher in the chip-based APCI source, but selective discrimination of saturated esters was observed. There was a technical reason for the discrimination of FAMES with higher boiling points. The limit for electric current flowing through the platinum heater of the chip nebulizer was rather low, which prevented us to use sufficiently high temperatures to efficiently vaporize long-chain esters. Detectability of esters differing by the number of double bonds was compared for FAMES with 18 carbons and both ion sources. An equimolar mixture of C18:0, C18:1n-9, C18:2n-6, and C18:3n-6 provided chromatograms shown in Figure 3. The detectability of saturated FAMES was much lower than of unsaturated FAMES, particularly for the chip-based APCI. Similar phenomena were observed in APCI-MS of other neutral lipids [38,41], and can likely be explained by the differences in proton affinities and vapor pressures. The detection sensitivity of unsaturated FAMES was significantly higher with the chip-based APCI compared to the

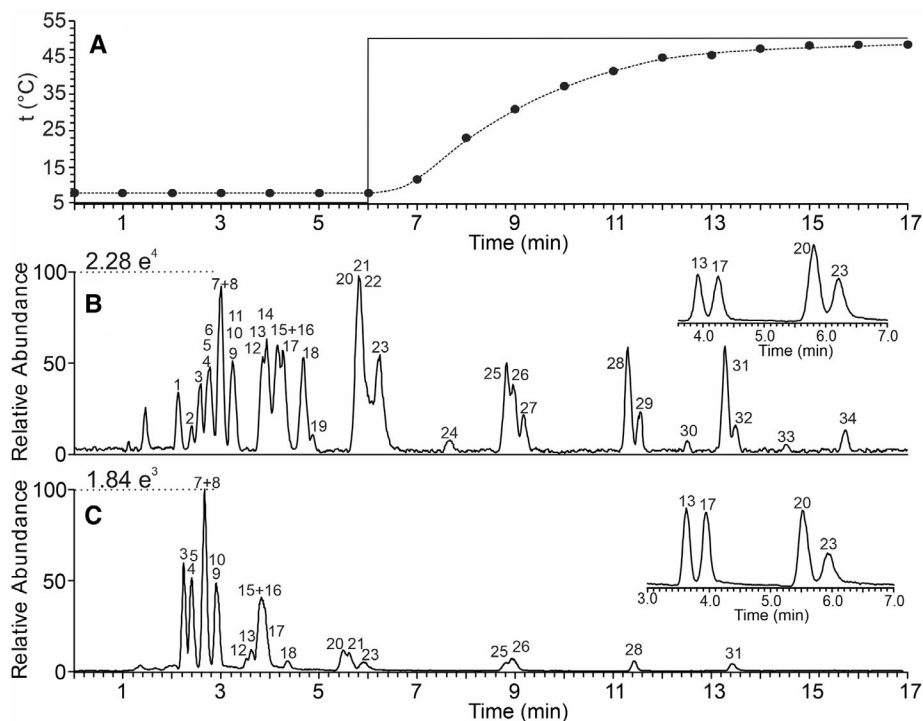


**FIGURE 2** Temperature program (solid line) and the measured temperature (dotted line) in the column oven (A); temperature-programmed capillary HPLC–APCI–MS chromatograms of FAMEs (total concentration 1 mg/mL) detected by the conventional APCI (B) and chip-based APCI (C) sources; insets: separation of 18:2n-6, 18:2n-6t, 18:1n-9, and 18:1n-9t; flow rate 10  $\mu$ L/min, acetonitrile with 0.1% FA; for other conditions and peak identifications, see Section 2 and Figure 1, respectively

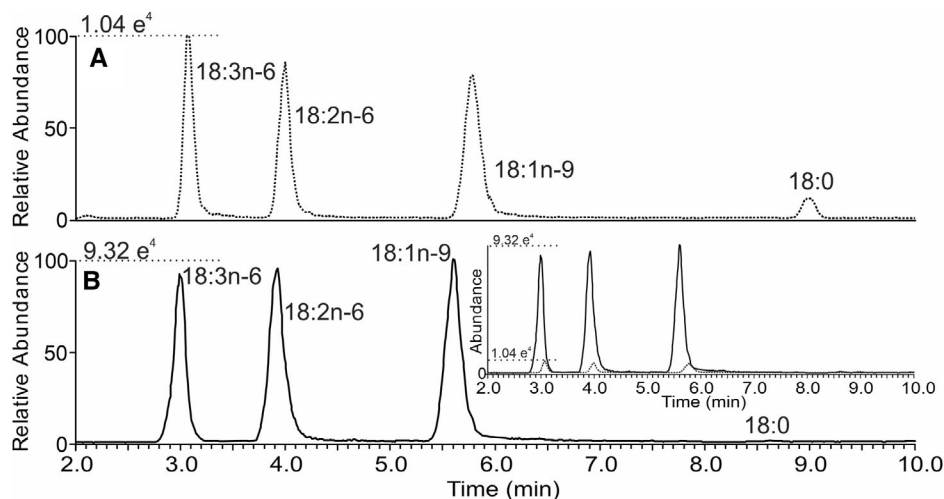


**FIGURE 3** Temperature-programmed capillary HPLC–APCI–MS chromatograms of FAMEs (1 mmol/L of each) detected by the conventional APCI (A, dotted line) and chip-based APCI (B, solid line) sources; inset: overlaid chromatograms; for other conditions, see Section 2

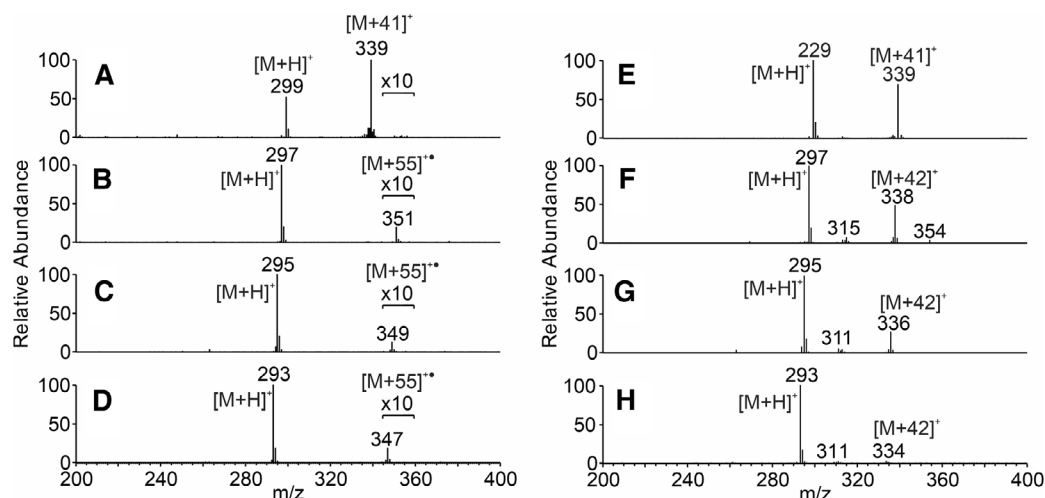
conventional APCI. However, for saturated FAMEs no gain in sensitivity was achieved, see the inset in Figure 3.

The analytical figures of merit were evaluated for 18:2n-6 using selected ion monitoring detection ( $m/z$  295.2). Each point of the calibration curve was measured three to five times with averaged RSD values of 5.8% for the chip-based ion source and 6.8% for the conventional ion source, indicating comparable measurement repeatability for the ion

sources. The detection limit, sensitivity, and linearity values are summarized in Table 1. The conventional APCI source provided approximately eight times higher detection limit and the sensitivity was about three times lower when compared to the chip-based ion source. The higher sensitivity of the chip-based APCI–MS detection was likely due to more efficient ionization and ion transfer in the well-focused jet of vapors. The calibration curve based on the peak area showed good

**TABLE 1** Analytical figures of merit of FAME 18:2n-6 obtained for the conventional APCI and chip-based APCI sources

APCI source	LOD ( $\mu\text{g/mL}$ )	LOD ( $\mu\text{g}$ )	Sensitivity ( $\text{mL}/\mu\text{g}$ )	Linear dynamic range	$R^2$
Conventional	3.45	207	49.9	3.45 mg/mL to >10 mg/mL	0.9985
Chip-based	0.42	25.2	139	0.42 $\mu\text{g/mL}$ to >2.5 mg/mL	0.9991

**FIGURE 4** Ion trap mass spectra of 18:0 (A and E), 18:1n-9 (B and F), 18:2n-6 (C and G), 18:3n-6 (D and H) obtained by conventional APCI (A–D) and chip-based APCI (E–H) sources. The spectra were collected during chromatographic runs; the analyte concentrations were 1 mmol/L except for the spectrum (E), which corresponds to 5 mmol/L

linearity for both ion sources. Calibration curves were linear from the detection limit up to the highest measured concentrations (10 and 2.5 mg/mL for conventional APCI and chip-based APCI source, respectively). Therefore, the linear dynamic range was at least 3.5 orders of magnitude for both detectors. The method precision was further tested for the conventional APCI source and FAMES with 18 carbons (FAMES 18:0, 18:1n-9, 18:1n-9t, 18:2n-6, 18:2n-6t, and 18:3n-3/18:3n-6). Run-to-run precision (repeatability) was evaluated for three consecutive measurements. The RSDs ranged from 1.6 to 14.7% with an average of 8.6%. Day-to-day precision (intermediate precision) was calculated for three measurements within 7 days. The RSDs ranged from 1.0 to 13.8% with an average of 6.0%.

The mass spectra obtained with two different APCI detectors were not the same (Figure 4). All unsaturated FAMES provided  $[M + H]^+$  as the most abundant ion in both ion sources. In addition to this ion, adducts related to acetonitrile were detected. While the unsaturated FAMES provided molecular adducts  $[M + 42]^+$  ( $[M + \text{CH}_3\text{CN} + \text{H}]^+$ ) [36,42] in the chip-based ion source, the conventional APCI source showed  $[M + 55]^{+*}$  ( $[M + \text{C}_3\text{H}_5\text{N}]^{+*}$ ) peaks. These ions are known to be formed in conventional high-flow APCI–MS conditions and they can be used to localize double bonds in various lipids including FAMES [28,34–36]. The formation of different types of ions can be explained by the ion sources design. While the ion source housing in

the conventional source prevents ambient air from entering the corona discharge region, the chip-based source is open to the atmosphere. Oxygen can be involved in ionization mechanisms in the chip source and thus affects the formation of acetonitrile-related adducts [43,44]. The saturated FAME 18:0 yielded abundant molecular adducts  $[M + H]^+$  and  $[M + 41]^+$  in both APCI sources (Figure 4A and E).

### 3.3 | Analysis of seed oil fatty acid methyl esters

The applicability of the temperature-programming HPLC–APCI–MS was demonstrated for trans-esterified seed oils. Two seed oils were used: (i) triacylglycerol-based blackcurrant seed oil and (ii) wax ester-based jojoba seed oil. The samples were processed and trans-esterified as described previously [37–39] and the reaction products were directly injected onto the column. The analyses were carried out with both types of APCI–MS detectors to compare their performance for real samples (Figure 5A and B). FAMES of blackcurrant seed oil were identified based on their mass spectra, retention times, and literature data [30]. The sample contained mostly unsaturated fatty acids with 18 carbons, namely FAME 18:4n-3, 18:3n-3, 18:3n-6, 18:2n-6, and 18:1n-9, together with 20:1n-9. The retention times of the isomeric FAME 18:3n-3 and 18:3n-6 were the same, which did not allow us to distinguish them in the full scan spectra.



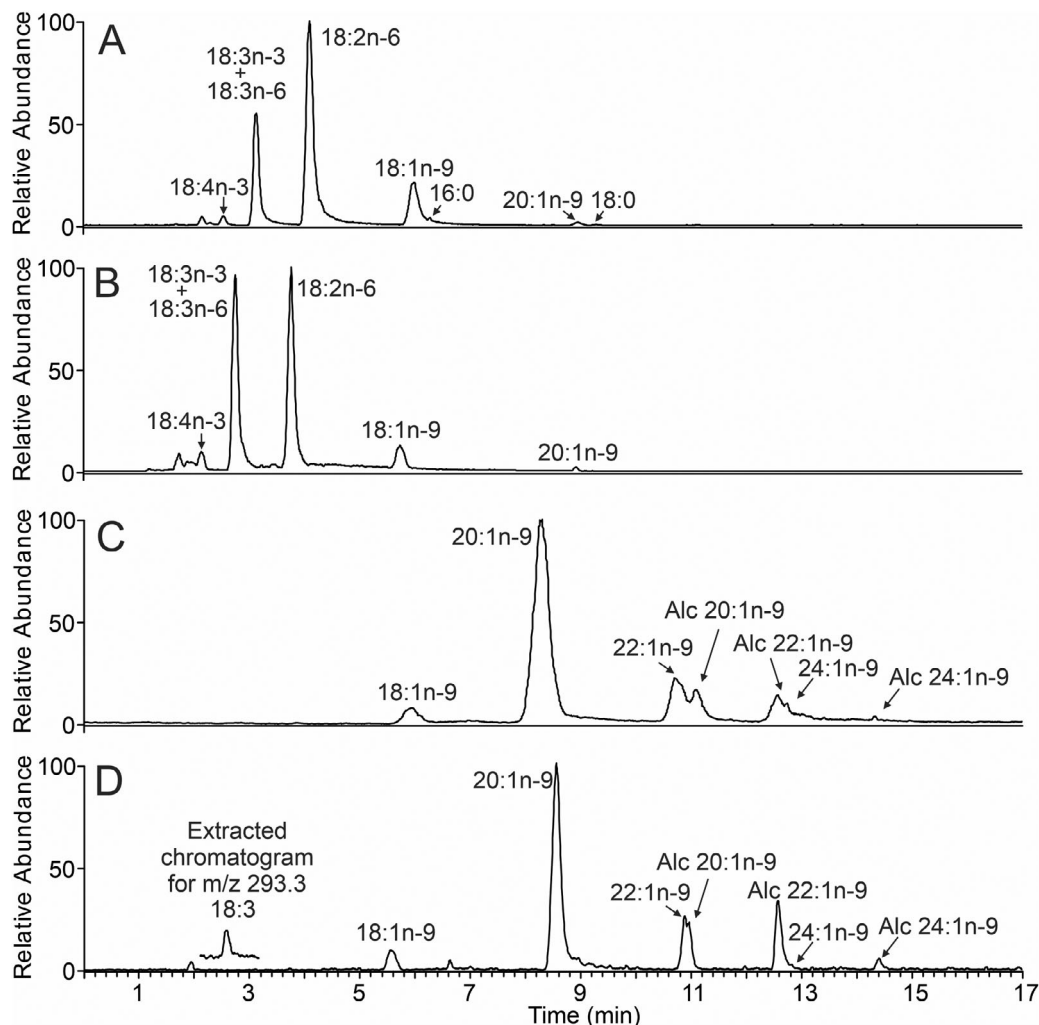


**FIGURE 5** Temperature-programmed capillary HPLC-APCI-MS base-peak chromatogram of FAMES from triacylglycerol fraction of blackcurrant seed oil (4 mg/mL) (A and B) and wax esters fraction of jojoba oil (3.5 mg/mL) (C and D) ionized by conventional APCI (A and C) and chip-based APCI (B and D) sources; flow rate 10  $\mu$ L/min, acetonitrile with 0.1% FA; for other conditions, see Section 2

However, we were able to prove both isomers using MS/MS spectra of the  $[M + C_3H_5N]^+$  ions [45]. The sample also contained saturated FAMES 16:0 and 18:0; their peaks were small in the conventional APCI source and almost missing in the chip-based APCI-MS detector.

The wax esters in jojoba oil consist mainly of long-chain monounsaturated alcohols esterified to monounsaturated fatty acids [38,46]. The temperature-programmed capillary HPLC-APCI-MS allowed us to detect both moieties of wax esters. In agreement with the literature, FAMES 18:1n-9, 20:1n-9, 22:1n-9, and 24:1n-9 and alcohols Alc 20:1n-9, Alc 22:1n-9, and Alc 24:1n-9 were detected in both ion sources (Figure 5C and D). In the conventional APCI source, the alcohols provided  $[M + H]^+$ ,  $[M + 42]^+$ , and minor peaks of  $[M + C_3H_5N]^+$  (Figure 6A). The MS/MS spectra of  $[M + C_3H_5N]^+$  contained fragments that made it possible to determine the position of the double bond (Figure 6B). Similarly to other lipid classes [30,34-36], the frag-

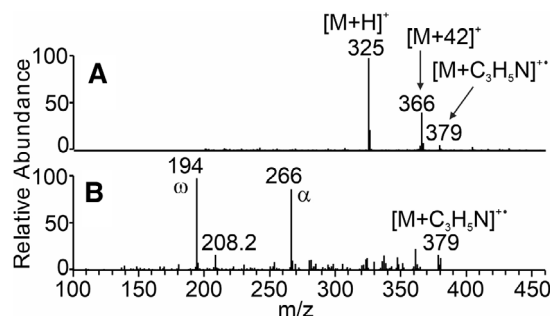


**FIGURE 6** Ion trap full MS spectrum of Alc 22:1n-9 (A) and MS/MS spectrum of  $[M + C_3H_5N]^+$  from which the position of the double bond can be determined (B). The spectra were collected under chromatographic conditions (Figure 5C)

ments corresponded to the cleavages of C-C bonds next to the original double bond. The  $\alpha$  fragment contained hydroxyl, while the  $\omega$  fragment contained the chain terminus. The

MS/MS spectra of  $[M + C_3H_5N]^+$  of all FAMES and alcohols from the trans-esterified jojoba oil are shown in Supporting Information Figures S2 and S3. The higher sensitivity of the chip-based APCI source allowed us to detect low abundant FAME 18:3 (Figure 5D), which was undetectable by the conventional ion source.

## 4 | CONCLUSIONS

A method for analyzing FAMES using temperature-programmed HPLC was developed. The temperature program was achieved in a simple way, using a standard column oven from a conventional liquid chromatograph. Good reproducibility of the temperature profile and retention times were observed. Increasing the column temperature during the isocratic HPLC run had a similar effect as a solvent gradient. Lately eluting compounds provided narrower peaks with shorter retention times, which increased sensitivity and shortened the overall analysis time. FAMES and fatty alcohols were detected using APCI-MS. Since there are no dedicated APCI-MS detectors for low flow rates on the market, a conventional high-flow rate detector and the in-house device with chip-based nebulizer were used. Both detectors could detect FAMES, but their performance was different. The enclosed conventional source provided better detectability of saturated FAMES and made it possible to determine the double bond positions in FAMES using acetonitrile-related adducts, but its overall sensitivity was low. The open chip-based ion source tended to provide narrower and more symmetrical peaks likely due to lower dead volumes (the chip had an integrated fused silica capillary). It provided better analytical figures of merit for unsaturated FAMES, but its applicability to saturated FAMES was poor and it did not offer localization of double bonds. Apparently, a better APCI source for capillary HPLC is needed. The method was successfully applied to trans-esterified seed oils. Temperature programming in isocratic HPLC is a promising method for analyzing neutral lipids in lipidomics and other applications.

## ACKNOWLEDGEMENTS

This project was financially supported by the Czech Science Foundation (Project No. 16-01639S), Charles University in Prague (Project SVV), and European Regional Development Fund; OP RDE; Project: “Chemical biology for drugging undruggable targets (ChemBioDrug)” (No. CZ.02.1.01/0.0/0.0/16\_019/0000729). The authors are indebted to Risto Kostianen and Markus Haapala from the University of Helsinki for the microchips, and the Development Center of the IOCB, Prague for indispensable assistance on this project.

## CONFLICT OF INTEREST

The authors have declared no conflict of interest.

## ORCID

Josef Cvačka  <https://orcid.org/0000-0002-3590-9009>

## REFERENCES

- Teutenberg T., High-Temperature Liquid Chromatography: A User's Guide for Method Development. Royal Soc Chemistry, Cambridge, UK 2010.
- Tran J. V., Molander P., Greibrokk T., Lundanes E., Temperature effects on retention in reversed phase liquid chromatography. *J. Sep. Sci.* 2001, 24, 930–940.
- Sander L. C., Wise S. A., The influence of column temperature on selectivity in reversed-phase liquid chromatography for shape-constrained solutes. *J. Sep. Sci.* 2001, 24, 910–920.
- Hazotte A., Libong D., Chaminade P., High-temperature micro liquid chromatography for lipid molecular species analysis with evaporative light scattering detection. *J. Chromatogr. A* 2007, 1140, 131–139.
- Hesse G., Engelhardt H., Temperaturprogrammierung bei der adsorptionschromatographie von lösungen. *J. Chromatogr. A* 1966, 21, 228–238.
- Chen M. H., Horvath C., Temperature programming and gradient elution in reversed-phase chromatography with packed capillary columns. *J. Chromatogr. A* 1997, 788, 51–61.
- Teutenberg T., Potential of high temperature liquid chromatography for the improvement of separation efficiency-A review. *Anal. Chim. Acta* 2009, 643, 1–12.
- Vanhoenacker G., Sandra P., High temperature and temperature programmed HPLC: possibilities and limitations. *Anal. Bioanal. Chem.* 2008, 390, 245–248.
- Trones R., Andersen T., Greibrokk T., Hegna D. R., Hindered amine stabilizers investigated by the use of packed capillary temperature-programmed liquid chromatography I. Poly((1,1,3,3-tetramethylbutyl)-amino)-1,3,5-triazine-2,4-diyl(2,2,6,6-tetramethyl-4-piperidyl)imino)-1,6-hexanediyl ((2,2,6,6-tetramethyl-4-piperidyl)imino)). *J. Chromatogr. A* 2000, 874, 65–71.
- Molander P., Thomassen A., Kristoffersen L., Greibrokk T., Lundanes E., Simultaneous determination of citalopram, fluoxetine, paroxetine and their metabolites in plasma by temperature-programmed packed capillary liquid chromatography with on-column focusing of large injection volumes. *J. Chromatogr. B* 2002, 766, 77–87.
- Yoo J. S., Watson J. T., McGuffin V. L., Temperature-programmed microcolumn liquid chromatography/mass spectrometry. *J. Microcolumn Sep.* 1992, 4, 349–362.
- Teutenberg T., Goetze H. J., Tuerk J., Ploeger J., Kiffmeyer T. K., Schmidt K. G., Kohorst W. G., Rohe T., Jansen H. D., Weber H., Development and application of a specially designed heating system for temperature-programmed high-performance liquid chromatography using subcritical water as the mobile phase. *J. Chromatogr. A* 2006, 1114, 89–96.
- <https://sunchrom.de/column-oven-2/> (last time accessed: March 31, 2020).

14. <https://sim-gmbh.de/en/products/liquid-chromatography/736-ht-hplc-200-column-oven.html> (last time accessed: March 31, 2020).
15. Urban J., Current trends in the development of porous polymer monoliths for the separation of small molecules. *J. Sep. Sci.* 2016, 39, 51–68.
16. Zajickova Z., Advances in the development and applications of organic–silica hybrid monoliths. *J. Sep. Sci.* 2017, 40, 25–48.
17. Čajka T., Fiehn O., Comprehensive analysis of lipids in biological systems by liquid chromatography-mass spectrometry. *TrAC-Trends Anal. Chem.* 2014, 61, 192–206.
18. Han X., *Lipidomics: Comprehensive Mass Spectrometry of Lipids*. John Wiley & Sons Inc, Hoboken 2016.
19. Ion Max and Ion Max-S API Source, Hardware Manual, 97055-97044 Revision D, Thermo Fisher Scientific 2008.
20. Nyholm L. M., Sjoberg P. J. R., Markides K. E., High-temperature open tubular liquid chromatography coupled to atmospheric pressure chemical ionisation mass spectrometry. *J. Chromatogr. A* 1996, 755, 153–164.
21. Strmeň T., Vrkoslav V., Pačes O., Cvačka J., Evaluation of an ion source with a tubular nebulizer for microflow atmospheric pressure chemical ionization. *Mon. Chem.* 2018, 149, 987–994.
22. Takeda S., Tanaka Y., Yamane M., Siroma Z., Wakida S., Otsuka K., Terabe S., Ionization of dichlorophenols for their analysis by capillary electrophoresis-mass spectrometry. *J. Chromatogr. A* 2001, 924, 415–420.
23. Ostman P., Marttila S. J., Kotiaho T., Franssila S., Kostiaainen R., Microchip atmospheric pressure chemical ionization source for mass spectrometry. *Anal. Chem.* 2004, 76, 6659–6664.
24. Ostman P., Jantti S., Grigoros K., Saarela V., Ketola R. A., Franssila S., Kotiaho T., Kostiaainen R., Capillary liquid chromatography-microchip atmospheric pressure chemical ionization-mass spectrometry. *Lab Chip* 2006, 6, 948–953.
25. Vrkoslav V., Rumlová B., Strmeň T., Nekvasilová P., Šulc M., Cvačka J., Applicability of low-flow atmospheric pressure chemical ionization and photoionization mass spectrometry with a microfabricated nebulizer for neutral lipids. *Rapid Commun. Mass Spectrom.* 2018, 32, 639–648.
26. Kromidas S., *Gradient HPLC for Practitioners: RP, LC-MS, Ion Analytics, Biochromatography, SFC, HILIC*. Wiley-VCH, Weinheim 2019.
27. Böhm V., Use of column temperature to optimize carotenoid isomer separation by C30 high performance liquid chromatography. *J. Sep. Sci.* 2001, 24, 955–959.
28. Sander L. C., Craft N. E., Device for subambient temperature control in liquid chromatography. *Anal. Chem.* 1990, 62, 1545–1547.
29. Řezanka T., Analysis of very long chain polyunsaturated fatty acids using high-performance liquid chromatography - atmospheric pressure chemical ionization mass spectrometry. *Biochem. Syst. Ecol.* 2000, 28, 847–856.
30. Vrkoslav V., Cvačka J., Identification of the double-bond position in fatty acid methyl esters by liquid chromatography/atmospheric pressure chemical ionisation mass spectrometry. *J. Chromatogr. A* 2012, 1259, 244–250.
31. Nikolova-Damyanova B., Christie W. W., Herslof B., Silver ion high-performance liquid chromatography of esters of isomeric octadecenoic fatty acids with short-chain monounsaturated alcohols. *J. Chromatogr. A* 1995, 693, 235–239.
32. Sehat N., Rickert R., Mossoba M. M., Kramer J. K. G., Yurawecz M. P., Roach J. A. G., Adlof R. O., Morehouse K. M., Fritsche J., Eulitz K. D., Steinhart H., Ku Y., Improved separation of conjugated fatty acid methyl esters by silver ion-high-performance liquid chromatography. *Lipids* 1999, 34, 407–413.
33. Kuhnt K., Degen C., Jahreis G., 2-Propanol in the mobile phase reduces the time of analysis of CLA isomers by silver ion-HPLC. *J. Chromatogr. B* 2010, 878, 88–91.
34. Vrkoslav V., Háková M., Pecková K., Urbanová K., Cvačka J., Localization of double bonds in wax esters by high-performance liquid chromatography/atmospheric pressure chemical ionization mass spectrometry utilizing the fragmentation of acetonitrile-related adducts. *Anal. Chem.* 2011, 83, 2978–2986.
35. Šubčíková L., Hoskovec M., Vrkoslav V., Čmelíková T., Háková E., Míková R., Coufal P., Doležal A., Plavka R., Cvačka J., Analysis of 1,2-diol diesters in vernix caseosa by high-performance liquid chromatography - atmospheric pressure chemical ionization mass spectrometry. *J. Chromatogr. A* 2015, 1378, 8–18.
36. Háková E., Vrkoslav V., Míková R., Schwarzová-Pecková K., Bosáková Z., Cvačka J., Localization of double bonds in triacylglycerols using high-performance liquid chromatography/atmospheric pressure chemical ionization ion-trap mass spectrometry. *Anal. Bioanal. Chem.* 2015, 407, 5175–5188.
37. Vacek M., Zarevúcka M., Wimmer Z., Stranský K., Koutek B., Macková M., Demnerová K., Lipase-mediated hydrolysis of blackcurrant oil. *Enzyme Microb. Technol.* 2000, 27, 531–536.
38. Vrkoslav V., Urbanová K., Cvačka J., Analysis of wax ester molecular species by high performance liquid chromatography/atmospheric pressure chemical ionisation mass spectrometry. *J. Chromatogr. A* 2010, 1217, 4184–4194.
39. Stranský K., Jursik T., Simple quantitative transesterification of lipids .1. Introduction. *Fett-Lipid* 1996, 98, 65–71.
40. Krúve A., Haapala M., Saarela V., Franssila S., Kostiaainen R., Kotiaho T., Ketola R. A., Feasibility of capillary liquid chromatography-microchip-atmospheric pressure photoionization-mass spectrometry for pesticide analysis in tomato. *Anal. Chim. Acta* 2011, 696, 77–83.
41. Holčápek M., Lída M., Jandera P., Kabátová N., Quantitation of triacylglycerols in plant oils using HPLC with APCI-MS, evaporative light-scattering, and UV detection. *J. Sep. Sci.* 2005, 28, 1315–1333.
42. Konstantinova O. V., Antonchick A. P., Oldham N. J., Zhabinskii V. N., Khrupach V. A., Schneider B., Analysis of underivatized brassinosteroids by HPLC/APCI-MS. Occurrence of 3-epibrassinolide in *Arabidopsis thaliana*. *Collect. Czech. Chem. Commun.* 2001, 66, 1729–1734.
43. Kolakowski B. A., Grossert J. S., Ramaley L., Studies on the positive-ion mass spectra from atmospheric pressure chemical ionization of gases and solvents used in liquid chromatography and direct liquid injection. *J. Am. Soc. Mass Spectrom* 2004, 15, 311–324.
44. Strmeň T., Vrkoslav V., Bosáková Z., Cvačka J., Atmospheric pressure chemical ionization mass spectrometry at low flow rates:

- Importance of ion source housing. *Rapid Commun. Mass Spectrom.* <https://doi.org/10.1002/rcm.8722>
45. Vrkoslav V., Rumlová B., Cvačka J., Temperature-programed micro-HPLC analysis of fatty acid methyl esters with APCI-MS detection. In: 15<sup>th</sup> International Interdisciplinary Meeting on Bioanalysis. Foret F., Křenková J., Drobníková I., Klepárník K., Příkryl J. (Eds.), Institute of Analytical Chemistry of the CAS, v. i., Brno 2018, pp. 320–324. [http://www.ce-ce.org/user\\_uploads/program/CECE%202018%20Proceedings\\_WOS.pdf](http://www.ce-ce.org/user_uploads/program/CECE%202018%20Proceedings_WOS.pdf) (last time accessed: March 31, 2020).
46. Medvedovici A., Lazou K., d'Oosterlinck A., Zhao Y., Sandra P., Analysis of jojoba oil by LC-coordination ion spray-MS (LC-CIS-MS). *J. Sep. Sci.* 2002, 25, 173–178.

## SUPPORTING INFORMATION

Additional supporting information may be found online in the Supporting Information section at the end of the article.

**How to cite this article:** Vrkoslav V, Rumlová B, Strmeň T, Cvačka J. Temperature-programmed capillary high-performance liquid chromatography with atmospheric pressure chemical ionization mass spectrometry for analysis of fatty acid methyl esters. *J Sep Sci.* 2020;43:2579–2588. <https://doi.org/10.1002/jssc.201901235>

# Temperature-programmed capillary-HPLC/atmospheric pressure chemical ionization-MS for analysis of fatty acid methyl esters

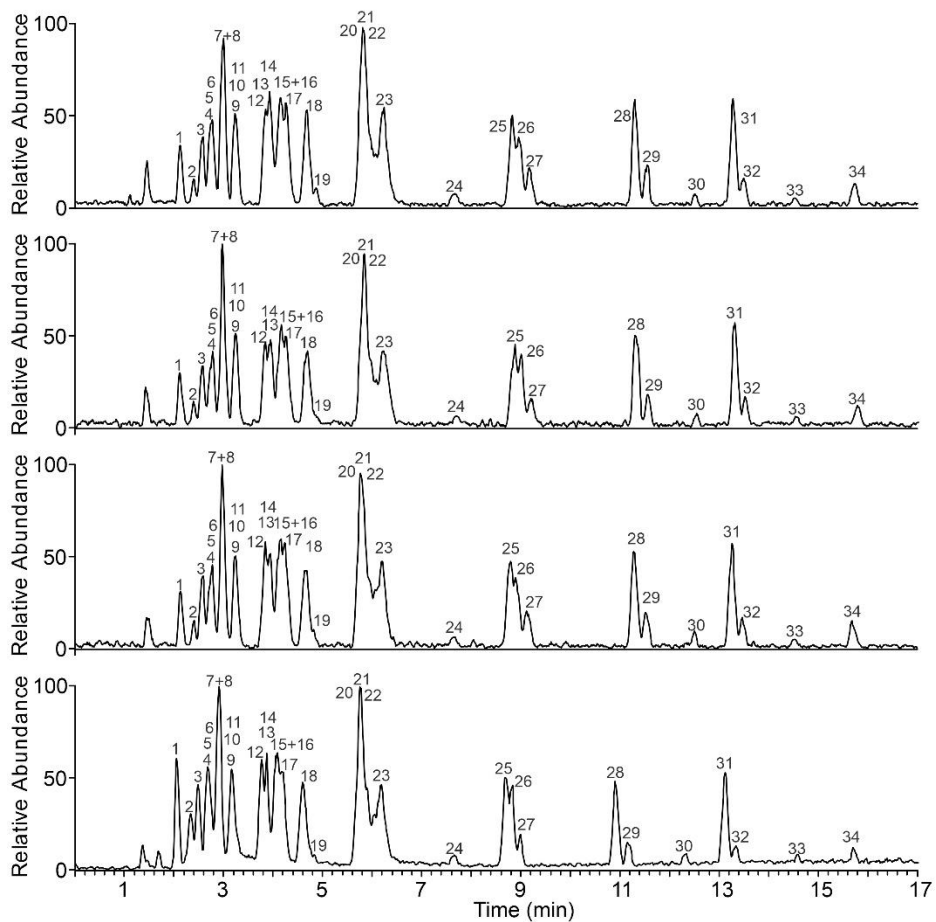
Vladimír Vrkoslav<sup>1</sup>, Barbora Rumlová<sup>1,2</sup>, Timotej Strmeň<sup>1,2</sup>, Josef Cvačka<sup>1,2</sup>

<sup>1</sup> *Institute of Organic Chemistry and Biochemistry of the Czech Academy of Sciences, Flemingovo nám. 2, CZ-166 10 Prague 6, Czech Republic*

<sup>2</sup> *Department of Analytical Chemistry, Faculty of Science, Charles University in Prague, CZ-128 43 Prague 2, Czech Republic*

*Correspondence:* Dr. Josef Cvačka, Institute of Organic Chemistry and Biochemistry of the Czech Academy of Sciences, Flemingovo nám. 2, CZ-166 10 Prague 6, Czech Republic; *E-mail:* josef.cvacka@uochb.cas.cz

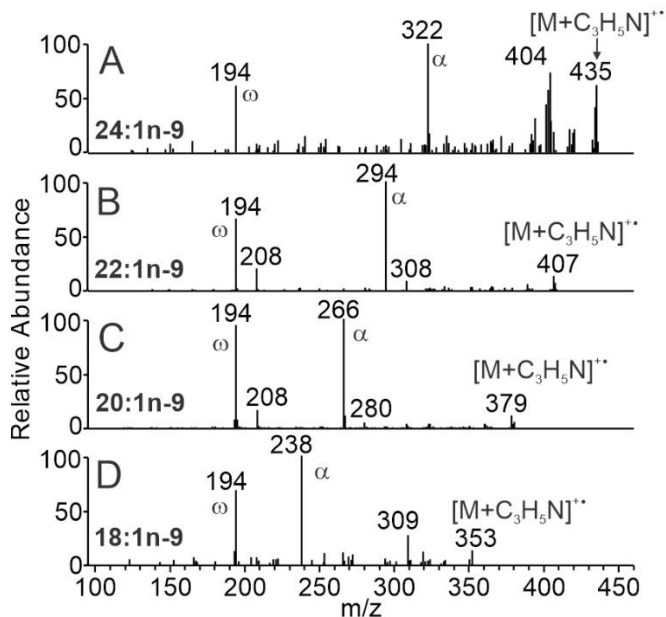
## Supporting information



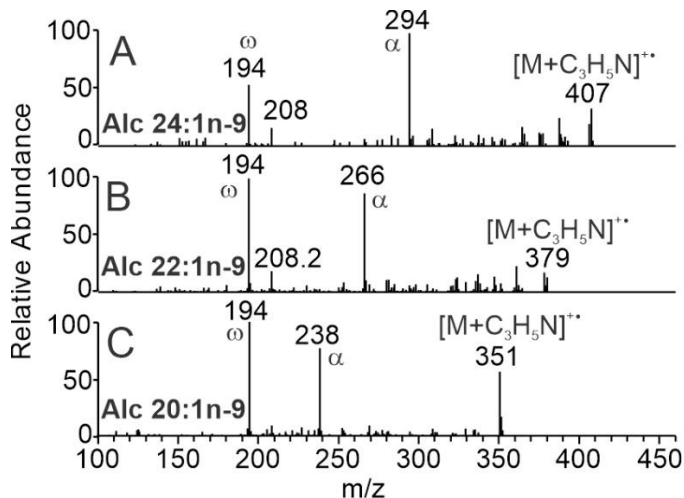
1. 10:0	6. 12:0	11. 13:0	16. 20:3n-3	21. 20:2n-6	26. 22:2n-6	31. 24:1n-9
2. 11:0	7. 18:3n-3	12. 16:1n-7	17. 18:2n-6t	22. 16:0	27. 18:0	32. 22:0
3. 20:5n-3	8. 18:3n-6	13. 18:2n-6	18. 17:1n-7	23. 18:1n-9t	28. 22:1n-9	33. 23:0
4. 22:6n-3	9. 20:4n-6	14. 14:0	19. 15:0	24. 17:0	29. 20:0	34. 24:0
5. 14:1n-5	10. 15:1n-5	15. 20:3n-6	20. 18:1n-9	25. 20:1n-9	30. 21:0	

SUPPORTING FIGURE 1. Temperature-programmed capillary HPLC/APCI-MS chromatograms of the mixture of FAME standards (total concentration 1 mg/ml) recorded over a period of seven days. The analytes were detected with the conventional APCI source; for the conditions see the Materials and Methods section.

Supporting information



SUPPORTING FIGURE 2. Ion trap MS/MS spectra of  $[M + C_3H_5N]^{++}$  adducts of FAMEs: 24:1n-9 (A), 22:1n-9 (b), 20:1n-9 (c), 18:1n-9 (d). The  $\alpha$  and  $\omega$  fragments determine position of the double bond. The spectra were collected under chromatographic conditions (FIGURE 5C).



SUPPORTING FIGURE 3. Ion trap MS/MS spectra of  $[M + C_3H_5N]^{++}$  adducts of alcohols: 24:1 (n-9) (a), 22:1n-9 (b) and 20:1n-9 (c). The  $\alpha$  and  $\omega$  fragments determine position of the double bond. The spectra were collected under chromatographic conditions (FIGURE 5C).